PhD degree in Systems Medicine

(curriculum in Molecular Oncology)

European School of Molecular Medicine (SEMM),

University of Milan and University of Naples "Federico II"

Settore disciplinare: MED/4

In vivo modeling and characterization of *MYC/BCL2* Double Hit Lymphoma

Giorgia Ceccotti

IEO, Milan

Matricola n. R11760

Supervisor: Dr. Bruno Amati,

European Institute of Oncology (IEO), Milan

Added Supervisor: Dr. Andrea Bisso,

European Institute of Oncology (IEO), Milan

Anno accademico 2019-2020

Table of contents

1 List of abbreviations

Aa = amino acid

AML = Acute Myelocytic leukemia

APC = Antigen presenting cells

BCR = B cell receptor

bHLH-LZ = basic helix-loop-helix leucine zipper

BL = Burkitt lymphoma

BM = bone marrow

CLL = Chronic Lymphocytic Leukemia

CLPs = Common lymphoid progenitors

DC = dendritic cells

DEG = differentially expressed genes

DHL = Double hit lymphoma

DLBCL = Diffuse large B-cell lymphoma

DNA = deoxyribonucleic acid

DZ = Dark zone

E-box = Enhancer box

FL = Follicular lymphoma

FO = Follicular Zone B-cells

GC = germinal center

GC = Germinal center

GEP = Gene expression profile

HSCs = hematopoietic stem cells

KD = knock down

KO = knock out

LPL = Lymphoplasmablastic lymphoma

Ly = lymphoma

LZ = Light zone

MB = Myc box

mDHL = mouse double hit lymphoma

MEFs = mouse embryonic fibroblasts

mESCs = mouse embryonic stem cells

MZ = Marginal Zone B-cells

NK = natural killer

NKT = natural killer T-cells

PC = Plasma cell

pre-GC = Pre-germinal center

preT = pre-tumoral

rDNA = ribosomal DNA

RNA = ribonucleic acid

RPKM = reads per kilo base per million mapped reads

rRNA = ribosomal RNA

T = tumor

T1 = Transitional Type 1 B-cells

T2 = Transitional Type 2 B-cells

T3 = Transitional Type 3 B-cells

TAD = transactivation domain

UTR = untranslated region

VDJ recombination = Variable, diversity, and joining recombination

WT = wild type

2 Figure Index

3 Table index

4 Abstract

Double-hit lymphoma (DHL) arises from Germinal Center (GC) B-cells that undergo chromosomal translocations activating the *MYC* and *BCL2* oncogenes and constitutes an aggressive group of tumors that show dismal prognosis with current therapeutic regimens. Full understanding of the pathophysiology of DHL and its exploitation for pre-clinical development depend upon the availability of a mouse model that faithfully represents the physio-pathological features of the human disease, and in particular its GC origin – a characteristic trait that is missing in the models developed do far. Here, we have pursued this goal by combining conditional *lox-stop-lox(lsl)-MYC* and *lsl-BCL2* alleles with the GC-specific transgene Cγ1-*Cre*: while either oncogene alone showed limited effects, their co-activation led to the development of fully penetrant lymphomas (median onset of 213 days) that showed a Dark Zone-like GC phenotype and a number of other DHL-like features, including extensive infiltration of multiple organs (e.g. liver, spleen, kidney, lung, brain), high levels of proliferation and apoptosis, and extensive macrophage infiltration. Careful examination by expert pathologists classified these tumors as high-grade B-cell lymphomas, similar to human DHL, and transcriptional profiling confirmed their GCB cell of origin. The tumors were transplantable and expanded in immunodeficient mice while retaining their original GC phenotype. These lymphomas were also stabilized for *in vitro* growth, thus creating stable DHL cell lines that can be used for further experiments. This model expands the available tools to characterize DHL at the biological, pathological and pre-clinical levels, and shall provide an advanced experimental platform for pre-clinical testing of novel therapeutic combinations. Altogether, these complementary lines of investigation shall provide deep insights into the biology and molecular underpinnings of DHL, and point to new therapeutic solutions against this aggressive lymphoma subtype.

5 Introduction

The occurrence of various B cell lymphoma (BCL) subtypes is associated with chromosomal translocations that occur at the Germinal Center (GC) stage and involve characteristic proto-oncogenes such as *MYC*, *BCL2*, or *BCL6* (Basso and Dalla-Favera, 2015; Kuppers and Dalla-Favera, 2001; Rosenquist et al., 2017). For example, Burkitt's (BL) and Follicular Lymphoma (FL) are initiated by activation of *MYC* and *BCL2*, respectively. The same genes can be activated at later stages in a subset of other BCL subtypes, as seen for *MYC* during progression of FL from the indolent to the transformed stage (Bakhshi et al., 1985; Cleary et al., 1980; Pasqualucci et al., 2014; Tsujimoto et al., 1984). Diffuse Large-B Cell Lymphomas (DLBCL) can show translocation of either oncogene, and in a subset of cases accumulate concurrent translocations giving rise to particularly aggressive double-hit lymphomas (DHL), which show dismal prognosis in the face of current front-line therapies (Anderson et al., 2016; Basso and Dalla-Favera, 2015; Friedberg, 2017; Karube and Campo, 2015; Rosenquist et al., 2017; Rosenthal and Younes, 2017; Sarkozy et al., 2015; Sesques and Johnson, 2017). While traditionally considered as a subtype of DLBCL – and still frequently so – the updated WHO classification now places it as a separate group of high-grade B-cell lymphoma (HGBL) (Swerdlow et al., 2016).

5.1 *MYC*

The *MYC* proto-oncogene (or c-*myc*), originally identified as the cellular homolog of the avian retroviral oncogene v-*myc* (Roussel et al., 1979; Vennstrom et al., 1982), is the founding member of a family of three related genes that also includes N- and L-*myc* (or *MYCN* and *MYCL*). *MYC* family members are expressed in the majority of tissues during mouse development, with c-*myc* expressed mostly in dividing cells of all tissues at the newborn and post-natal stages while N-*myc* is restricted to brain, kidney, intestine and lungs, and L-*myc* to kidney and lungs (Zimmerman et al., 1986). The importance of *MYC* family members in early

embryonic development has been investigated by generating homozygous null mice for either c-*myc*, N-*myc* or L-*myc*: embryos lacking c-*myc* die between 9.5 and 10.5 days post coitus (dpc) due to abnormal heart, neural tube and yolk sac development (Davis et al., 1993). The knockout of N-*myc* also causes embryonic lethality around mid-gestation, with its specific deletion in neural stem and precursors cells leading to severe disruption of murine brain growth, specifically of the cerebellum (Charron et al., 1992; Stanton et al., 1992). L-*myc* null mice do not show any congenital defects and a life span comparable to that of WT siblings (Hatton et al., 1996), possibly owing to compensation by c-*myc* and N-*myc*, which have been detected in all L-*myc* expressing tissues (Hatton et al., 1996). In mouse embryonic stem cells (ESCs) grown in minimal in 2i medium, c-*myc* or N-*myc* single KO cells did not show any detectable phenotype and were capable of multilineage differentiation both in vitro and in vivo, while joint elimination of the two genes caused proliferative arrest, demonstrating that *MYC* activity is essential, but c- and N-*myc* are redundant in this setting (Scognamiglio et al., 2016). Moreover, substitution of both c-*myc* alleles with the N-*myc* coding region supports the survival of viable offspring (Malynn et al., 2000), supporting the idea of functional redundancy among *MYC*-family proteins. This concept is not restricted to the embryo but may also apply to somatic stem cells (Cheung and Rando, 2013; Latil et al., 2012; Sosa et al., 2014; Wagner et al., 1993; Wilson et al., 2008). For example, in the hematopoietic system, both N- *myc* and c-*myc* play a pivotal role such as the exit of HSCs from dormancy triggered by interferon-α associated to the upregulation of c-*Myc* (Ehninger et al., 2014). Additionally, upon conditional deletion of both c-*myc* and N-*myc* in the bone marrow, the only blood cells that are preserved are dormant HSCs, while non-stem cells undergo rapid apoptosis (Laurenti et al., 2008).

MYC activity has a significant impact on longevity and multiple aspects of mammalian health. In a recent study, *MYC*+/– mice were shown to have an increased lifespan compared to their *MYC* +/+ littermates (Hofmann et al., 2015). Most noteworthy here, mice carrying a

hypomorphic c-*myc* allele are smaller than the wild type, due to decreased overall cell numbers (Trumpp et al., 2001).

5.1.1 Structure of the MYC protein

Proteins belonging to the *MYC* family, are composed by two major region: an N-terminal transcriptional activation domain (TAD) (Amati et al., 1992; Kato et al., 1990) and a C-terminal basic Helix-Loop-Lelix Leucine Zipper domain (bHLH-LZ), required for dimerization and DNA binding, transcriptional activation and oncogenic activity (Conacci-Sorrell et al., 2014; Reddy et al., 1992; Tansey, 2014) (Figure 5.1). Their sequence show six highly conserved regions (*MYC* boxes or MBs) which spread through the TAD region and the central portion of the protein, followed by the bHLH-LZ (Meyer and Penn, 2008).

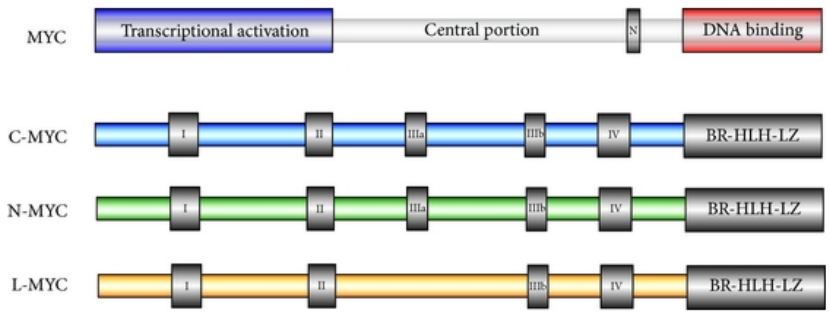

Figure 5.1: Structure of *MYC* protein family.

The main structural domains of *MYC* are shown at the top of the figure. Transcriptional activation, central portion canonical nuclear localization sequence 'N' and region of DNA, binding via interaction with *MAX* are reported. A representation of the different family members (c, N and L-*MYC*) is shown. Modified from (Tansey, 2014).

The TAD itself (aa 1-143), originally mapped through chimeric constructs fusing portions of *MYC* to a heterologous DNA binding domain (Kato et al., 1990), is characterized by the presence of two MBs, MBI (aa 43-63) and MBII (aa 128-143), which are highly conserved among *MYC* family members (Figure 5.2). A proteomic profiling of the *MYC* interactome suggested that half of the *MYC* interactors require one or more MBs for binding (Kalkat et al., 2018). Besides its role in gene activation (Su et al., 2018), MBI is also important for

ubiquitin/proteasomal degradation of *MYC*: this region is characterized by the presence of Threonine 58 (T58) and Serine 62 (S62), the phosphorylation of which regulates the activity and stability of *MYC* (Pulverer et al., 1994; Sears et al., 2000). Stabilization of *MYC* happens via phosphorylation of S62, which in turn primes for T58 phosphorylation (Sears et al., 2000); on the other hand, T58 triggers the dephosphorylation of the stabilizing phosphate group S62 (Arnold and Sears, 2006; Yeh et al., 2004). Most noteworthy here MBI, and in particular T58, is also a hot spot for point mutations in Burkitt's lymphoma, which occur as secondary events in the translocated MYC oncogene (Bemark and Neuberger, 2000; Bhatia et al., 1993; Bhatia et al., 1994; Giulino-Roth et al., 2012; Reddy et al., 2017). Besides *MYC* stability, point mutation in this region may also impacts the transforming and apoptotic activities of *MYC* (Hemann et al., 2005).

MBII is a key domain important for binding coactivators, such as TRRAP (McMahon et al., 1998) and the associated histone-acetyl-transferase complexes Tip60/NuA4 or GCN5/STAGA (Figure 5.2) (Tu et al., 2015). At the functional level, MBII is important for *MYC* transforming activity, as well as for gene activation (Kalkat et al., 2018; Oster et al., 2002).

The central portion of the MYC protein is its least studied part. This region includes a bipartite nuclear localization sequence, composed by the peptides M1 (PAAKRVKLD, aa 320-328) and M2 (RQRRNELKRSP, aa 364-374) (Dang and Lee, 1988), and three other conserved elements: MBIIIa, MBIIIb and MBIV. MBIIIa (aa 180-199) is the least conserved among *MYC* family members, since it is lost in L-*MYC*. It has been reported that this region is important for transcriptional repression by *MYC* and for transformation, both *in vitro* and in a mouse model of lymphomagenesis (Herbst et al., 2005). MBIIIb (aa 259-270) was recently shown to interact directly with WDR5 (WD repeat-containing protein 5), which is part of various chromatin remodelling complexes, such as H3K4 methyltransferases, and could facilitate *MYC* recruitment to open chromatin (Thomas et al., 2015b). Interestingly, disruption of the *MYC*-

WDR5 interaction promotes tumor regression in vivo (Thomas et al., 2019). MBIV (aa 304-324) has been reported to be involved in different *MYC* functions: its deletion impairs *MYC*-induced apoptosis and partially reduces its transforming potential, but it does not have any effects on cellular proliferation (Cowling et al., 2006).

The best characterized domain of *MYC* is the bHLH-LZ, which mediates heterodimerization of *MYC* with its partner, *MAX* (Blackwood and Eisenman, 1991; Luscher and Larsson, 1999). The fact that *MYC* homodimers are never detected at physiological levels (Dang et al., 1991; Smith et al., 1990), highlights the importance of *MAX* for *MYC* activity. Indeed, dimerization with *MAX* is required for *MYC* to bind DNA, drive E-box dependent transcription *in vivo*, proliferation, transformation and apoptosis (Amati et al., 1992; Amati and Land, 1994; Littlewood and Evan, 1995).

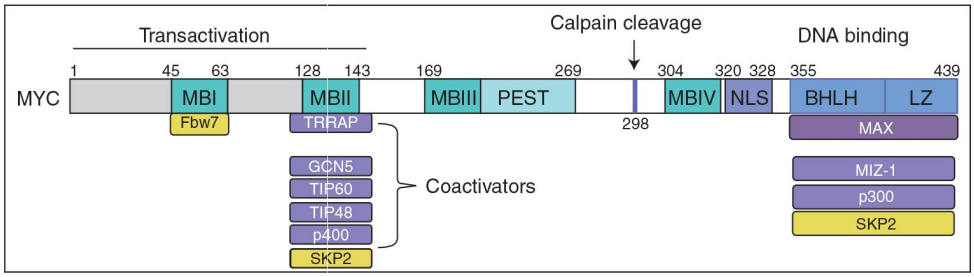

Figure 5.2 Schematic representation of *MYC* domains and some of its cofactors.
In yellow are depicted major ligases responsible for *MYC* turnover and in violet are transcriptional binding partners of *MYC*. Modified from (Conacci-Sorrell et al., 2014).

5.1.2 Regulation of *MYC* expression and activity

The abundance and activities of *MYC* are tightly regulated by a complex signaling network that may act at different biological steps, as described below.

- Transcriptional control.

The first level of *MYC* regulation is the control of the transcription of its own gene. As originally shown in fibroblasts, *MYC* expression levels are very low in quiescent cells, and rapidly induced upon mitogenic stimulation, classifying it an immediate-early gene (Kelly et

al., 1983; Winkles, 1998). After stimulation, *MYC* levels need to be lowered again to avoid uncontrolled proliferation (Bentley and Groudine, 1986; Eick and Bornkamm, 1986; Krystal et al., 1988; Xu et al., 1991). The direct regulation of *MYC* by mitogenic stimuli was confirmed in diverse cell types, with a variety of growth factors and signaling pathways. For example, Notch, WNT, Hedgehog and and Janus kinase (JAK)–signal transducer and activator of transcription 3 (STAT3) signalling induce *MYC* transcription, whereas transforming growth factor-β (TGFβ) signalling represses it. The mTOR complex 1 (mTORC1)–S6K1 (REFS 167,168), MAPK–HNRPK169 and MAPK–FOXO3A170 signalling cascades affect the efficiency of MYC translation, whereas the cooperative action of the PI3K and RAS signalling pathways increases the stability of MYC (Kress et al., 2015b) (Figure 5.3A).

- Post-transcriptional control.

Upon transcription of the *MYC* mRNA, its export to the cytoplasm is controlled by the translation initiation factor eIF4E (Culjkovic et al., 2006), which is also activated by mitogenic stimuli. The half-life of *MYC* mRNA is very short (Dani et al., 1984) and controlled by a number of miRNAs and RNA binding proteins (RBPs), such as TIAR, AUF1 and HuR (Kim et al., 2009; Liao et al., 2007).

- Translational control.

In eukaryotes, the assembly of ribonucleoprotein complexes is a fundamental step for initiation of translation, and mRNAs with long and complex 5'UTR, such as the one encoding for *MYC*, are impaired in translation initiation (Kozak, 1989) providing additional regulatory potential. For example, S6 Kinase 1 (S6K1), a target and effector of mTORC1, enhances *MYC* translation efficiency by modulating the phosphorylation of eIF4B, critical for unwinding of the *Myc* 5' UTR (Csibi et al., 2014). In addition, in the *MYC* mRNA, the presence of a ribosome internal entry site (IRES) can drive cap-independent initiation of translation (Stoneley et al., 1998) and

mutations in this element can result in increased MYC protein production in multiple myeloma cells (Chappell et al., 2000; Paulin et al., 1998).

Synthesis of the MYC protein can be halted in response to UVC irradiation, which causes association of the TIAR protein with the 3' UTR of many key regulators, including *MYC*, ultimately suppressing their translation (Mazan-Mamczarz et al., 2006).

- Post-translational control.

The MYC protein undergoes many different post-translational modifications, such as phosphorylation, acetylation, ubiquitination and sumoylation, that have a role in *MYC* stabilization and degradation (Rabellino et al., 2016; Sabò et al., 2014a; Vervoorts et al., 2006). The main route for controlling MYC protein levels is trough ubiquitin-proteasome system (UPS) (Farrell and Sears, 2014; Thomas and Tansey, 2011). In particular, one of the best characterized Ub-ligase complexes controlling *MYC* levels is SCF^{Fwb7}, which depends upon interaction of its F-box subunit Fbw7 with the phospho-T58 form of *MYC* (Welcker et al., 2004; Yada et al., 2004). SCFFwb7 is not the only enzyme involved in *MYC* ubiquitination: for example, Skp2 also promotes poly-ubiquitination of *MYC*, and does so independently from its phosphorylation (Kim et al., 2003). On the contrary, ubiquitination by β-TrCP appears to increase MYC protein stability (Popov et al., 2010). Recently, the importance of post-translational control of *MYC* levels in both normal and tumor tissues was highlighted by demonstrating that S62 phosphorylation and Pin1-mediated isomerization of *MYC* control its spatial localization in the nucleus and further allow for optimal regulation of gene expression in response to extrinsic signals (Su et al., 2018).

Taking into account that *MYC* can be also acetylated and that both acetylation and ubiquitination occur on Lysine residues, it has been hypothesized that these modifications may be compete with each other. Indeed, it has been shown that acetylation increases the stability of *MYC* and is negatively correlated with ubiquitination (Faiola et al., 2005; Vervoorts et al.,

2003). Moreover, *MYC* can also be a substrate for addition of small ubiquitin-like modifier (SUMO) proteins (Gonzalez-Prieto et al., 2015; Kalkat et al., 2014; Sabò et al., 2014a). In c-*MYC*, mass spectrometry analysis identified several SUMO acceptor lysines, K52, K148, K157, K317, K323, K326, K389, K392, K398 and K430 (Gonzalez-Prieto et al., 2015; Kalkat et al., 2014). However, in N-*MYC* only Lysine 349 has been reported to be modified by SUMOylation (Sabo et al., 2014a). Both c-*MYC* and N-*MYC* SUMOylation can have a role in MYC protein regulation, e.g. multiple SUMO monomers have been associated with ubiquitin-proteasome pathway (Gonzalez-Prieto et al., 2015), while *MYC* phosphorylation and dephosphorylation of S62 and T58 could be a SUMO-dependent process (Rabellino et al., 2016).

5.1.3 Physiological functions of *MYC*

In normal conditions, cells express c-*myc* only upon exposure to mitogenic stimuli and in turn, leads to variety of transcriptional changes that foster cell growth and proliferation, mainly regulating key components of biosynthetic and metabolic processes necessary to maintain cellular growth (Dang, 2013; de Alboran et al., 2001; Kress et al., 2015a; Perna et al., 2012; Tesi et al., 2019a; Wang et al., 2011a). In line with these findings, *MYC* acts as a direct sensor of activating signals in both B- and T-cells, and is required for several steps of cellular activation, such as metabolic reprograming, ATP synthesis, ATP-dependent chromatin decompaction, RNA accumulation and cell growth (de Alboran et al., 2004; Kieffer-Kwon et al., 2017; Murn et al., 2009; Wang et al., 2011b) (Figure 5.3B). Altogether, *MYC* constitutes central node in cell signaling, providing cells with a direct readout of mitogenic stimuli, and contributing to their response to those same signals.

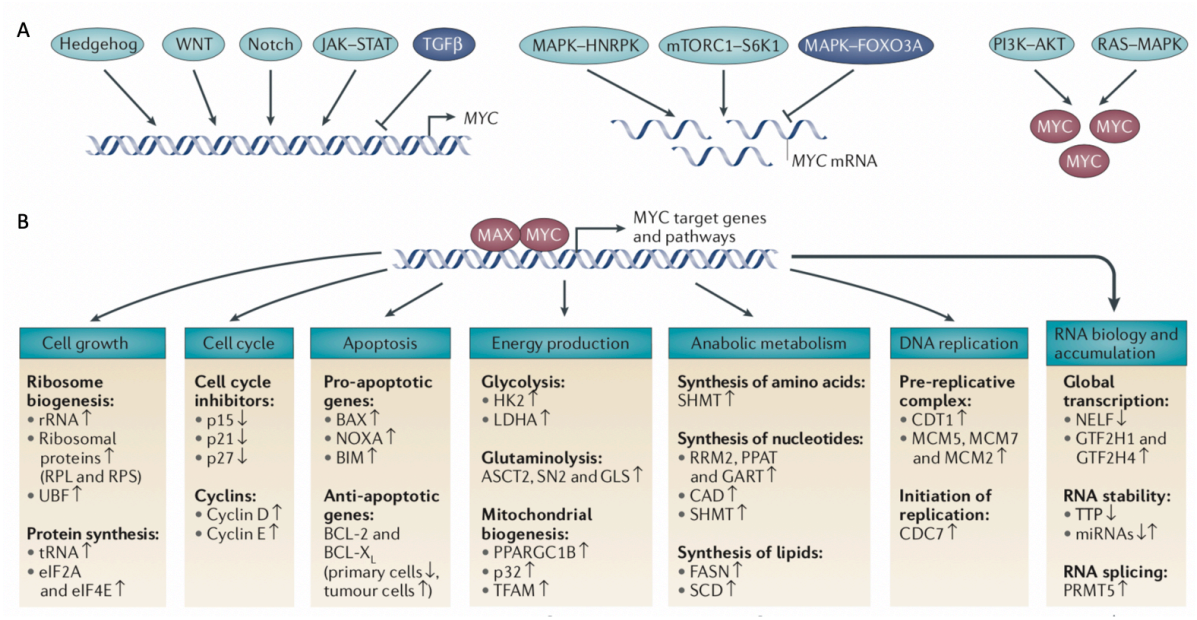

Figure 5.3 Examples of *MYC*-dependent genes and cellular processes (Kress et al., 2015b)

5.1.4 Alterations of *MYC* in cancer

The central role of *MYC* in mitogenic signaling endows it with strong oncogenic activity when aberrantly expressed. Indeed, up to 70% of human tumors show *MYC* overexpression (Dang, 2012; Meyer and Penn, 2008; Tansey, 2014). *MYC* can be oncogenically activated either through direct alterations of its locus (see below) or, in the absence of direct oncogenic lesions, through aberrant activation of upstream signaling pathways (Figure 5.3A). The first alterations to be described in *Myc* were translocations, which are a defining landmark in Burkitt's B cell lymphomas (Kuppers and Dalla-Favera, 2001), but also occur in a subset of follicular B cell lymphoma (FL), diffuse large B cell lymphoma (DLBCL), chronic lymphocytic leukemia (CLL) and multiple myeloma (Bisso et al., 2019; Grande et al., 2019; Huh et al., 2008; Pasqualucci and Dalla-Favera, 2018; Pasqualucci et al., 2014; Shou et al., 2000). In all of these cancers, *MYC* deregulation generally correlates with a more aggressive phenotype and poor prognosis (Barrans et al., 2010; Bisso et al., 2019; Gabay et al., 2014; Pasqualucci and Dalla-Favera, 2018). *Myc*'s oncogenic potential can also be achieved through amplification of its locus, as observed in

diverse solid tumors (Beroukhim et al., 2010). Most frequently, *MYC* is activated in an indirect manner, as its overexpression is triggered by upstream oncogenic events that activate pathways such as Wnt in colon cancer (He et al., 1998; Sansom et al., 2007), Notch in T-cell leukemia (Palomero et al., 2006; Weng et al., 2006) or JAK-STAT signaling in prostate cancer, hematopoietic malignancies and sarcomas (Bromberg et al., 1999; Kiuchi et al., 1999) (Figure 5.3A).

Among its multiple effects, oncogenic *MYC* can increase the number of divisions in cycling cells and the size of cells (Iritani and Eisenman, 1999). In certain conditions, *MYC* overexpression can cause proliferative arrest (Felsher et al., 2000) or cellular senescence (Campaner et al., 2010; Grandori et al., 2003). When *MYC* overexpression co-occurs with other oncogenic event, such as Ras activation or overexpression of *BCL2*, it eventually leads to transformation of the cells and tumor initiation (Clegg et al., 2011; DeoCampo et al., 2000; Land et al., 1983; Strasser et al., 1990b; Welm et al., 2005). When oncogenic *MYC* is switched off in already established tumors, it causes tumor involution, based on either growth arrest, apoptosis, block in differentiation, as well as a number of systemic alterations in the tumor microenvironment, demonstrating that tumors are addicted to continuous *MYC* overexpression at multiple levels (Felsher and Bishop, 1999; Gabay et al., 2014; Jain et al., 2002; Kortlever et al., 2017; Kress et al., 2016; Shachaf et al., 2004; Sodir et al., 2020). Even in tumors driven by other oncogenes (e.g KrasG12D or SV40 large T antigen), inhibition of *MYC* leads to tumor regression (Soucek et al., 2013), implying that *MYC* is generally required for tumor maintenance.

5.1.5 The *MYC*/*MAX* dimer

As outlined above, *MYC* associates with *MAX* to specifically bind DNA and activate transcription from promoters containing the consensus binding motif CACGTG (or E-box) (Amati et al., 1992; Blackwood and Eisenman, 1991; Prendergast et al., 1991). The formation of the *MYC*/*MAX* heterodimer is fundamental for the biological activities of *MYC* such as DNA binding to the E-box (Blackwood and Eisenman, 1991; Prendergast et al., 1991), transcriptional activation (Amati et al., 1992; Crouch et al., 1993; Kretzner et al., 1992; Reddy et al., 1992), cell proliferation, apoptosis and transformation (Amati et al., 1993a; Amati et al., 1993b), and *MYC*-dependent gene regulation (Mao et al., 2003). A recent publication dissected the functional interplay between c-*myc* and *MAX* in B lymphocytic differentiation by using either c-myc KO, *MAX* KO or double KO mice, showing that *MYC* requires *MAX* in primary B lymphocytes in order to exert its function, while cell differentiation and DNA replication can be initiated without the formation of *MYC*/*MAX* heterodimers, but requires these dimers the maintenance, amplification or fine-tuning of these functions upon their initial activation (Perez-Olivares et al., 2018). Another recent publication showed that loss of *MAX* in B cells leads to downregulation of numerous transcriptional targets of *MYC*/*MAX* and abrogates lymphomagenesis in the Eμ-myc mouse model, confirming the importance of *MAX* for *MYC* activity (Mathsyaraja et al., 2019).

5.1.6 *MYC* as a transcription factor

Early on, and still before the emergence of technologies allowing genome-wide analysis, the discovery of *MAX* and of the transcriptional activity of the MYC/MAX dimer led to the notion that the effects of *MYC* in physiology and disease were driven by specific target genes. While a plethora of studies pointed in this direction, a number of controversies have developed in recent years, concerning the activities of *MYC* when associated with DNA, the

extent of its interactions with the genome, or the specificity of *MYC*-dependent transcriptional programs. These debates will be introduced below.

Initial DNA binding and gene expression profiles suggested that *MYC* binds to and potentially regulates transcription of around ~15% of the genome (Fernandez et al., 2003; Zeller et al., 2006). Genomic regions found to be enriched at *MYC* binding sites were CpG island (Luscher and Vervoorts, 2012; Zeller et al., 2006), and more in general chromatin regions enriched for epigenetic marks of open and active chromatin, such as tri- and di-methylation of lysine 4 as well as acetylation of lysine 27 of the histone H3 (H3K4me3, H3K4me2, H3K27ac respectively) (Guccione et al., 2006; Sabò and Amati, 2014). So far, it has not been reported that *MYC* can bind to heterochromatin, even though the E-boxes could be present in those regions (Lin et al., 2012; Sabo et al., 2014b). Hence, chromatin has to be open prior to *MYC* binding to its target sites.

Apart from being marked by H3K4me3, regions that are bound by *MYC* can also be pre-bound by transcriptional regulators such as *WDR5* or *BPTF*, which can facilitate recruitment of *MYC* to its target sites (Richart et al., 2016; Thomas et al., 2015a; Thomas et al., 2015b). Once bound to DNA, *MYC* in turn recruits a number of transcription co-factors that lack sequence specificity, such as TRRAP (McMahon et al., 2000), *HDAC*s (Matsuoka et al., 2008), Tip60 or *GCN5* (Frank et al., 2003; McMahon et al., 2000). Moreover, *MYC* can interact with general transcription factors, such as *P-TEFB* (cyclin T-CDK9 complex) which mediates RNAPolII CTD phosphorylation, and such interaction has been proposed to lead to the stimulation of transcriptional elongation (Bouchard et al., 2004; Eberhardy and Farnham, 2002; Lin et al., 2012; Rahl et al., 2010). In addition, *MYC* can associate with the H3K4me3 demethylases JARID1A/KDM5A and Jarid1B/Kdm5b and different subunits of ATP-dependent chromatin remodeling complexes such as SWI/SNF (Cheng et al., 1999; Pal et al., 2003; Park et al., 2002; Secombe and Eisenman, 2007).

MYC can interact also with other proteins through its C-terminal domain (CTD), such as the transcription factor *MIZ1*: this interaction has been linked to *MYC*-dependent repression, which is thought to occur mainly through blockade of the activating action of *MIZ1* (Staller et al., 2001; Walz et al., 2014). An example of a *MYC*/ *MIZ1*-repressed gene is *CDK1NA*: upon UV irradiation in mammalian cells, *MIZ1* promotes transcription of *CDK1NA* in order to trigger the DNA damage-induced cell cycle arrest; on the other hand, *MYC* antagonize *MIZ1* activity and facilitate recovery of proliferation after the arrest (Herold et al., 2002). Since both *MYC* and *MIZ1* are transcriptional activators, but together block the activating action of *MIZ1*, it has been proposed that the ratio of *MYC*/ *MIZ1* bound to promoters correlates with the direction of response: in case of *MYC* upregulated genes this ratio is bigger than 1, while for *MYC*-repressed genes is close to 1 (Walz et al.2014). However, an integrative analysis of genomic and transcriptomic data from different in vitro and in vivo systems suggested that the relative abundance of *MYC* at promoters – rather than the *MYC*/*MIZ1* ratio – is a more accurate predictor of transcriptional outcome (de Pretis et al., 2017).

5.1.7 Regulatory models: selective transcription versus general transcriptional amplification

Traditionally, it has been thought that *MYC*-dependent transcriptional activation occurs upon its direct binding to a target sequence on promoter DNA (Kress et al., 2015b; Sabò and Amati, 2014), while *MYC*-dependent repression in most cases is a result of its indirect DNA binding through other transcription factors of whom *MYC* would antagonize the function (Staller et al., 2001). In 2012, two studies challenged this view proposing that *MYC* act as a general amplifier of transcription of all expressed genes (Lin et al., 2012; Nie et al., 2012). This model was based on the observation that, in cancer cells, the widespread binding of *MYC* to basically all accessible regions of the genome (active promoters and enhancers) is often coupled with an increase in global RNA levels, termed “RNA amplification”. The authors thus

concluded that *MYC* binds broadly trough the genome and provides non-specific amplification of already expressed genes, mainly through enhancement of transcription elongation via its interaction with the p-Tefb complex (Lin et al., 2012; Nie et al., 2012). However, the transcriptional amplification model failed to consider a fundamental aspect: *MYC* can trigger a series of cellular processes which dramatically impact cell physiology and may thus also foster a general increase in transcription. One of the ways in which the phenomenon of RNA amplification may be explained is by a variety of metabolic changes that rely on *MYC* and, in turn, impact the global RNA synthesis and turnover (Kress et al., 2015b). For example, it has been known for decades that differences in total RNA content may be used as a discriminating marker for cycling and quiescent cells in yeast (which has no *MYC* homologue) (Darzynkiewicz et al., 1980) and changes in *MYC* levels often co-occur with changes in the proliferative state of the cells, e.g. tumor versus normal tissue (Sabo et al., 2014b), or quiescent B cells versus LPS-stimulated cells (Nie et al., 2012; Sabo et al., 2014b; Tesi et al., 2019b; Zeller et al., 2006). Moreover, *MYC* invasion and RNA amplification are distinct, separable events that can occur independently: in serum-stimulated fibroblasts, increased RNA levels are observed in cells transitioning from G1 to S-phase, while *MYC* does not completely invade the open chromatin (Sabo et al., 2014b) and contributes to the activation of an earlier transcription program in G1 (Perna et al., 2012). On the contrary, overexpressed *MYC* can be detected at all active chromatin domains in already proliferating fibroblast, without triggering RNA amplification (Kress et al., 2015b; Sabo et al., 2014b). Finally, the idea of *MYC* as a transcriptional amplifier postulates a cause-to-effect relation between *MYC* binding and gene regulation, without considering the possible existence of different binding modalities; in fact, discriminating productive from non-productive binding events is a challenging issue in the field, and is true for all transcription factors. Indeed, careful analysis of available datasets revealed that DNA binding is not predictive of actual regulation of gene transcription (Kress

et al., 2015b). In a recent work from our lab, we observed that promiscuous chromatin interaction profiles seems to encompass diverse DNA-binding modalities, driving defined, sequence-dependent transcriptional responses (Pellanda et al., 2020)

Altogether these observations strongly support the long-standing concept that *MYC* acts as a "traditional" transcription factor, which is able to up- and down-regulate specific sets of genes in response to the environmental stimuli (Kress et al., 2015b).

5.1.8 DNA replication

DNA replication is one of the key cellular processes in which *MYC* was proposed to play a direct role (Dominguez-Sola and Gautier, 2014; Dominguez-Sola et al., 2007). Different studies reported protein-protein interactions between MYC and factors of the pre-replication complex, such as the Origin Replication Complex 1 and 2 (ORC1, ORC2) (Dominguez-Sola et al., 2007; Takayama et al., 2000b), MCM 2-7 (Dominguez-Sola et al., 2007), CDC6 (Takayama et al., 2000a) and Cdt1 (Dominguez-Sola et al., 2012). The *CDT1* gene has also been characterized as a *MYC* target gene (Valovka et al., 2013). Moreover, data in Xenopus cell-free extracts suggested that *MYC* controls DNA replication independently from its transcriptional activity (Dominguez-Sola et al., 2007). All this notwithstanding, it remains to be confirmed whether the effects of *MYC* on S-phase entry and progression are due to direct regulation of DNA replication or – perhaps more likely – to its impact on cell cycle control, mediated by the transcriptional control of gene that regulate this process (Kress et al., 2015a): examples of the latter include up-regulation of *cyclin D* (Perez-Roger et al., 1999; Yu et al., 2005) and *cyclin E* (Beier et al., 2000), or repression of $p21^{Cip1}$ and $p15^{INK4b}$ (Gartel et al., 2001; Seoane et al., 2001). Most noteworthy in this context *MYC* can also counteract the action of two related inhibitors, $p27^{KiPl}$ and $p16^{INK4a}$, without suppressing their levels (Alevizopoulos et al., 1997; Vlach et al., 1996). Finally, the products of *MYC*-activated genes can impact on the

biosynthesis of DNA and of other macromolecules (RNA, proteins) through the metabolism of precursors (nucleotides, amino acids) (Kress et al., 2015a), energy production, mitochondrial biogenesis or glycolysis (Dejure and Eilers, 2017; Kim et al., 2007; Li et al., 2005; Zhang et al., 2007).

5.1.9 rRNA biology, ribosome biogenesis and translation

A number of studies have linked *MYC* to the regulation of ribosome biogenesis and mRNA translation. First, *MYC* can control multiple stages of ribosome biogenesis by regulating the transcription of ribosomal RNA (rRNA) trough recruitment of RNA polymerase I (RNAPolI) co-factors and chromatin remodelling of ribosomal DNA (rDNA) loci and (Arabi et al., 2005; Grandori et al., 2005; Grewal et al., 2005; Poortinga et al., 2004; Shiue et al., 2009). Whether this effect is truly direct, however, remains unclear: while preliminary binding data in mammalian cells were used to support a direct action of *MYC* on rDNA (Arabi et al., 2005; Grandori et al., 2005), ChIP-seq experiments in our own group failed to confirm this effect (B. Amati, personal communication) while clearly mapping other factors along the mouse rDNA repeat (Pistoni et al., 2010). Most importantly, the regulation of RNAPolI activity by *MYC* occurs indirectly in Drosophila (Grewal et al., 2005), suggesting that the same may be true in mammalian cells. In line with this concept, *MYC* regulates the RNA polymerase II (RNAPolII)-dependent transcription of genes encoding ribosomal protein, as well as regulators of ribosomal subunit transport (Maggi et al., 2008; Wu et al., 2008; Zeller et al., 2001) and rRNA processing, such as Nucleolin, nucleoplasmin, Nop56 and others (Greasley et al., 2000; Schlosser et al., 2003). Therefore, *MYC* regulated a large number of protein-coding RNAPII-transcribed genes, the products of which control not only rRNA synthesis by RNAPI, but also rRNA processing, ribosome maturation and function.

Finally, besides the above general effects on the translation machinery, *MYC* can also modulate translation of select mRNAs, most likely through the transcriptional control of translation factors such as eIF4E (Schmidt, 2004). An example is the translational control of mRNAs encoding immune checkpoint proteins, such as PD-L1, which leads to more aggressive cancers (Xu et al., 2019).

5.1.10 *MYC*, Proliferation and Apoptosis

As mentioned above, *MYC* has a central role in the control of cell proliferation in response to mitogenic stimuli, and may promote cell cycle progression and cell division in multiple ways, including the regulation of genes such as cyclin D (Perez-Roger et al., 1999; Yu et al., 2005) and cyclin E (Beier et al., 2000), among many others. *MYC* also impacts proliferation by regulating the biological processes needed to support cell it, such as energy production. In order to provide the energy required for the cycling cell, *MYC* is upregulating genes implicated in different metabolic processes, such as mitochondrial biogenesis and glycolysis (Dejure and Eilers, 2017; Kim et al., 2007; Li et al., 2005; Zhang et al., 2007).

The ability of *MYC* to promote proliferation is counter-balanced by its propensity to trigger cell death in particular conditions. Indeed, it is believed that the ability of *MYC* to tightly control proliferation on one side, and to trigger cell death on the other, is a safeguard mechanism to prevent uncontrolled cell divisions due to *MYC* deregulation. For example, in the absence of survival signals, such as growth hormones or cytokines, deregulated *MYC* expression can induce apoptosis (Bissonnette et al., 1992; Evan et al., 1992) in both p53-dependent and p53-independet ways. First, *MYC* deregulation leads to the increase in the ARF protein expression (Zindy et al., 1998), which inhibits Mdm2, a negative regulator of p53 (Weber et al., 1999). Activation of p53 can increase Puma and Noxa levels that further downregulate anti-apoptotic factors – *BCL2* and Bcl-X_L (Eischen et al., 2001b; Maclean et

al., 2003; Oda et al., 2000). P53 can also activate pro-apoptotic protein Bax which subsequently causes permeabilization of the mitochondrial outer membrane that leads to induction of cell death (Chipuk et al., 2004).

Disruption of the equilibrium between pro-apoptotic and anti-apoptotic proteins by *MYC*-dependent mechanisms is another way how *MYC* induces apoptosis (Eischen et al., 2001b; Mitchell et al., 2000; Oster et al., 2002).

5.2 *BCL2* and apoptosis

BCL2 is the first molecularly defined regulator of the cell suicide program to be identified. Indeed the hallmark t(14;18) chromosome translocation in human follicular lymphoma linked the immunoglobulin heavy chain locus to a novel gene, then denoted *BCL2* (Tsujimoto et al., 1984). This gene was shown to promote cellular survival rather than proliferation, unlike the previously identified oncogenes (Vaux et al., 1988). The identification of *BCL2* together with apoptotic protease-activating factor-1 (Apaf1) in mammalian cells from the studies of Caenorhabditis elegans development in the 1990s (Hengartner et al., 1992; Hengartner and Horvitz, 1994; Yuan and Horvitz, 1992) marks the beginning of an era of molecular apoptosis research that triggered the rapid expansion of regulated cell death research.

The term apoptosis was coined for the first time in 1972 by John Kerr, Andrew Wyllie, and Alastair Currie (Kerr et al., 1972), and the molecular mechanisms regulating this process have been extensively investigated in multiple organisms over the last 30 years (Tang et al., 2019). Apoptosis is essential in both shaping the embryo and ensuring homeostasis within adult tissues (Fuchs and Steller, 2011). When the apoptotic process is ongoing, cells shrink, fragment their DNA, bleb and break up into ‘apoptotic bodies’, which are then engulfed by phagocytes (Kerr et al., 1972). Importantly, no inflammation ensues because the plasma membrane is not breached.

In mammals, apoptosis can be prompted through two different mechanisms: the intrinsic pathway and the extrinsic pathway (Figure 5.4). The extrinsic pathway is activated in response to external stimuli such as the engagement of the Fas or TNFα ligands to their receptors on cell surface as part of the effector phase of an immune response (Schulze-Osthoff et al., 1998) (Bredesen et al., 2004). in contrast, the intrinsic pathway is initiated when cells receive intrinsic death stimuli, such as excessive oncogene activation, DNA damage, or the unfolded protein response (UPR) (Chipuk et al., 2006). The intrinsic, and partially the extrinsic patway converge at the level of the mitochondrial outer membrane (MOM). Mitochondrial outer membrane permeabilization (MOMP) is tightly controlled by the *BCL2* family, including pro-apoptotic (e.g., BCL2 associated X, apoptosis regulator [*BAX*]) members (Czabotar et al., 2014; Singh et al., 2019). MOMP is considered to be the 'point of no return' during apoptosis as it results in the diffusion to the cytosol of numerous proteins that normally reside in the space between the mitochondrial inner and outer membranes (Von Ahsen et al., 2000). Among these is cytochrome c, which serves as a cofactor for Apaf-1 to trigger the formation of the apoptosome and subsequent activation of the initiator and executioner caspases, normally caspase-9 and -3, respectively. MOMP itself is a complex process regulated by numerous BCL2 proteins, culminating in formation of pores by the core components BAX, BAK and/or BOK) (see section 5.2.2) (Chipuk et al., 2006).

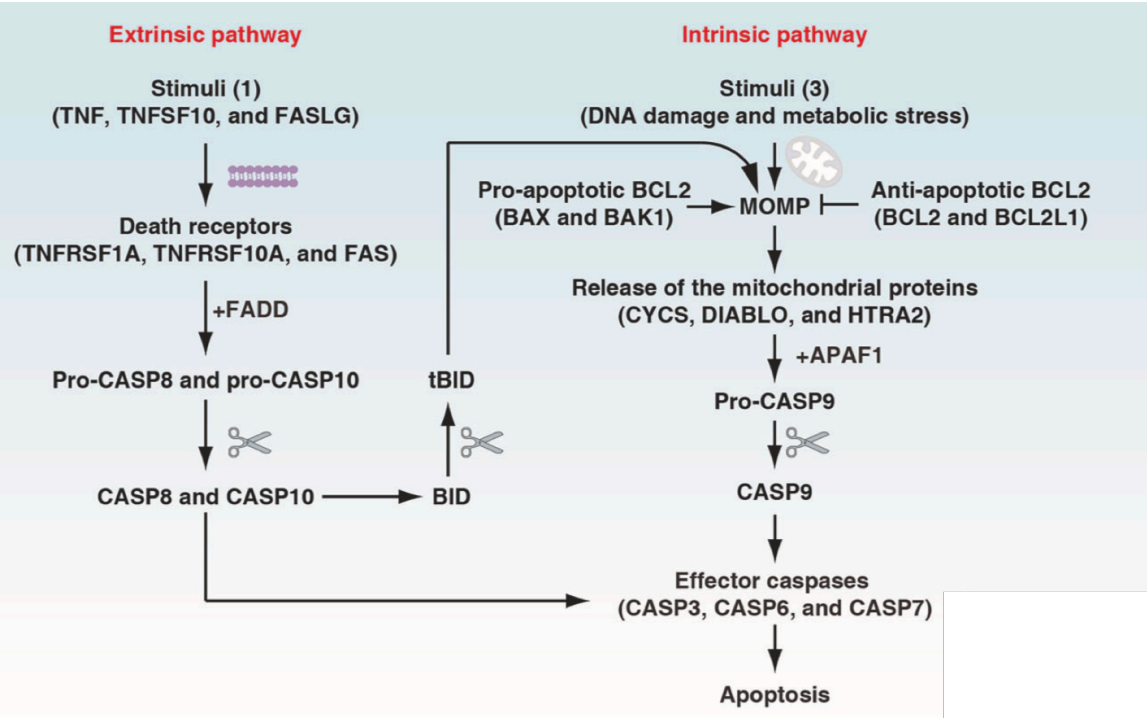

Figure 5.4 Apoptosis.
Extrinsic and intrinsic apoptosis. Extrinsic apoptosis is induced by the addition of death receptor ligands or by the withdrawal of dependence receptor ligands. CASP8 and CASP10 initiate death receptor-mediated extrinsic apoptosis, whereas CASP9 initiates the withdrawal of dependence receptor ligand-mediated extrinsic apoptosis. Pro-CASP8 and pro-CASP10 are enzymatically inactive until they interact with FADD (Fas-associated via death domain), which is activated upon binding to cell death receptors responding to their ligands. DNA damage, hypoxia, metabolic stress, and other factors can induce intrinsic apoptosis, which begins with MOMP and leads to the release of mitochondrial proteins (e.g., CYCS) into the cytosol. Cytosolic CYCS interacts with APAF1, which recruits pro-CASP9 to form the apoptosome. MOMP is tightly controlled by the BCL2 family, including its pro-apoptotic and anti-apoptotic members. CASP3, CASP6, and CASP7 are considered the common effector caspases for both extrinsic and intrinsic apoptosis. In addition, the extrinsic pathway can trigger intrinsic mitochondrial apoptosis through the generation of truncated BID (tBID) by activated CASP8. tBID can further translocate to mitochondria and cause MOMP through the activation of BAX and BAK1. Modified from (Tang et al., 2019).

5.2.1 The *BCL2* family

The *BCL2* family includes more than 20 proteins (Hardwick and Youle, 2009) with either pro-apoptotic or anti-apoptotic functions and is divided into three groups based on their primary functions (Figure 5.5) : anti-apoptotic (BCL2, BCL-XL, BCL-W, MCL-1, BFL-1/A1), pro-apoptotic BH3-only proteins (BAD, BID, BIK, BIM, BMF, HRK, NOXA, PUMA) and pore-forming proteins (BAX, BAK, BOK). All proteins belonging to the BCL2 family bear from one to four of the co-called BCL2 Homology (BH) domains (Adams and Cory, 2018; Lomonosova and Chinnadurai, 2008) (Figure 5.5).

BH3-only proteins are so called because their only homology to BCL2 is the BH3 domain, through which they engage multi-BH domain relatives (Adams and Cory, 2018) : this domain is essential for the binding of BH3-only proteins to the anti-apoptotic members of the family and for their ability to kill cells (Huang and Strasser, 2000). Hetero-dimerization is mediated by the insertion of the BH3 domain of the pro-apoptotic molecules into a hydrophobic cleft formed by the BH1, BH2 and BH3 domains on the surface of the anti-apoptotic proteins (Sattler et al., 1997). Many pro- as well as anti-apoptotic members of the *BCL2* family also have a C-terminal transmembrane domain, which can target these proteins to the cytoplasmic side of intracellular membranes of the nucleus, endoplasmic reticulum and mitochondria (Chen-Levy and Cleary, 1990; Lithgow et al., 1994). Interactions between these proteins determine whether cells live or die. The pro-survival members can bind with high affinity to members of both the *BAX/BAK* and the BH3-only subgroups, via association of the BH3 domain of the pro-apoptotic proteins with a hydrophobic groove on the surface of the pro-survival proteins (Sattler et al., 1997). These interactions, however, exhibit specificity. The affinities of BH3-only proteins for the pro- survival proteins differ markedly (Chen et al., 2005; Kuwana et al., 2005). *BIM, PUMA* and perhaps *TBID* show high affinity for *BAX/BAK,* whereas other BH3-only proteins show more selectivity. Hence, enforced expression of either *BIM* or *PUMA* potently kills cells, whereas Bad and *NOXA* can efficiently induce cell death only if co-expressed (Chen et al., 2005). *BAX* and *BAK* also differ in their interaction with the pro-survival proteins. *BAK* can be bound tightly by *BCL-XL* and *MCL-1* but only poorly by *BCL2* (Willis et al., 2005), whereas all the pro-survival proteins probably can constrain *BAX* activity (Willis et al., 2007).

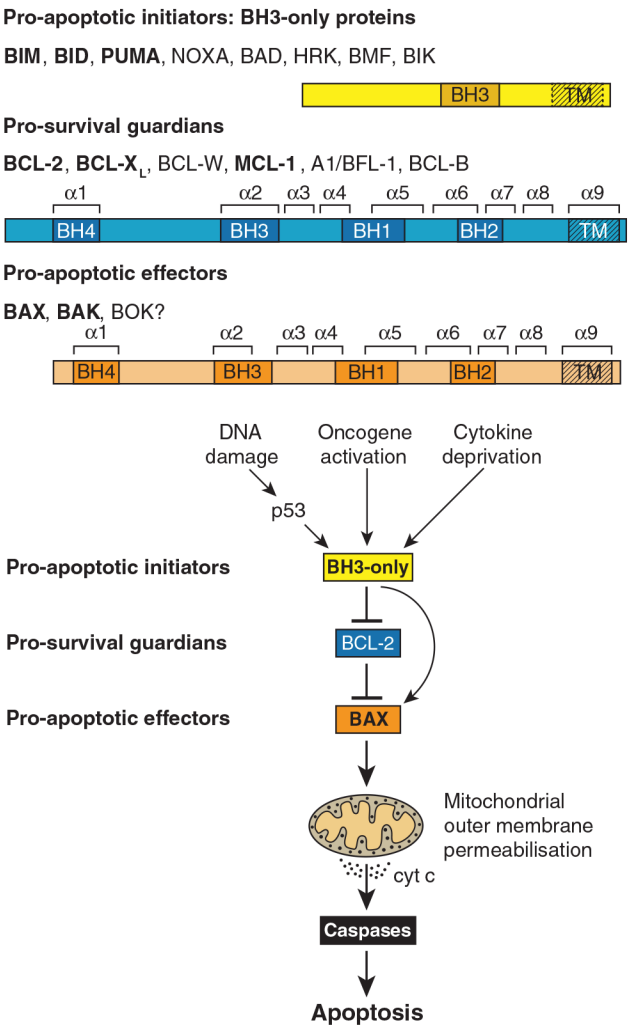

Figure 5.5 The BCL2 protein family.
The initiator, guardian and effector factions of the family. Domains of shared BCL2 Homology (BH), and the nine α-helices in the multi-BH domain members are indicated. (Effectors BAX and BAK, and the related BOK, have a BH4 domain if both structural and sequence homology are considered.29) BOK seems to drive apoptosis only in special circumstances. Faction members most important for controlling apoptosis are in bold. All multi-BH domain family members and some BH3-only proteins (BIM, BID, BIK, HRK) have a C-terminal transmembrane (TM) domain for anchoring to organelles, most notably the MOM. How the BCL2 protein family controls cell life and death is shown. In healthy cells, the pro-survival guardians prevent activation of BAX and BAK, at least in part by binding the BH3 domain (α2) of any destabilised BAX or BAK monomers. Various stress signals activate BH3-only proteins that avidly bind their pro-survival relatives, preventing their constraint of BAX or BAK. In addition, certain BH3-only proteins, namely BIM, cleaved (active) BID and probably PUMA, can directly activate BAX and BAK, which then homo-oligomerise and permeabilise the MOM, releasing cytochrome c to initiate caspase activation and cellular demolition. Modified from (Cory et al., 2016)

5.2.2 Physiological functions of *BCL2* family members

In healthy cells, proteins belonging to the *BCL2* family are involved in many physiological processes that also go beyond their apoptotic function. Thanks to the use of transgenic and gene-knockout mice, many studies have contributed to the understanding of the

biological functions of *BCL2* family members. In particular, overexpression of either *BCL2* (McDonnell et al., 1989; Sentman et al., 1991; Strasser et al., 1990b), *BCL-XL* (Grillot et al., 1995), *MCL-1* (Campbell et al., 2010; Zhou et al., 1998) or *A1* (Chuang et al., 2002) in lymphoid and other haemopoietic cells revealed to be protecting against diverse cytotoxic signals, both physiological (e.g. cytokine deprivation) or imposed (e.g. γ-irradiation, chemotherapeutic drugs). Notably, overexpression of pro-survival proteins in lymphocytes caused lymphadenopathy, which, in the case of *BCL2* and *MCL-1*, can progress at low (but significant) incidence to malignant lymphoma (Campbell et al., 2010; Egle et al., 2004; Korsmeyer et al., 1990; Strasser et al., 1993; Zhou et al., 2001). *BCL2* (but not *MCL-1*) overexpression can also provoke a fatal kidney disease similar to human systemic lupus erythematosus (SLE) (Egle et al., 2004; Strasser et al., 1990b; Zhou et al., 2001) establishing that apoptotic defects can promote autoimmune disease. Different cell types vary in their dependence on individual pro-survival proteins, presumably due to variable expression patterns and selectivity of interactions. For example, *BCL2*$^{-/-}$ mice developed a fatal polycystic kidney disease (PKD), due to the death of renal epithelial stem/progenitor cells in the embryonic kidney, premature greying due to death of melanocyte progenitors, and immunodeficiency due to B- and T-cell attrition (Veis et al., 1993). Remarkably, these degenerative disorders were eliminated by concomitant loss of *BIM* (in the case of PKD, even loss of a single *BIM* allele) (Bouillet et al., 2001), demonstrating that *BIM* and *BCL2* are the major mutually antagonistic regulators of the life/death switch in these cell types. The function of other *BCL2*-family members is discussed separately below.

- <u>*BCL-X*</u>: the cell types most affected by *BCL-X* loss include fetal erythroid progenitors, certain neuronal populations, male germ cells, immature ($CD4^+$ $CD8^+$) thymocytes, hepatocytes and platelets (Kasai et al., 2003; Mason et al., 2007; Motoyama et al., 1995). *Bcl-x*$^{-/-}$ mice die around E14–15 due to severe anemia and neuronal degeneration (Motoyama et al.,

1995) et al, 1995) and *bcl-x*$^{+/-}$ males have profoundly reduced fertility (Kasai et al., 2003). Interestingly, *Bim* loss restored fertility in *bcl-x*$^{+/-}$ males and prevented the erythroid attrition caused by complete *bcl-x* loss but did not rescue the neurons, so bim$^{-/-}$ *bcl-x*$^{-/-}$embryos still die around E15 (Akhtar et al., 2008). Thus, the *Bim–Bcl-xL* interaction determines the fate of erythroid progenitors and male germ cells, but *Bim* is not the sole BH3-only protein regulating neuronal survival.

- *MCL-1*: Loss of *MCL-1* has profound effects. Its complete loss caused pre-implantation embryonic lethality (Rinkenberger et al., 2000) and conditional deletion studies have shown that Mcl-1 is important for the survival of haemopoietic stem cells (Opferman et al., 2005), immature B and T lymphoid progenitors and their mature resting progeny (Opferman et al., 2003), activated germinal center B cells (Vikstrom et al., 2010) granulocytes and activated macrophages (Steimer et al., 2009), certain neuronal populations in the embryonic brain (Arbour et al., 2008) and hepatocytes (Vick et al., 2009).

- *BCL-W* and *A1*: *BCL-W* and *A1* may have more restricted roles. Although *BCL-W* is broadly expressed, its loss provoked noticeable defects only in adult spermatogenesis (Print et al., 1998; Ross et al., 1998) and in epithelial cells in the small intestine, which became more sensitive to DNA damage (Pritchard et al., 2000). The mouse has at least three expressed a1 genes, and loss of one of them (a1a) accelerated the apoptosis of granulocytes (Hamasaki et al., 1998) and mast cells (Xiang et al., 2001). Targeting all the *A1* genes might well reveal additional defects, since diverse stimuli induce *A1* expression in many cell types.

- *BAX* and *BAK*: studies with mice lacking either BAX, BAK or both have shown that their functions largely overlap. No abnormalities are discernible in *bak*$^{-/-}$ mice (Lindsten et al., 2000), except a modest rise in platelets (Mason et al., 2007), and *bax*$^{-/-}$ mice exhibit only mild lymphoid hyperplasia and male sterility, the latter because proper spermatogenesis requires the

death of excess testicular germ cells (Lindsten et al., 2000). In striking contrast, more than 90% of *Bax*$^{-/-}$*Bak*$^{-/-}$ compound mutant mice die perinatally for still unknown reasons. The few survivors exhibited several phenotypic abnormalities, including webbed feet, substantial neuronal and lymphoid cell accumulation, as well as profound resistance of their lymphocytes (and other cell types) to a broad range of apoptotic stimuli (Cheng et al., 2001; Lindsten et al., 2000). Perhaps surprisingly, several tissues in these *Bax*$^{-/-}$*Bak*$^{-/-}$ mutants such as the bladder, liver, heart and pancreas still developed and functioned normally (Lindsten et al., 2000), suggesting that another protein may be involved in the activation of the effector phase of apoptosis in some circumstances. One such candidate is BOK, a BCL2 family member showing >70% amino acid sequence homology to BAX and BAK

- BH3-only proteins: BH3-only proteins have distinctive physiological roles. For example, BIM, one of the most prominent players, is essential in many cell types for apoptosis induced by growth factor deprivation (Bouillet et al., 1999) and for the deletion of autoreactive thymocytes and immature B cells (Bouillet et al., 2002) (Enders et al., 2003). The *PUMA* and *NOXA* genes are both direct transcriptional targets of the tumor suppressor p53 (Vousden and Lane, 2007). Significantly, lymphocytes and certain other cell types from puma$^{-/-}$ mice are highly resistant to γ-irradiation and DNA damage-inducing chemotherapeutic drugs (e.g. etoposide) (Jeffers et al., 2003; Villunger et al., 2003), demonstrating that Puma is the major mediator of the p53 apoptotic response in those cells. No abnormalities appeared in *bik*$^{-/-}$ mice or cells (Coultas et al., 2004), but males lacking both BIM and BIK were infertile due to impaired apoptosis of immature testicular progenitor cells (Coultas et al., 2005) as in *bax*$^{-/-}$ males. The association of Beclin-1 with *BCL2*, *BCL-XL* or *MCL-1* reportedly blocks its ability to activate the PI3 kinase *VPS34* and trigger autophagy (Maiuri et al., 2007; Pattingre et al., 2005). Accordingly, a BH3-only protein of higher affinity (as most are), or a BH3 mimetic compound such as ABT-737 (see below), can displace Beclin-1 and allow autophagy. Beclin-

1 can also be freed by several other mechanisms (Kang et al., 2011) including mono-ubiquitination or phosphorylation of its BH3 domain.

Collectively, the above observations support the concept that the survival of most if not all cells in vertebrates relies upon one or more of the *BCL2*-like guardians. This is consistent with the view that death is the default for most cells unless they receive positive signals from other cells (Raff, 1992). Most likely, paracrine signals conveyed by growth factors and cell–cell or cell–matrix contacts promote the survival of most cell types by up-regulating various anti-apoptotic *BCL2* family members, as well as by curtailing expression and/or activity of particular BH3-only proteins (Youle and Strasser, 2008).

5.2.3 *BCL2* family and *MYC*-induced apoptosis

As described above, *MYC* is a potent inducer of apoptosis (Evan et al., 1992). In 1992 it was shown that *BCL2* expression specifically abrogates *MYC*-induced apoptosis without affecting its mitogenic function in Rat fibroblasts and Chinese hamster ovary (CHO) cells (Bissonnette et al., 1992; Fanidi et al., 1992). Most importantly, these findings provided a strong rationale for the cooperativity between *MYC* and *BCL2* in B cell lymphomagenesis, that had just been independently demonstrated in transgenic mice (Strasser et al., 1990b). Taking advantage of a mutant MYC proteins which retain its ability to stimulate proliferation and activate p53, but is defective at promoting apoptosis (because not able to induce BIM and effectively inhibit *BCL2)* it has been demonstrated that enforced expression of BCL2, thus abrogation of apoptosis, enables wild-type MYC to produce lymphomas as efficiently as mutant MYC (Hemann et al., 2005).

In a subsequent work BIM has been depicted as the primary regulator of *MYC*-induced apoptosis (using both *in vitro* and *in vivo* systems) (Muthalagu et al., 2014). Altogether, the

above studies provided fundamental insight into the oncogenic cooperation between *MYC* and *BCL2* family members, relevant to both carcinogenesis and the evolution of drug resistance in tumors.

5.2.4 Role of the *BCL2* family members in cancer

Many of the initial observations concerning *BCL2* and related proteins were made in the context of the lymphoid or other hematopoietic cells, or malignancies originating from these same compartments. Cloning of portions of the human *BCL2* gene was first reported by Tsujimoto et al who cloned the breakpoints from t(14;18) chromosomal translocations observed in non-Hodgkin lymphomas. Soon thereafter, *BCL2* was shown to prevent the death of cytokine-deprived haemopoietic cells in vitro and to cooperate with *MYC* in immortalization of lymphoid cells (Vaux et al., 1988) and in lymphomagenesis (Strasser et al., 1990b). This was the first identification of a gene that regulates cell survival (in any species) and the first evidence that evasion of apoptosis contributes to neoplastic transformation. *BCL2* transgenes linked to an Igh gene enhancer, mimicking the human t[14;18] translocation, produced plasma cell tumors and lymphocytic leukemias, but not follicular lymphoma (McDonnell and Korsmeyer, 1991; Strasser et al., 1993). Subsequently, however, a VavP-*BCL2* transgene expressed widely in the haemopoietic compartment did provoke follicular lymphoma, preceded by a huge germinal center hyperplasia dependent on CD4+ T cells, which also accumulated due to the high *BCL2* levels (Egle et al., 2004). These observations indicate that the *BCL2* translocation by itself can cause human follicular lymphoma directly or by chronic T-cell stimulation. Furthermore, the long latency of tumor development (McDonnell and Korsmeyer, 1991; Strasser et al., 1993) pointed to a need for additional oncogenic mutations.

MCL-1 and *BCL-XL* are also important players in tumorigenesis. *MCL-1* overexpression predisposes mice to diverse B cell lymphomas (Zhou et al., 2001) and, notably, haemopoietic

stem/progenitor cell tumors (Campbell et al., 2010). Also, Bcl-xL (Boylan et al., 2007; Cheung et al., 2004; Swanson et al., 2004) and Mcl-1 (Campbell et al., 2010) synergizes with *MYC* in the induction of lymphoma and plasmacytoma, and all the pro-survival family members accelerate *MYC*-induced myeloid leukemia (Beverly and Varmus, 2009). In humans, *MCL-1* expression is elevated in many cases of acute myeloid leukemia (AML) and multiple myeloma, and diverse cancers exhibit amplified *MCL-1* or *BCL-X* genes (Beroukhim et al., 2010).

Just as antiapoptotic *BCL2*-family proteins promote tumorigenesis, pro-apoptotic family members can function as tumor suppressors. *MYC*-induced lymphomagenesis in particular was accelerated by loss of either *BAX* (Eischen et al., 2001a), *BIM* (Egle et al., 2004), Puma (Garrison et al., 2008; Michalak et al., 2009), *BMF* or Bad (Frenzel et al., 2010), suggesting that all of these proteins contribute to *MYC*-induced apoptosis. *BAX* loss also accelerated brain tumor development in a transgenic model (Yin et al., 1997), and γ-irradiation-induced thymic lymphomagenesis was enhanced by loss of *NOXA* (Michalak et al., 2009), *BMF* (Labi et al., 2008) or both *BIM* and *BAD* (Kelly et al., 2010). Mice lacking both *BIM* and *PUMA* had enhanced lymphocyte accumulation and some spontaneously develop lymphoma (Erlacher et al., 2006). Importantly, loss or suppression of pro-apoptotic family members is also found in human cancer. *BAX* frameshift mutations appear in 50% of colon carcinomas in patients with a DNA mismatch repair defect, due to slippage during replication of an eight G run in the human *BAX* gene (Rampino et al., 1997). Moreover, 17% of mantle cell lymphomas have homozygous *BIM* deletions (Tagawa et al., 2005), and the *BOK* and *PUMA* genes have suffered allelic deletions in diverse cancers (Beroukhim et al., 2010). In many Burkitt lymphomas, *BIM* or puma are epigenetically silenced (Garrison et al., 2008; Richter-Larrea et al., 2010). Notably, *BIM* hypermethylation correlated with lower remission and shorter survival, (Richter-Larrea et al., 2010).

5.2.5 *BCL2* family members and upstream oncogenic pathways

Since a relatively small proportion of human malignancies carry abnormalities that directly affect genes of the *BCL2* or death receptor families, the survival of cells undergoing neoplastic transformation most likely often relies upon upstream oncogenic pathways that alter expression of *BCL2* family members. For example, gene expression databases show high *BCL2* levels in most human lymphoid malignancies, including not only follicular lymphoma (due to the t[14;18] translocation), but also B-chronic lymphocytic leukemia (CLL) and multiple myeloma. Notably, over half of B-CLL cases exhibit deletions or mutations in micro-RNAs (miR-15a, miR-16-1) that down-regulate *BCL2* mRNA (Iorio and Croce, 2009). Perhaps surprisingly, although *BCL2* overexpression enhances *MYC*-induced lymphomagenesis (Strasser et al., 1990b) and is required for sustained growth of such lymphomas (Letai et al., 2004), loss of endogenous *BCL2* does not impair *MYC*-induced lymphomagenesis (Kelly et al., 2010). Presumably, other pro-survival relatives sustain the pre-leukemic cells while they acquire the mutations allowing transformation and progression. In line with this notion, loss of even a single mcl-1 allele protected mice from developing *MYC*-induced AML (Xiang et al., 2001).

5.3 B cells

The production of B cells is a lifelong process starting in the fetal liver and continuing in the bone marrow (BM) in postnatal life: like all hematopoietic lineages, B cells originate from a pool of multipotent hematopoietic stem cells (HSCs) and undergo a characteristic, stepwise differentiation process (Figure 5.6) (Era et al., 1991; Hardy et al., 1991; Hardy and Hayakawa, 1991; Matthias and Rolink, 2005). Extensive research over the past decades has dissected B cell lymphopoiesis to great detail, which has allowed the identification of surface markers and molecular events, as well a high-resolution assessment of B cell function at defined steps of lymphopoiesis.

5.3.1 Early step of B cell development

HSCs are identified on the basis of a combination of surface markers as well as the absence of lineage-specific markers (Ikuta and Weissman, 1992; Li and Johnson, 1995). Stem-cell daughter cells give rise to lymphoid-primed multipotent progenitors (LMPPs), which, in turn, can give rise to either myeloid or lymphoid cells. LMPPs then produce common lymphoid progenitors (CLPs), which can generate T cells, B cells, natural killer (NK) cells, and dendritic cells (DCs) (Matthias and Rolink, 2005; Nagasawa, 2006).

B lymphopoiesis proceeds as a result of the concerted action of cytokines including *FLT3* (fms-related tyrosine kinase 3) and IL-7 released by stromal cells in the BM, and the instructive function of TFs including *PU.1* (DeKoter and Singh, 2000), *IKAROS* (Ng et al., 2009; Papathanasiou et al., 2009), E2A (Kwon et al., 2008); EBF1(Hagman et al., 1993) and PAX5 (paired box 5) (Cobaleda et al., 2007; Nutt et al., 1999).

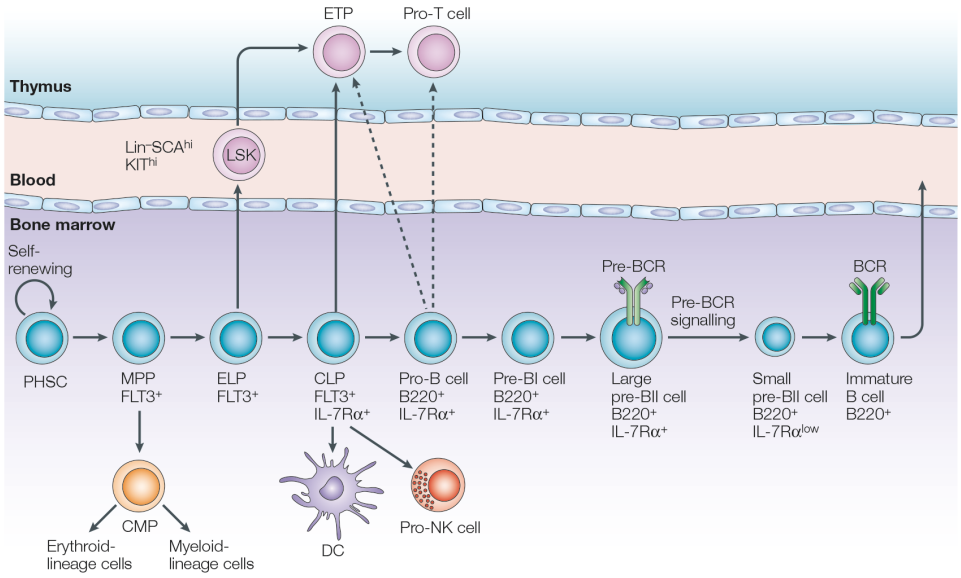

Figure 5.6 Schematic view of B cell development.
The main compartments — bone marrow, thymus and blood — are shown. The various developmental stages that have been defined are indicated, as well as their relative order. Pluripotent haematopoietic stem cells (PHSCs), multipotential progenitors (MPPs), common myeloid progenitors (CMPs), early lymphoid progenitors (ELPs) and common lymphoid progenitors (CLPs) are known as lineage (Lin)− cells; these cells lack detectable expression of any of the markers that are associated with cells of the mature blood lineages or their committed progenitors: that is, CD3, CD8, B220, CD11b, CD19, GR1 and TER119. Cells that are defined as LSK are Lin− stem-cell antigen (SCA)hiKIThi, which is a possible precursor stage to early T-cell-lineage progenitors (ETPs). B cell development is typically viewed as a linear progression through different stages of differentiation. The various steps in immunoglobulin (Ig) rearrangement and the pattern of expression of these surface molecules can be used to characterize stages in B cell development From (Matthias and Rolink, 2005).

5.3.2 VDJ recombination

During their differentiation from common lymphoid progenitors (CLPs), B cells (and T-cells) undergo rearrangements of their genetic material in order to establish a plethora of antigen receptors (one for each clonal population) which is necessary for their protective immune function. Each B cell is characterized by the expression of a B cell receptor (BCR) composed of membrane-bound immunoglobulin and the Igα/Igβ heterodimer (Figure 5.7). The Ig molecule consists of two polypeptide chains, a heavy (H) and a light (L) chain, each of which includes a variable (V) and a constant region (C). These chains form monomers which then combine into dimers, or higher-order oligomers to form a full Ig molecule. Both constant and variable regions contain domains from the heavy and light chains (Dreyer and Bennett, 1965). Functionally, the constant region confers effector properties such as complement binding, stable interactions with cellular Fc receptors (FcRs), and the class, or isotype, of the Ig. In both humans and mice, there are four IgG, or γ-chain isotypes that are important for the identification and clearance of many peptide and polysaccharide antigens (Ags) (Tonegawa, 1983). In contrast, the V region confers specificity to the Ig molecule by functioning as the direct contact between the Ig and its cognate antigen.

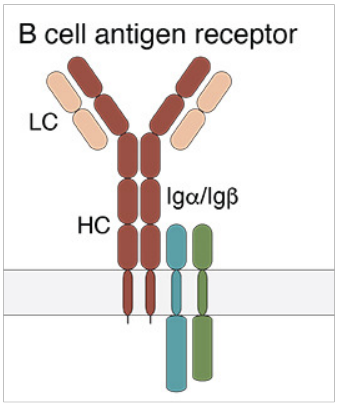

Figure 5.7 B cell receptor.
Schematic representation of a membrane bound immunoglobulin composed of two heavy chains and two light chains. Both the heavy chain and the light chain comprise a variable and a constant region.

The variable region of each receptor is generated by a gene rearrangement process called VDJ recombination. VDJ recombination joins together a unique variable (V), diversity (D) and joining (J) gene segment (only V and J segments for the Ig light chain of the BCR and the alpha chain of the TCR) in lymphoid precursors (Matthias and Rolink, 2005; Nagasawa, 2006). VDJ recombination is triggered by the product of the Recombination activation genes (Rag)-1 and -2. Rag proteins bind and cleave DNA at specific recombination signal sequences (RSSs) flanking each V, D and J gene segment (Figure 5.8). Through the action of Rag proteins V, D and J gene segments are brought in close proximity and joined ultimately by components of the classical non-homologous end joining (NHEJ) repair pathway (Figure 5.8).

VDJ recombination leads first to the assembly of an Ig Heavy (IgH) chain. A functional IgH chain expression interrupts further rearrangements at the second IgH locus (Bergman, 1999). This process is called allelic exclusion (Cedar and Bergman, 2008). Pairing of the IgH chains with surrogate Ig light (IgL) chains triggers clonal expansion of pre-B cells, which ultimately exit the cell cycle and complete IgL rearrangements. Pairing of functional IgH and IgL chains leads to the generation of immature B cells with surface expression of the B cell receptor (BCR). Productive assembly of IgH and IgL V-region exons allows the expression of IgH and IgL chains as cell-surface IgM by newly generated B cells. These cells are allowed to exit the BM and complete their differentiation to become mature B cells in secondary lymphoid organs where they can undergo further antigen-driven immunoglobulin-gene diversification through somatic hypermutation (SHM) and class-switch recombination (CSR) (Chaudhuri and Alt, 2004).

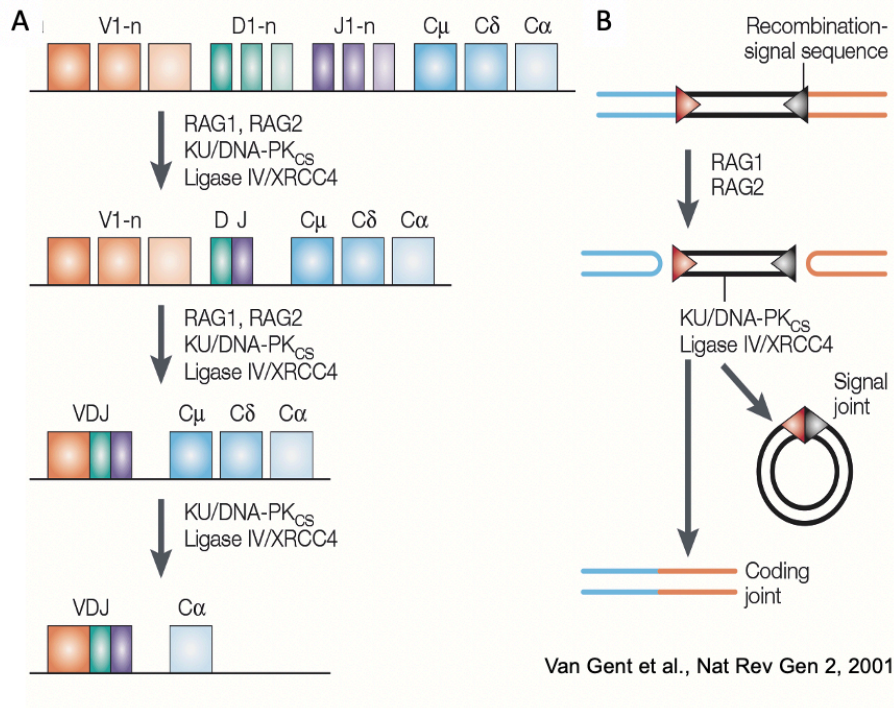

Figure 5.8 The process of VDJ recombination.
A: For successful VDJ recombination a concerted action of Rag proteins with DSB recognition and repair proteins is necessary. First a D segment is coupled to a J segment, which is followed by a V segment joining to the DJ assembly, to give rise to a functional Ig heavy chain gene. **B:** The mechanism of VDJ recombination initiates with Rag proteins inducing a DSB at the RSS. This leads to deletion of the nicked DNA sequence. Subsequently, the DSB is repaired by the NHEJ machinery (Ku70/80, DNA-PKs, DNA ligase IV and Xrcc4). Modified from

5.3.3 Peripheral B cell development

Immature B cells in the spleen, also called ttransitional B cells, are the first B cells to exit from the BM. They are divided in two main subsets, based on the expression of the CD23 surface marker and IgM: T1 cells ($B220^{lo}IgM^{+}CD23^{-}$) are the earliest BM emigrants and include a fraction of self-reactive B cells committed to death (Carsetti et al., 1995; Pillai et al., 2004); T2 cells ($B220^{lo}IgM^{high}CD23^{+}$) derived from T1 cells and are direct precursors of long-lived mature B cells. The three major mature B cell subsets are follicular (FO) ($B220^{+}CD21^{int}CD23^{+}$), marginal zone (MZ) ($B220^{+}CD21^{high}CD23^{lo}$) and B1 B cells ($B220^{+}CD21^{low}CD23^{low}$). MZ and B1 B cells are not part of the adaptive immune response but have an important role in the production of antibodies, as they respond fast to T-cell independent antigens by differentiating into low-affinity antibodies secreting plasma cells

(Song and Cerny, 2003). On the other hand, FO B cells are the main players in T-cell dependent antigen responses and, once exposed to a T-cell dependent antigen, form germinal centers (GCs) in which they undergo affinity maturation.

5.4 The Germinal Center

Germinal Centers (GCs) are dynamic micro-anatomical structures in which B cells capable to produce high affinity antibodies are generated, selected and expanded further (Basso and Dalla-Favera, 2015). This process (called the GC reaction) happens upon the concurrent encounter of naïve B cells with antigen-presenting cells and CD4+ T-cells, resulting in B cell activation (Victora and Nussenzweig, 2012). Histologically, GCs are composed by two topologically distinct zones: the so-called dark zone (DZ), which consists of densely packed highly proliferating B cells referred to as centroblasts and the light zone (LZ), consisting mainly of non-dividing centrocytes (Allen et al., 2004; MacLennan, 1994; McHeyzer-Williams et al., 2009; Victora et al., 2010) (Figure 5.9). These compartments are characterized by the differential expression of a series of surface markers such as the CXC-chemokine receptor 4 (CXCR4), CD83 and CD86: in particular, $CXCR4^{hi}CD83^{low}CD86^{low}$ and $CXCR4^{low}CD83^{high}CD86^{high}$ profiles define DZ and LZ zone B cells, respectively (Allen et al., 2004; Caron et al., 2009; Victora et al., 2012; Victora et al., 2010). A large body of work has revealed that the DZ and LZ are the sites of specific, inter-dependent processes that determine the highly dynamic nature of the GC reaction (Figure 5.9) and will be synthetically described here.

In the DZ, highly proliferating CBs undergo diversification of their Ig V gene repertoire through a process called somatic hypermutation (SHM). As a result, clonally-related GC B cells express BCRs with different affinities to the antigen (Wagner and Neuberger, 1996). These cells migrate to the light zone to become CCs, where they establish intimate contacts

with antigen-presenting FDCs and undergo affinity-based selection (Allen et al., 2007; Schwickert et al., 2007). Indeed, GCBs are highly susceptible to undergo apoptosis (Liu et al., 1989; MacLennan, 1994), as they lack expression of most anti-apoptotic factors (Klein et al., 2003; Liu et al., 1989; MacLennan, 1994) and instead express high levels of several pro-apoptotic proteins, such as the death receptor CD95 (FAS) (MacLennan, 1994; Martinez-Valdez et al., 1996). Since FDCs expressed the cognate ligand CD95L (FASL) (Verbeke et al., 1999), the LZ provides a highly pro-apoptotic environment, ensuring the rapid demise of GCBs, unless rescued by survival signals emanating mainly from BCR engagement. As a result of this process, only few CCs expressing high-affinity BCRs succeed to bind the antigen and to receive the necessary co-stimulatory survival and differentiation signals by a limiting number of T_{FH} cells (McHeyzer-Williams et al., 2009; Schwickert et al., 2007; Victora et al., 2010).

Besides their role in affinity-selection, T_{FH} cells also release cytokines that induce GCBs to undergo class switch recombination (CSR, also called isotype switching), a process that leads to the replacement of the initial IgM constant region with that of another class, including IgG3, IgG1, IgG2a, IgG2b, IgE and IgA (Chaudhuri and Alt, 2004). As a result of isotype switching, the effector function of the encoded Ig molecules is modified, resulting in the production of the various classes of secreted antibodies (Stavnezer and Amemiya, 2004). Most noteworthy here, recent work demonstrated that naive B cells undergo CSR upon interacting with antigen and receiving T cell help prior to GC entry, and thus before undergoing somatic hypermutation (Roco et al., 2019): as a result CSR is a relatively rare event in GCs, limiting the occurrence of pathogenic double-strand breaks and recombination events.

The signals received by antigen-selected GC B cells upon interaction with T_{FH} cells promote differentiation into long-lived antibodies secreting cells (ASCs) (Radbruch et al.,

2006). A fraction of GC–derived ASCs home to the BM where they eventually mature into long-lived plasma cells (PCs). PCs provide a lifelong resource of high-affinity antibodies while memory B cells instead are long-lived surface Ig^+ B cells, which re-circulate in the blood and get preferentially recruited into secondary immune responses, during which they undergo either terminal differentiation into PCs or additional rounds of SHM and selection within the GC to generate a new pool of memory B cells, with even higher affinity for the antigen (Radbruch et al., 2006).

The segregation of proliferation and hypermutation in the DZ from antigen-driven selection in the LZ requires that cells migrate between these two zones for affinity maturation to occur, and early studies proposed that iterative cycles of SHM followed by selection (in DZ and LZ, respectively) would be required to achieve the degree of affinity maturation observed in vivo, a framework known as cyclic re-entry (Kepler and Perelson, 1993; Oprea and Perelson, 1997). According to this model, now widely accepted in the field, a fraction of LZ B cells with improved affinity is allowed to re-enter the DZ for further rounds of proliferation and SHM; indeed, studies have provided experimental evidence for the re-entry of selected B cells from LZ to DZ upon antigen-driven selection (Allen et al., 2007; Gitlin et al., 2014; Schwickert et al., 2007; Victora et al., 2010).

Further studies led to the unraveling of additional complexity within the GC compartments. In particular, two parallel studies addressed the role of the transcription factor Foxo1 in GC B cells (Dominguez-Sola et al., 2015; Sander et al., 2015): deletion of a loxP-flanked allele of Foxo1 in GC B cells results in "DZ-less" GCs, in which all B cells display a LZ surface phenotype ($CXCR4^{low}CD86^{hi}$), suggesting that Foxo1 is essential for the proliferating GC in the DZ. Finally, recently published data proposed a separation of the GC into three different cell populations trough a multidimensional analysis (Kennedy et al., 2020):

in particular, the authors proposed that following selection in the LZ, B cells migrated to specialized sites within the canonical DZ that contained tingible body macrophages and were sites of ongoing cell division. Proliferating DZ (DZp) cells then transited into the larger DZ to become differentiating DZ (DZd) cells before re-entering the LZ. Altogether, we surmise that the GC might be constituted by a continuum of cell states that await more accurate description, in partucular at the phenotypic and transcriptional levels.

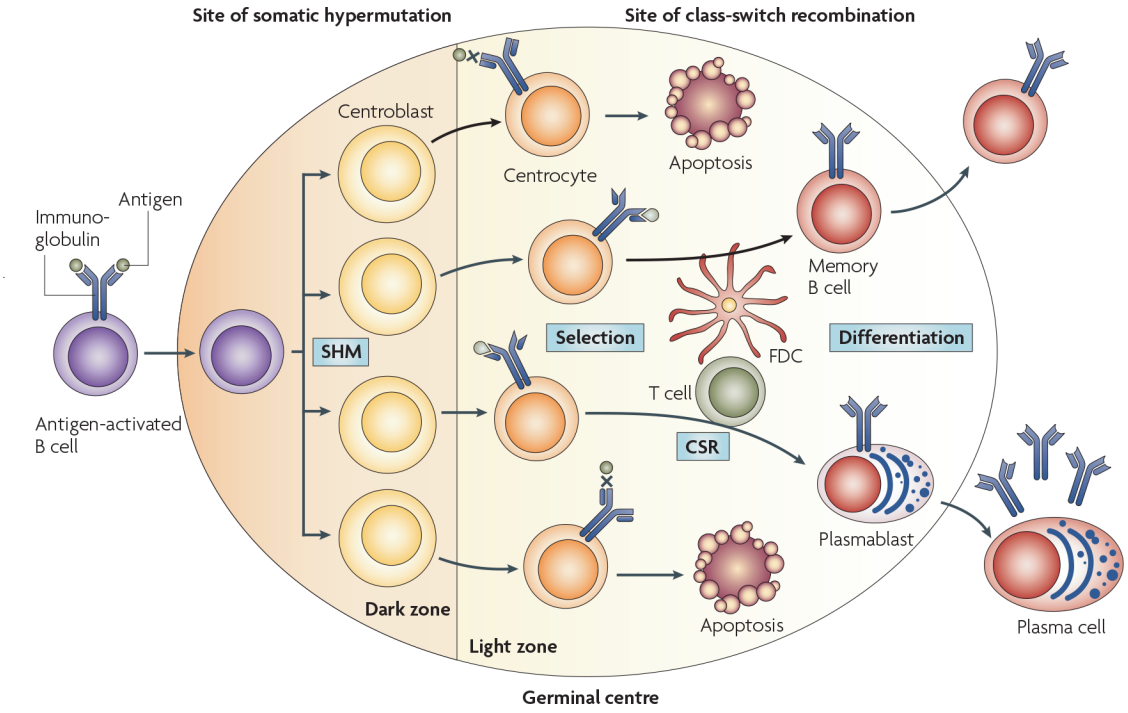

Figure 5.9: Schematic view of the GC reaction.

During T cell driven immune response, FO B cells enter the GC reaction. GC reaction is characterized by massive B cell proliferation coupled to Ig gene mutations (SHM) followed by selection of high-affinity BCR expressing B cells (FDCs present antigen on their surface and together with TFH cells provide survival signals to B cells upon antigen recognition). Low-affinity or non-functional Ig expressing B cells undergo apoptosis. GC B cells switch their isotype from IgM to IgG1 (during CSR) and undergo terminal differentiation towards PCs or memory B cells Modified from: (Klein and Dalla-Favera, 2008).

5.4.1 Role of *MYC* in the GC

MYC plays a central role in the maintenance and regulation of physiological B cell proliferation, differentiation, and apoptosis (Bisso et al., 2019; Meyer and Penn, 2008). In particular, *MYC* expression is required for the survival, proliferation and proper differentiation

of B cell precursors into mature B cells (de Alboran et al., 2001; Huang et al., 2008; Sabo et al., 2014b; Tesi et al., 2019a; Vallespinos et al., 2011). Instead, a role of *MYC* in GCs has been controversial in the field: although some studies reported increased *MYC* expression in human and mouse GC B cells compared to other cells type (Cutrona et al., 1997a, b; Martinez-Valdez et al., 1996), others refuted these observations, detecting only low or absent *MYC* expression in these cells (Klein et al., 2003; Shaffer et al., 2001). However, two seminal studies in 2012 showed that that *MYC* is expressed in a fraction of GC B cells, and is essential for the GC reaction (Calado et al., 2012; Dominguez-Sola et al., 2012). In particular, *MYC* acts in a bimodal way during the GC reaction: its expression is induced in LZ upon GC B cells upon stimulation, it is transcriptionally repressed in DZ B cells and it is re-expressed in a subset of LZ B cells that are going to re-enter in the DZ. The role of *BCL6* deserves further attention here: in particular, during normal GC reaction, signals such as *IRF4* and *BCL6* itself, negatively regulate *BCL6* activity (Hatzi and Melnick, 2014).This would thus allow *MYC* to escape *BCL6* repression during the first rounds of cell division that will give rise to the bulk of GC B cells. The transient nature of these signals, and the decreasing number of positive selection events found in GC as they mature, would explain why *MYC* is not detectable in the majority of 'mature' GC B cells (Dominguez-Sola et al., 2012). The differential expression patterns of *MYC* and *BCL6* in the LZ and DZ compartments were recently confirmed through single-cell transcriptional profiles (Milpied et al., 2018). Hence, *MYC* and *BCL6* expression are mutually exclusive. Despite this, a small fraction of GC B cells (nearly 10%), is positive for the expression of both proteins (Calado et al., 2012; Dominguez-Sola et al., 2012). This could be explained by the presence of cells that transit in either direction between dark and light zone, but can also open the possibility of further layers of regulation, such as the inhibition of *BCL6* activity by acetylation (Bereshchenko et al., 2002). In a recent study (Kennedy et al., 2020), *MYC* locus specific enhancers were shown to be open in LZ B cells, correlating with deposition

of active enhancer epigenetic marks (H3K4me1^{+}H3K27Ac^{+}). Consistent with this, *MYC* mRNA abundance was highest in LZ B cells. A phosphorylated form of *MYC* was detected in both the LZ and a newly distinguished, proliferating "DZp" subset, the latter also showing highest expression of a *MYC*-dependent downstream program (Kennedy et al., 2020). Hence, this data provide a model in which *MYC* transcriptional activation in LZ B cells would be followed by phosphorylation and stabilization of *MYC* in DZp cells and execution of the *MYC*-dependent program (De Silva and Klein, 2015). In addition, in very recent publications, the turnover between DZ proliferation and LZ affinity selection of GC B cells is specifically regulated by the cell cycle regulator cyclin D3 expression (Ramezani-Rad et al., 2020) Pae et al., 2020 BioRxiv. Accordingly to one of these models, B cell receptor (BCR) stimulation of GC B cells downregulates cyclin D3 but induces c-Myc, which subsequently requires cyclin D3 to exert GC expansion (Ramezani-Rad et al., 2020). Altogether, the aforementioned data support a still open scenario in which *MYC* is induced by costimulatory signals in GC B cells and is required for the proliferative response to these signals, albeit in a spatially and temporally distinct manner.

5.5 *BCL2* in the GC

BCL2 is normally transiently expressed during B cell maturation (Menendez et al., 2004). Early studies showed that overproduced *BCL2* prevents the death of B cells cultured in vitro (Nunez et al., 1990; Strasser et al., 1991) and its expression decrease in germinal center B cells (Pezzella et al., 1990). In a later study, constitutive expression of a *BCL2* transgene (Eμ-bcl2-36) in B cells led to increased survival of germinal center cells which, in turn, revealed alterations in the selection process of memory B cells. In contrast, bone marrow AFCs are subjected to a stringent selection which is not influenced by the *BCL2* transgene.

This is consistent with the affinity threshold required by GC B cells for the selection into the plasma cell differentiation path (Smith et al., 2000).

5.5.1 *BCL2* deregulation in GC lymphomas

As explained above, GCs represent critical sites within lymphoid tissues, where B cell responses to antigen are amplified and refined through the mechanism of affinity maturation. 25% of DLBCL cases is carrying a *BCL2* t(14;18) translocation in (Iqbal et al., 2004; Willis and Dyer, 2000). The t(14;18) chromosomal recombines *BCL2*, located at 18q21, with the immunoglobulin (Ig) H-chain joining region (JH) at 14q32 (Hua et al., 1988). GC entry of naive B cells with t(14;18)(q32;q21) translocation is assumed to be a key step in the onset of follicular lymphoma (FL) by allowing *BCL2*-driven rescue of B cells with low-affinity receptors, and accumulation of developmentally blocked GC B cells (Roulland et al., 2011). The accumulation of activated GC B cells localized in the reactive follicle increase the chances to acquire other oncogenic hits thus promoting progression of the malignancy and its gradually spreading to distant lymphoid organs, including BM, to eventually manifest as a systemic disease (Swerdlow et al., 2016).

The tumorigenic potential of *BCL2* has been studied in different transgenic mouse models (McDonnell et al., 1989; McDonnell and Korsmeyer, 1991; Strasser et al., 1993; Strasser et al., 1990b). In these studies, enforced expression of *BCL2* was found to increase the risk of the risk of B-lymphoid neoplasia, but the incidence was low, and the tumors were pre-B lymphomas, immunoblastic lymphomas, and plasmacytomas rather than follicular lymphomas. The *VavP-Bcl2* transgenic mice (Ogilvy et al., 1999) is engineered to overexpress *BCL2* in cells of all hematopoietic lineages. These mice are highly predisposed and develop a disease with typical features of follicular lymphoma, including enlarged lymphoid organs. Since these cells accumulate in such large numbers in the spleen, they hypothesize that *BCL2* overexpression

led to inefficient exit from the germinal center reaction and a prolonged permanence time in this state. Cells within this population would presumably have an increased probability of acquiring additional somatic mutations, including oncogenic mutations. Altogether, these data describe the dysregulation of *BCL2* as a principal event prior to the expansion of a precursor population for follicular lymphoma.

5.6 Diffuse large B cell lymphoma (DLBCL)

Diffuse large B cell lymphoma (DLBCL), a member of the diverse group of mature B cell lymphomas, represents the most common type of aggressive B-NHLs in the US and Europe (Sant et al., 2010). A fundamental step in the classification of DLBCL is the transcriptome-based recognition of the cell of origin, as either germinal center B cell (GCB), or activated B cell (ABC); this feature is now routinely monitored in the clinic, using IHC or mRNA profiling (Scott et al., 2015; Scott et al., 2014; Swerdlow et al., 2016; Wright et al., 2020). This subdivision has proven prognostic value and correlates with significant differences in the molecular pathogenesis of the tumors. Recent studies also have shown that ABC compared with GCB lymphomas exhibit differential sensitivity to certain drugs such as the immune/chemo-therapeutic regimen R-CHOP, consisting of rituximab plus cyclophosphamide, doxorubicin, vincristine, and prednisone (Roschewski et al., 2014). Recent studies have integrated mutational clustering methodologies and allowed the classification of DLBCL subsets (Chapuy et al., 2018; Schmitz et al., 2018). However, there is a limit in clustering methods. For example, the necessity to assign tumor samples to no more than single subtype could result in a wrong classification given the high heterogeneity of DLBCL genetic aberrations; moreover, the fact that the subtype assignment of a particular tumor can vary when different tumors are included during the clustering process could make the result less reliable. In order to overcome this limitation, a recent work developed an algorithm based probabilistic study that allowed the identification of seven DLBCL genetic subtypes that differ with respect

to oncogenic pathway engagement, gene expression phenotype, tumor microenvironment, survival rates, and potential therapeutic targets (Wright et al., 2020). Among all these DLBCL classifications, DHL deserves particular attention here, and will be discussed separately in the next section.

5.7 Double-hit Lymphoma

The term DHL commonly refers to a subset of DLBCLs that present concurrent rearrangements of *MYC* and *BCL2* (less commonly, *BCL6*). *MYC* and *BCL2* activation, are initiating events in Burkitt's (BL) and Follicular Lymphoma (FL), respectively, but also occur in other subtypes, such as DLBCL (Rosenquist et al., 2017; Scott et al., 2018). While direct information is generally missing on the order of activation events, complex translocations can occur that simultaneously hit both oncogenes (Dyer et al., 1996). Progression from the *BCL2*-translocated indolent form of FL to the transformed stage (tFL) is associated in ca. 25% of cases with secondary translocation of *MYC* (Dyer et al., 1996; Pasqualucci et al., 2014; Rosenquist et al., 2017; Scott et al., 2018). Regardless of their specific history, the resulting "double-hit" lymphomas (DHL) are highly aggressive malignancies with dismal prognosis in the face of current front-line therapies (Friedberg, 2017). At the morphological level, most DHLs show intermediate features between DLBCL and Burkitt lymphoma: cells are derived from the GC, are medium-sized, with a very high proliferation rate (Le Gouill et al., 2007; Momose et al., 2015). DHL represents 5%-10% of DLBCL patients (Anderson et al., 2016; Burotto et al., 2016; Friedberg, 2017; Rosenthal and Younes, 2017; Roulland et al., 2011; Sarkozy et al., 2015; Sesques and Johnson, 2017).

The most recent revision of the WHO classification defined high-grade B cell lymphoma with MYC and BCL2 and/or BCL6 chromosomal rearrangements (HGBL-DH/TH) (Swerdlow et al., 2016) a subset comprising tumors with either DLBCL or high-grade B cell

lymphoma features. Approximately 8% of tumors with DLBCL morphology are HGBL-DH/TH, and all HGBL-DH/TH with BCL2 translocations of DLBCL morphology belong to the GCB molecular subgroup. In contrast, Double Expressor Lymphomas (DEL) tends to be ABC cell of origin (Friedberg, 2017). Recently, a subgroup of GCB DLBCL has been identified by a distinct DHIT gene expression signature. (Ennishi et al., 2019; Sha et al., 2019). DHITsig-positive patients had inferior outcomes after R-CHOP therapy compared with DHITsig-negative patients (5-year time to progression rate, 57% and 81%, respectively;), irrespective of HGBL-DH/TH-BCL2 status (Ennishi et al., 2019). Indeed, only half of tumors belonging to the DHITsig-positive harbored MYC and BCl2 rearrangements (Ennishi et al., 2019). Altogether, the poor outcome after standard chemoimmunotherapy of DEL but especially of High-grade B-cell lymphoma with MYC and BCL2 and/or BCL6 rearrangements (HGBL-DH/TH) as well as the presence of other aggressive lymphomas which did not score as DHL, called for a deep study of their biological/molecular characteristics to efficiently guide patients management

5.7.1 Mouse models of DHL

The cooperativity between *MYC* and *BCL2* in lymphomagenesis was demonstrated in 1990 (Strasser et al., 1990a) and was confirmed multiple times since then, based on various combinations of transgenic mouse strains and/or gene-transfer experiments in either mouse or human cells (Hemann et al., 2005; Leskov et al., 2013; Letai et al., 2004; Marin et al., 1995; McDonnell and Korsmeyer, 1991; Ortega-Molina et al., 2015; Schmitt et al., 2002; Schuster et al., 2011). Strasser and colleagues, demonstrated that double-transgenic mice expressing both *BCL2* and c-myc under the control of the immunoglobulin enhancer (Eμ) develop an immature lymphoblastic leukemia within few days of birth. Mice show hyperproliferation of pre-B and B cells and develop tumors much faster than Eμ-myc mice. Suprisingly, the tumors derive from

a cell with the hallmarks of a primitive haemopoietic cell, perhaps a lymphoid-committed stem cell (Strasser et al., 1993). Later on, thanks to the generation of mice expressing a conditional *BCL2* gene and constitutive c-myc and developing lymphoblastic leukemia, it was demonstrated that eliminating *BCL2* yielded rapid loss of leukemic cells and significantly prolonged survival, formally validating *BCL2* as a rational target for cancer therapy (Letai et al., 2004). In 2011, a humanized mouse model of *MYC*/*BCL2*-driven DHL was generated by engrafting human HSCs transduced with both oncogenes into immunodeficient mice. This humanized-*MYC*/*BCL2*-model (hMB) recapitulates some of the histopathological and clinical features of steroid-, chemotherapy- and rituximab-resistant human DHL (Leskov et al., 2013).

In all of the aforementioned models, the resulting tumors did not arise from GC B cells as in human DHL, but rather from earlier stages of B cell differentiation (Leskov et al., 2013; Letai et al., 2004; Strasser et al., 1990a). Hence, the pre-clinical models available so far suffer from major limitations, failing to reproduce the correct developmental stage of the human tumors. In recent work, Caeser et al. circumvented this limitation by direct transduction of both oncogenes in human GC B cells followed by xenografting in immune-deficient mice (Caeser et al., 2019).

Altogether, the available models of DHL suffer from a series of limitations: on one hand, xenograft-based models, while allowing to test drugs that are toxic to tumor cells, do not allow us to assess the contribution of the immune system and/or immune-targeted therapies. On the other, while the cooperative action of *MYC* and *BCL2* in B cell lymphomagenesis was documented multiple times in immune-competent mice, the tumors obtained in these models were composed of primitive lymphoid rather than GC B cells and no mouse model was described that would faithfully reproduce the GC origin, differentiation stage and cellular phenotype of human DHL.

5.8 Aim of the project

The occurrence of various B cell lymphoma (BCL) subtypes is associated with chromosomal translocations that occur at the Germinal Center (GC) stage and involve characteristic proto-oncogenes such as *MYC* and *BCL2.* In a subset of diffuse Large-B Cell Lymphomas (DLBCL), concurrent *MYC* and *BCL2* translocations accumulate and give rise to particularly aggressive double-hit lymphomas (DHL), which show dismal prognosis in the face of current front-line therapies. In this scenario, a mouse model that accurately recapitulates the human disease is fundamental in order to fully understand the biology of this disease and to develop pre-clinical studies.

Although the cooperativity of *MYC* and *BCL2 in* lymphomagenesis has been described in multiple transgenic models, the resulting tumors did not arise from GC B cells, but rather from earlier stages of B cell differentiation. Other models were based on xenografting, not allowing to assess the contribution of the immune system and/or immune-targeted therapies. Hence, the field still lacks an immune-competent mouse model that would faithfully recapitulate the cellular origin and physio-pathological features of human DHL.

On this basis, the general aim of our project was to determine whether specific GC activation of *MYC* and *BCL2* could result in the development of a better DHL model. In order to investigate this scenario, we took advantage of the Germinal Center (GC)-specific transgene Cγ1-*Cre* and conditional *lox-stop-lox(lsl)-MYC* and *lsl-BCL2* alleles, that we combined to concomitantly activate both oncogenes in GC B cells.

The specific aims of the project were the following:

I. to phenotypically characterize DHL-tumors developed upon activation of *MYC* and *BCL2* in GC B cells;
II. to evaluate the consequences of the activation of *MYC* and/or *BCL2* in cell undergoing the GC reaction;
III. to profile transcriptional programs in DHL and compare them with the profiles of human B-cells and lymphomas;

6 Material and methods

6.1 Mice

R26-lsl-CAG-MYC-ires-hCD2 mice (Calado et al., 2012) were purchased from Jackson Laboratory (Maine; Stock No.: 020458). With the aim to obtain a mouse model that reflects the GC origin of human DHL, we combined the Cγ1-*Cre* transgene(Casola et al., 2006), expressing the *Cre* recombinase specifically in GC B-cells, with the *Cre* -inducible alleles R26-CAG-lsl-MYC-IRES-hCD2 (*MYC*) (Calado et al., 2012; Sander et al., 2012) and R26-lsl-BCL2-IRES-GFP (*BCL2*) (Knittel et al., 2016) that allow the overexpression of *MYC* and *BCL2* respectively. We then generated experimental cohorts by transplanting lethally irradiated RAG1 mice with bone marrow from transgenic donors, and monitored tumor development in reconstituted animals. For tumor-free survival analysis, Cγ1- *Cre* ; R26-lsl-MYC-IRES-hCD2 ; R26-lsl-BCL2-IRES-GFP (henceforth Cγ1- *Cre; lsl-MYC; lsl-BCL2*) mice were monitored three times per week and euthanized when showing wight loss equal or greater than 10% of the initial body weight, indicative of illness attributed to tumor formation. Infiltrated spleen or liver were dissected and either processed freshly or frozen and stored at −80°C until further analysis. NSG mice (purchased from Charles River Laboratories, Calco, Italy) were injected intravenously with 3×10^6 DHL cells and monitored until lymphoma onset. Experiments involving animals were done in accordance with the Italian Laws (D. lgs. 26/2014), which enforce Dir. 2010/63/EU (Directive 2010/63/EU of the European Parliament and of the Council of September 22, 2010 on the protection of animals used for scientific purposes) and authorized by the Italian Minister of Health with project 602/2018 PR.

6.1 Genotyping

Genomic DNA was extracted from tail biopsies by overnight digestion in lysis buffer (100 mM TrisHCl pH 8. 5,5 mM EDTA pH 8, 0, 2% SDS, 0,2 M NaCl and 0,1 mg/ml freshly

added Proteinase K) at 55°C, followed by heat inactivation (5 minutes at 100°C) and dilution with 10 volumes of water, and then used to evaluate offspring genotype by semi-quantitative PCR (GoTaq® G2 Hot Start Polymerase, #M7408). The primers used for genotyping are listed in Table 1.

	species	Amplicon	Forward sequence	Reverse sequence
Genotyping	mouse	$R26^{wt}$	GGAGTGTTGCAATACCTTTCTGGG AGTTC	TGTCCCTCCAATTTTACACCTGTTCAA TTC
		R26-lsl-CAG-MYC	ACAACCGAAAATGCACCAGC	TCACATTGCCAAAAGACGGC
		CG1-CRE	GGTGGCTGGACCAATGTAAATA	GTCATGGCAATGCCAAGGTCGCTAG
		R26-lsl-CAG-BCL2	GCAGGAAGCACTTGCTCTC	CGACAAGGCGTCTAGTTTATGTG
		$CD19\text{-}CRE^{wt}$	CCAGACTAGATACAGACCAG	AACCAGTCAACACCCTTCC
		$CD19\text{-}CRE^{-}$	CCAGACTAGATACAGACCAG	TCAGCTACACCAGAGACGG

Table 1: List of primers.

6.2 In vivo procedures

6.2.1 Whole-body irradiation

RAG1 mice were irradiated one day before being transplanted with Cγ1- *Cre; lsl-MYC; lsl-BCL2* BM at 7.5 Gy in order to ablate the immune system. Upon irradiation, mice were supplied with neomycin-treated water (2mg/mL) for 2 weeks.

6.2.2 Immunization

60 days after transplantation, mice were immunized by treatment with sheep red blood cell (SRBC) in order to boost the germinal center reaction. A certain volume of SRBC (depending on the amount of mice that need to be immunized) has been taken from the stock, diluted in 50mL of PBS and spin at 2500 RPM for 5 min at 4 °C. This wash has been repeated for 3 times.

After the third wash cells have been resuspended in 3-5 mL of cold PBS to aliquot and count cells by performing 1:10, 1:100 and 1:1000 serial dilution. The concentration has been adjusted with PBS at the final 10^9/0,3 mL. Cells have been then injected IV 300µl/mouse (10^9 SRBC/mouse).

6.2.3 Transplants

Bone marrow cells

0.5-1 x 10^6 BM cells counted directly from the bone marrow suspention resuspended in 0.3 ml of PBS and were injected intravenously in RAG1 mice (purchased from Charles River Laboratories). Animals were monitored by weight measurements, and sacrificed when the weight loss was equal or greater than 10% of the initial body weight.

Lymphoma cells

0.5-1 x 10^6 lymphoma cells were counted directly from the spleen suspension, resuspended in 0.3 ml of PBS and injected intravenously in either C57BL/6 mice (purchased from Charles River Laboratories) or NSG mice. Animals were monitored by weight measurements, and sacrificed when the weight loss was equal or greater than 10% of the initial body weight.

6.3 Western Blot

Protein extraction was performed resuspending cells in Lysis buffer (300 mM NaCl, 1% NP-40, 50 mM Tris-HCl pH 8.0, 1 mM EDTA) with freshly added protease inhibitors (cOmplete™ Mini Protease Inhibitor Cocktail, #11836153001 Roche-Merck) and phosphates inhibitors (PhosSTOP™, #4906845001, Roche-Merck). Cell lysates were then sonicated for 10 seconds, cleared by centrifugation at 13000 rpm for 20 minutes at 4°C and quantified by

Bradford assay (Bio-Rad Protein Assay, #5000006). Upon addition of 6X Laemmli buffer (375 mM Tris-HCl, 9% SDS, 50% glycerol, 9% β-mercaptoethanol and 0.03% bromophenol blue), lysates were boiled 5 minutes at 100°C and then analysed on 4-15% gradient pre-casted polyacrylamide gel (Bio-Rad, #5678084). Proteins were then transferred to a methylcellulose membrane (Bio-Rad, #1704271) for 30 min at 0.3 A with a Trans-Blot® SD Semi-Dry Transfer apparatus (BioRad, #1704150). Membranes were then washed in TBS-T (10 mM Tris-HCl, 100 mM NaCl, 0.1% Tween at pH7.4) and blocked with 5% milk in TBS-T for 30 minutes, and incubated over-night at 4°C with the indicated primary antibodies (Table 2). Next day membranes were washed three times for 5 minutes with TBS-T and then incubated at room temperature for 1 hour with the proper secondary antibodies. After three washes in TBS-T, chemiluminescence was detected using a CCD camera (ChemiDoc XRS+ System, Bio-Rad) using Calrity™ Wester ECL substrate (Bio-Rad, #1705060).

Target	Clone	Company	Dilution
c-MYC (Y69)	ab32072	Abcam	1:3000
HRP-conjugated goat-anti-mouse IgG	170-6516	Biorad	1:10000
HRP-conjugated goat-anti-rabbit IgG	170-6515	Biorad	1:10000

Table 2. Antibodies used for Western blotting.

6.4 Primary lymphoma cell lines and treatments

Lymphoma cells were isolated from DHL bearing mice spleen: total dissociated organs were added to the culture and keep in culture for at least 3 weeks before seeing cell growth. Cells were cultured at 37°C 5% CO_2 in B cell medium. B cell medium was composed by DMEM and Iscove's modified Eagle's media implemented with L-Glutamine 4mM, penicilline-streptomycin 100 Units/ ml, b-mercaptoethanol 25mM and 10% Fetal bovine serum. For treatments, cells where cultured for Tigecycline, and Venetoclax (all from Carbosynth) were

dissolved in dimethyl sulfoxide and added directly to the culture medium. Lymphoma cells were isolated from the spleen ot DHL bearing mice: total dissociated organs were added to the culture and kept in culture for at least 3 weeks before seeing cell growth. Cells were cultured at 37°C with 5% CO_2 in B cell medium, composed of ½ DMEM and ½ Iscove's modified Eagle's media implemented with 4mM L-Glutamine, 100 Units/ ml penicilline-streptomycin, 25mM β-mercaptoethanol and 10% Fetal bovine serum. For treatments, cells where cultured at a concentration of $3x10^6$ cells/mL. Tigecycline, and Venetoclax (all from Carbosynth) were dissolved in dimethyl sulfoxide and added directly to the culture medium at concentration indicated in Figure 7.13.

6.5 FACS analysis

All the cells used for FACS analysis were taken directly from organ dissociation. 1.5 x 10^6 cells have been counted and used for the staining. Specific fluorochrome-conjugated antibodies were added to the staining solution - MACS buffer (PBS 1x, 2 mM EDTA, 0.5% BSA) - mixed with specific for fluorochrome-conjugated antibodies (listed in Table 3), used at the dilution indicated. Cells were stained in FACS tubes for 1h at 4°C in dark and consecutively washed by spin at 2000 RPM and analysed with a FACSCelesta™ cytofluorimeter. Results were then further processed and analysed with FlowJo Version 10.4.0 software.

Antibody	Conjugate	Company	Clone	Species	Dilution used
CD19	PE-Cy7	Invitrogen (25-0193-82)	1D3	mouse	1:400
CD19	BB700	BD Pharmingen (#566412)	1D3	mouse	1:400
CD95	BV421	BD Pharmigen (#562633)	Jo2	mouse	1:200
CD38	BV650	BD Pharmigen (#740489)	90/CD38	mouse	1:200
CD86	PE	BD Pharmigen (#553692)	GL1	mouse	1:200
CD184 (CXCR4)	APC-R700	eBioScience (#565522)	2B11/CXCR4	mouse	1:100
hCD2	BV510	BioLegend (#300217)	RPA-2.10	mouse	1:100

Table 3: Antibodies used forFACS analysis

6.6 Cell sorting

Before sorting, cells were pre-enriched with Anti-CD19 MicroBeads and MACS column separation (Miltenyi Biotech, Cambridge, MA). B cells were stained with antibodies listed in Table 3 4 and cells were sorted according to hCD2 and GFP (EYFP for wt mice) reporter genes by a BDFACSAria Fusion Special Order System sorter (Becton Dickinson) using a 85um (pressure 45PSI) nozzle. In Cγ-*Cre; lsl-MYC; lsl-BCL2* mice, $hCD2^+/GFP^+$ cells are more than 90% GC B cells. Similarly, $EYFP^+$ cells in wild type mice are 90% GC B cells. The software utilized is BD FACSDiva software v8.0.2. Immediately after collection the cells were used for RNA extraction, followed by RNA-seq.

6.7 Immunohistochemistry

Freshly isolated tissue was washed in PBS, fixed in 4% paraformaldehyde at 4°C degrees for at least 16-24 hours, washed in PBS, and then stored in 70% ethanol at 4°C until further processing. The tissue was dehydrated with increasing concentrations of ethanol,

embedded in paraffin blocks, cut into 3/5-mm thick sections and mounted on glass slides. Sections were dewaxed and rehydrated through an ethanol scale, heated in citrate solution (BioGenex, #HK086-9K) in a water bath at 99°C for 30 minutes for antigen unmasking, washed once in water, and treated with 3% H_2O_2 for quenching of endogenous peroxidases. After overnight incubation at 4°C with the relevant primary antibody (Table 4), slides were washed twice with TBS and incubated with secondary antibodies (Table 4) for 45 minutes. The signal was revealed with DAB peroxidase substrate solution (Dako, #K3468) for 1 to 5 minutes. Slides were finally counterstained with Harris Hematoxylin (Sigma-Aldrich, #HHS80), dehydrated through alcoholic scale, and mounted with Eukitt (Bio-Optica, #09-00250). Pathological evaluations have been performed by two different human pathologists: Professor Stefano Pileri (European Institute of Oncology) and Claudio Tripodo (University of Palermo).

Target	Clone	Company	Dilution
c-MYC (Y69)	ab32072	Abcam	1:100
Ki67	RM-9106-R7	Thermo Scientific	1:200
Bcl2	Ab32124	Abcam	1:200
Peanut Agglutinin (PNA), Biotinylated	B-1075	Vector Lab	1:250
EnVision+ System- HRP Labelled Polymer Anti-mouse	K4000	Dako	ready to use
EnVision+ System- HRP Labelled Polymer Anti-rabbit	K4003	Dako	ready to use
HRP-Conjugated Streptavidin	P0397	Dako	1:100

Table 4: Antibodies used for IHC.

6.8 Apoptosis analysis

Expression of active caspase(s) was assessed by staining 1.5 x 10^6 of isolated splenocytes with Red-DEVD-FMK fluorescent-labelled CaspGLOW reagent according to the manufacturer's instructions (Biovision) and measured by FACS on cells stained with flow cytometry antibodies listed in Table 3.

6.9 RNA extraction and analysis

For RNA-seq experiments, total RNA was purified from lymphoma (Table 5) cell pellet onto Quick-RNA Miniprep columns (Zymo, #R1054) and treated on-column with DNaseI. RNA quality was checked with the Agilent 2100 Bioanalyser (Agilent Technologies). 0.5-1 µg were used to prepare libraries for RNA-seq with the TruSeq stranded total RNA Sample Prep Kit (Illumina, #20020596) following the manufacturer's instructions. RNA-seq libraries were then run on the Agilent 2100 Bioanalyser (Agilent Technologies) for quantification and quality control and pair-end sequenced on the Illumina 2000 or NovaSeq platforms.

Tumor ID		Originating tissue
DHL_241675	RAG1 primary lymphoma	Spleen
DHL_241879		
DHL_256874		
DHL_256875_ly		Lymphnodes
DHL_256875_sp		Spleen
DHL_91855		
DHL_91856		
DHL_241880		
DHL_237145_T2	NSG transplanted lymphoma	

Table 5: Lymphomas used for RNA-seq analysis

6.10 RNA-seq data filtering and quality assessment

RNA-seq reads (50 bp paired end) were filtered using the fastq_quality_trimmer and fastq_masker tools of the FASTX-Toolkit suite (http://hannonlab.cshl.edu/fastx_toolkit/). Their quality was evaluated and confirmed using the FastQC application (https://www.bioinformatics.babraham.ac.uk/projects/fastqc/). Pipelines for primary analysis (filtering and alignment to the reference genome of the raw reads) and secondary analysis (expression quantification, differential gene expression) have been integrated in the HTS-flow system (Bianchi et al., 2016). RNA-seq NGS reads were aligned to the mm10 mouse reference genome using the TopHat aligner (Kim et al., 2013) (version 2.0.8) with default parameters. In case of duplicated reads, only one read was kept. Read counts were associated to each gene (based on UCSC-derived mm10 GTF gene annotations), using the featureCounts software (http://bioinf.wehi.edu.au/featureCounts/) (Liao et al., 2014) setting the options -T 2 -p -P. Bioinformatic and statistical analyses were performed using R with Bioconductor (Liao et al., 2014) and comEpiTools (Liao et al., 2014) packages. Differentially expressed genes (DEGs) were identified using the Bioconductor Deseq2 package (Love et al., 2014) as genes whose q-value is lower than 0.05.

7 Results

7.1 GC-specific activation of *MYC* and *BCL2* provides a bona fide model of DHL

In order to generate a murine model that would faithfully recapitulate the cell of origin of human DHL, we intended to overexpress *MYC* and *BCL2* oncogenes specifically in B-cells that undergo the GC reaction. To do so, we took advantage of the germinal center specific transgene Cγ1-*Cre*, in which expression of the *Cre* recombinase is under control of the immunoglobulin Ig gamma1 constant region (Cgamma1) (Casola et al., 2006), which we combined with the *Cre*-induced conditional alleles R26lslCAG-MYC-IRES-hCD2 (Calado et al., 2012) and R26lslCAGBCL2-IRES-GFP (Knittel et al., 2016), hereafter indicated as *lsl-MYC* and *lsl-BCL2*. In *lsl-MYC*, the *MYC* open-reading frame is under the control of a strong synthetic promoter (CAG) and is followed by and internal ribosome entry site (IRES) driving expression of a truncated form of human CD2 as a reporter for *Cre*-mediated recombination (Figure 7.1). *lsl-BCL2* has a similar structure, with *BCL2* followed by a green fluorescent protein (GFP) expressing cassette. In the absence of *Cre*, expression of *MYC*, *BCL2* and the associated reporters is prevented by the presence of a LoxP-flanked STOP cassette, coupled with neomycin (NEO) resistance.

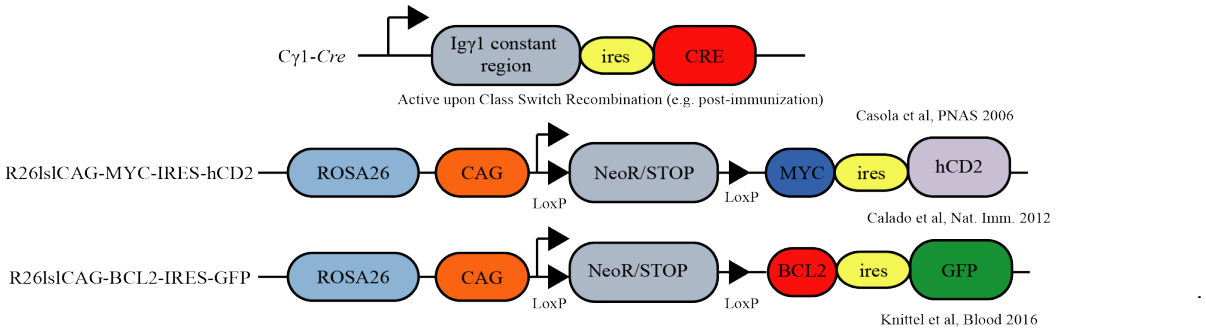

Figure 7.1 Alleles used in this study.
Schematic representation of the germinal center specific C**γ**1-Cre transgene (upper) and the Cre-inducible alleles R26lslCAG-MYC-IRES-hCD2 (middle) and R26lslCAGBCL2-IRES-GFP (bottom). The knock-in alleles are inserted into the ROSA26 locus and driven by a strong CAG promoter. Expression of Cre recombinase causes excision of the LoxP-flanked NeoR; STOP cassette, allowing constitutive expression of the downstream coding units, including MYC and hCD2, or BCL2 and GFP. The hCD2 and GFP reporters are translated from the same mRNAs as MYC and BCL2, respectively, by initiation from the intervening IRES (internal ribosomal entry site), as depicted.

In order to generate compound Cγ1-*Cre; lsl-MYC; lsl-BCL2* animals, we first crossed Cγ1-*Cre* and *lsl-BCL2* mice, and then bred the double-transgenic offspring with *lsl-MYC*. In order to obtain the required numbers of experimental animals in a timely manner, we followed a strategy that was previously described for the modeling of GC-derived Burkitt Lymphoma (BL) (Sander et al., 2012): briefly, the bone marrow (BM) of individual transgenic mice was transplanted into lethally irradiated, 8 weeks-old immunodeficient RAG1-null mice, which lack mature B and T lymphocytes, due to the absence of V(D)J recombination (Mombaerts et al., 1992). After BM transfer, the reconstituted recipient mice generate lymphocytes that are genotypically identical to the donor BM. For each transgenic donor of the various compound genotypes, we reconstituted a variable number of recipient animals (Figure 7.2A), thus allowing us to generate sizeable experimental cohorts for further study. The parallel cohorts were generated, expressing either both oncogenes (Cγ1-*Cre; lsl-MYC; lsl-BCL2*), each alone (Cγ1-*Cre; lsl-MYC* and *Cγ1-Cre; lsl-BCL2*) or none (Control: Cγ1-*Cre*). Eight weeks after transplantation, all mice were immunized by intraperitoneal (IP) injection of 10^9 cells of sheep red blood cells (SRBC) in order to stimulate the GC reaction, induce Cγ1-*Cre* (Casola et al., 2006) and trigger recombination of the target transgenes (Sander et al., 2012). The animals were then monitored for over one year for lymphoma development.

As summarized in Figure 7.2, activation of either *BCL2* or *MYC* and *BCL2* together led to the development of lymphomas, while *MYC* alone showed no effect. In particular, the Cγ1-*Cre*; *lsl-BCL2* cohort developed lymphoma about 9 months post BM transplantation (median survival 294 days), whereas the Cγ1-*Cre; lsl-MYC; lsl-BCL2* group developed fully penetrant lymphomas with a median latency of 7 months post BM transplantation (median survival 213 days). We decided to sacrifice them when the weight loss was equal or greater than 10% of the initial body weight. Besides general signs of illness and weight loss, suffering mice did not show any enlargement of lymph nodes. Upon necropsy, all mice of the Cγ1-*Cre*; *lsl-MYC; lsl-*

BCL2 group (of 25 analyzed) showed splenomegaly and hepatomegaly, with large tumors infiltrates present in both organs. A majority also displayed macroscopic signs of tumor infiltration in other non-lymphoid organs, such as lung (23/25), kidney (10/25), intestine (5/25), heart (3/25) or brain (1/25) (Figure 7.2B). Histological analysis by Giemsa staining was performed on 12 isolated spleen sections, revealing a characteristic "starry sky" phenotype (Figure 7.2C), a typical feature of high-grade B cell lymphoma due to extensive macrophage infiltration (Swerdlow et al., 2016). Remarkably, this cooperative effect of MYC and *BCL2* in promote lymphomagenesis was not due to a donor founder effect. Indeed, as shown in Figure 7.3, transplantation of the same Cγ1-*Cre*; *lsl-MYC; lsl-BCL2* BM resulted in a variable tumor latency in reconstituted recipient mice.

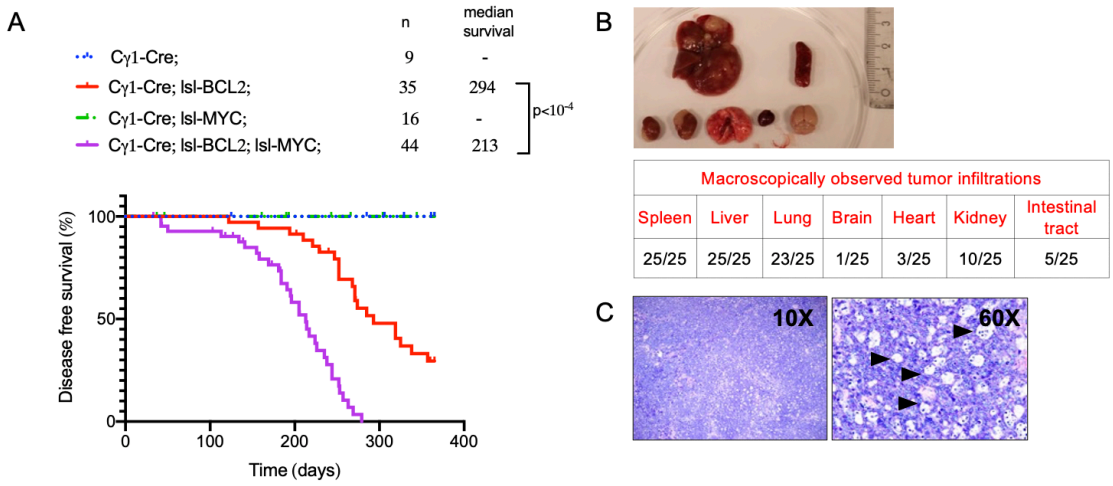

Figure 7.2 Concomitant *MYC* and *BCL2* GC activation resulted in lymphoma development.
A: Kaplan-Meier survival curve of mice reconstituted with BM of the indicated genotypes. Mice were scored as disease-positive and sacrificed when the weight loss was over 10% of total body weight. The numbers (n) represent the animals in each group. The median tumor-free survival is indicated (days); **B**: Examples of organs harvested from mice with a *MYC/BCL2* lymphoma showing enlargement of the spleen and the liver and infiltration of various organs (top); summary of infiltrated organs observed (bottom) **C**: Giemsa staining on spleen section allowed identification of the typical "starry sky" morphology due to admixed phagocytic macrophages (indicated with arrows).

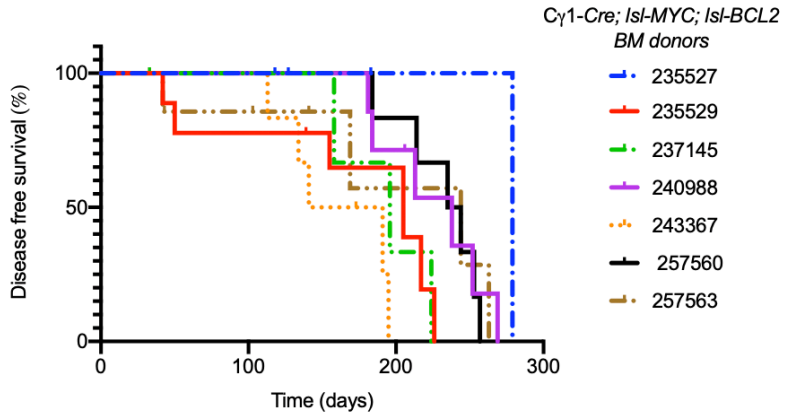

Figure 7.3 Cγ1-Cre; lsl-MYC; lsl-BCL2 BM transplantation does not cause a founder effect.
Kaplan-Meier survival curve of mice reconstituted with BM of the indicated Cγ1-*Cre*; *lsl-MYC; lsl-BCL2* donors. Reconstituted mice showed variable tumor latency upon transplantation with the same Cγ1-*Cre; lsl-MYC; lsl-BCL2 BM*

In order to determine the cellular phenotype of the tumors in Cγ1-*Cre*; *lsl-MYC; lsl-BCL2* reconstituted mice, we isolated splenocytes from sick mice and performed immune-staining with the B-cell surface markers CD19, CD95 and CD38, which allow to distinguish GC B-cells from other subset of non-GC B cells (which include follicular (FO), marginal zone (MZ) and eventually memory B cells) (Basso and Dalla-Favera, 2015; Monzon-Casanova et al., 2018). B-cells, defined by CD19 expression, were around 70% of total splenic cells analyzed in tumor-bearing mice (

Figure 7.4 A,B): gating on those $CD19^{+}$ cells revealed a $CD38^{low}/CD95^{hi}$ profile typical of GC B-cells (

Figure 7.4 C) (Basso and Dalla-Favera, 2015). Moreover, virtually all of those cells were positive for the hCD2 and GFP reporters, indicating that they had activated *MYC* and *BCL2* alleles (

Figure 7.4 A, D).

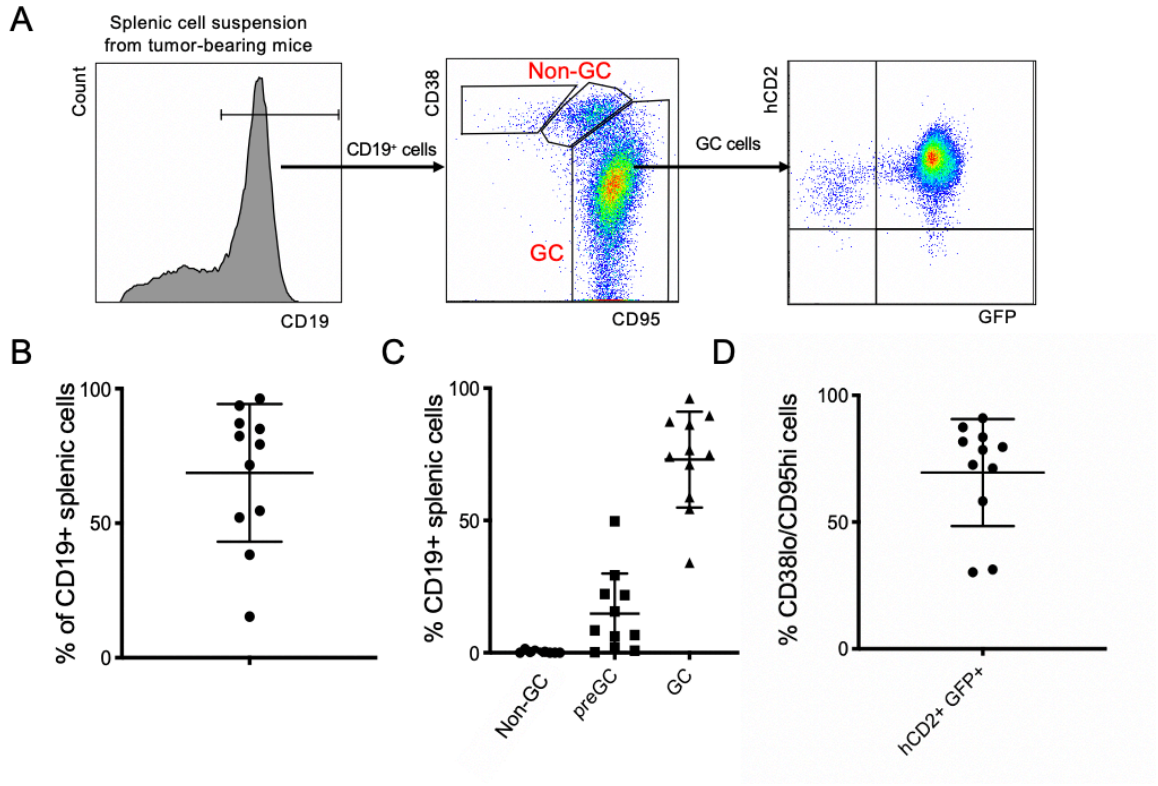

Figure 7.4 Germinal Center origin of Cγ1-*Cre; lsl-MYC; lsl-BCL2* lymphomas.
A: Representative immune-staining of the splenic cell suspension from tumor-bearing mice performed with B-cell surface marker: CD19, CD95 and CD38 which allowed us to mark Germinal Center and non-germinal center B cells (GC: $CD19^{+}$, $CD38^{low}$, $CD95^{hi}$) B cells. hCD2 and GFP activity was measured in GC B cell compartment **B-D**: distribution of the data for all mice analyzed for CD19 (B), CD38 and CD95 (C), and hCD2 and GFP (D).

GCs are polarized into two different zones: dark (DZ) and light zones (LZ) (Victora et al., 2012), which can be defined by distinct surface marker profiles, such as $CXCR4^{hi}CD83^{low}CD86^{low}$ and $CXCR4^{low}CD83^{high}CD86^{high}$, respectively (Allen et al., 2004; Caron et al., 2009; Victora et al., 2012; Victora et al., 2010). As assayed by immunophenotypic analysis of two of these markers, CXCR4 (CD184) and CD86, the lymphomas arising in our Cγ1-*Cre*; *lsl-MYC; lsl-BCL2* model showed a phenotype slightly promne to a DZ-like phenotype being composed of $CXCR4^{hi}CD86^{low}$ cells in a DZ/LZ ratio of 70/30 and considering that a wild type GC is 60/40 (Figure 7.5). In conclusion activation of *MYC* and *BCL2* and the GC B-cell stage gives rise to lymphomas (as confirmed from the

anatomopathological analysis described below) that reproduce the GC origin of human DHL with a DZ-like phenpotype.

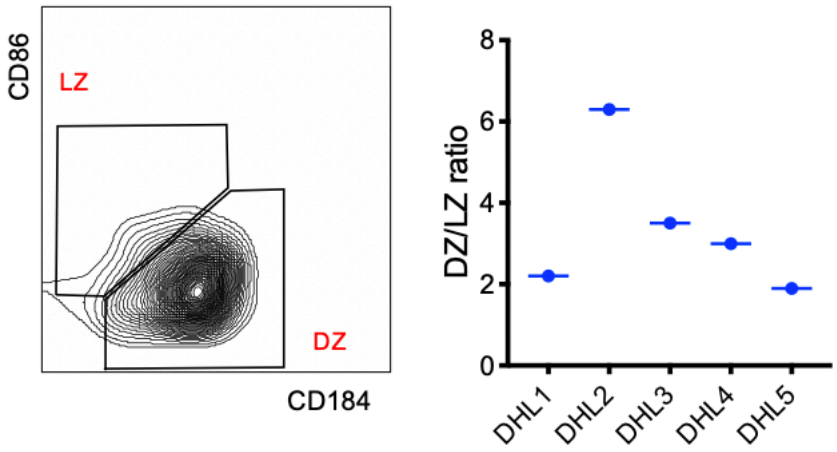

Figure 7.5 LZ/DZ composition of GC B cells in DHL.
Representative flow cytometric analysis of splenic GC B cells of Cγ1-*Cre*; *lsl-MYC; lsl-BCL2* tumor bearing mice stained for CD184 and CD86 surface markers. Gates define DZ ($CXCR4^{hi}CD86^{low}$) and LZ ($CXCR4^{low}CD86^{high}$) GC B cells. DZ/LZ ratio of 5 different Cγ1-*Cre*; *lsl-MYC; lsl-BCL2* reconstituted mice analyzed is shown.

7.2 Activation of *MYC* and *BCL2* at early stages of B-cell differentiation leads to lymphoma development

The onset of a GC-derived lymphoma, as described above, might have been driven by the GC-specific activation of *lsl-MYC* and *lsl-BCL2* or, alternatively, by a propensity of these oncogenes to instruct tumor initiation at the GC stage. In order to address this question, we substituted Cγ1-*Cre* by the CD19-*Cre* transgene, expressed in the whole B-cell lineage from the pre-B cell stage (Rickert et al., 1997). We thus crossed CD19-*Cre* with *lsl-MYC and lsl-BCL2* alleles to generate CD19-*Cre; lsl-MYC; lsl-BCL2* mice, and followed the animals over a period of one year for lymphoma development, without transplantation or immunization. The mice in each cohort were monitored twice a week for tumor development by macroscopic observation and weight measurement, and euthanized if showing signs of illness or weight loss. CD19-*Cre* driven activation of *MYC* and *BCL2*, but neither alone, led to the development of

aggressive tumors after 4-5 month (median survival of 165 days) (Figure 7.6 A), with splenomegaly and hepatomegaly. Upon necropsy, most CD19-*Cre; lsl-MYC; lsl-BCL2* animals showed tumor macroscopic infiltration in the spleen (12/19 cases), and less frequently in the liver (4/19), lung (5/19) and kidney (7/19) (Figure 7.6 B). Giemsa staining on spleen sections revealed the presence of an atypical plasmablastic proliferation which has not been associated with any human lymphoproliferative disease condition yet. However, the possibility that CD19-*Cre; lsl-MYC; lsl-BCL2* mice reflect lymphoproliferative abnormalities such as plasmablastic lymphoma or Waldenström's Macroglobulinemia has still to be addressed.

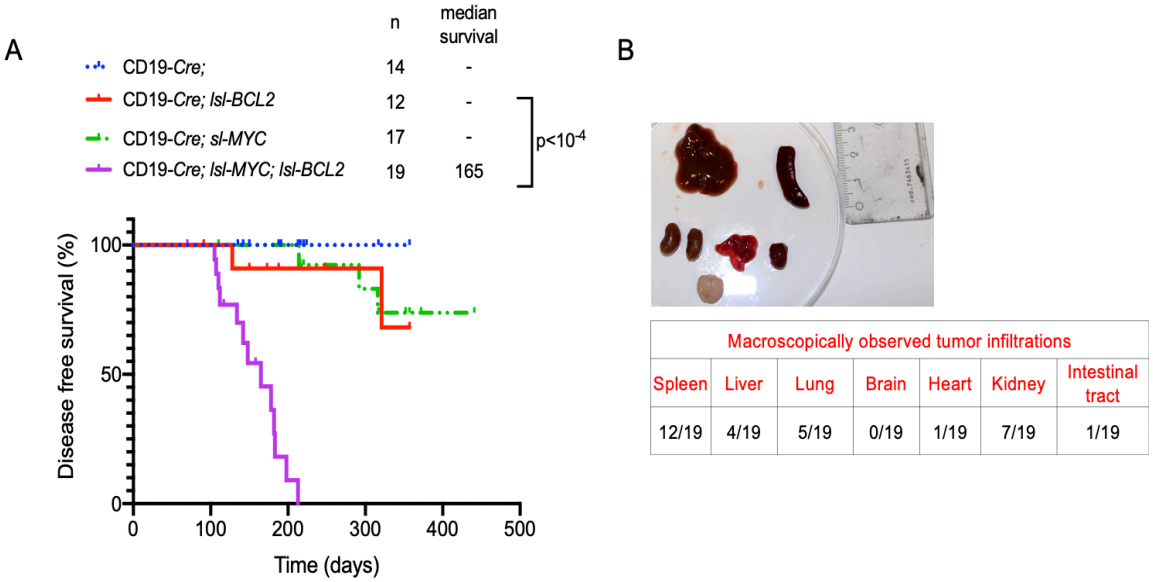

Macroscopically observed tumor infiltrations						
Spleen	Liver	Lung	Brain	Heart	Kidney	Intestinal tract
12/19	4/19	5/19	0/19	1/19	7/19	1/19

Figure 7.6 Concomitant *MYC* and *BCL2* activation at early B-cell differentiation stage resulted in lymphoma development.
A: Kaplan-Meier survival curve of CD19-*Cre; lsl-MYC; lsl-BCL2* mice. Group of mice with only *MYC* or only *BCL2* did not show acceleration of lymphomagenesis disease-free survival while concomitant *MYC* and *BCL2* activation resulted in tumor development. Mice were scored as disease-positive and sacrificed when the weight loss was over 10% of total body weight. The numbers (n) represent the animals in each group. The median tumor-free survival is indicated (days); **B**: Examples of organs harvested from mice with a *MYC/BCL2* lymphoma showing enlargement and infiltration of spleen and liver (top); summary of infiltrated organs observed (bottom)

Immunophenotypic analysis of CD19-*Cre; lsl-MYC; lsl-BCL2* lymphomas from the spleens of the sacrificed animals revealed high variability among mice analyzed , with the presence of a $CD19^{+}CD38^{hi}CD95^{hi}$ phenotype (**Error! Reference source not found.**A, C),

distinct from the characteristic GC-like CD19^{+}CD38^{low}CD95^{hi} profile of Cγ1-*Cre*; *lsl-MYC; lsl-BCL2* tumors (compare with

Figure 7.4 . Although we named this stage pre-GC, the nature and correct assignment of this stage remains to be fully evaluated. Indeed, it is likely that this interesting population is composed by activated B cells. However, they could be both pre-GC or post-GC B cells.

This aspect will be further review in the discussion section of this thesis. Moreover, while all positive cells for the *MYC*-associated marker hCD2, about 50% of the tumor cells scored negative for GFP (Fig. 1.6A,D), indicating that they had either lost *BCL2* expression, or failed to recombine the allele in the first place. In conclusion, activation of *MYC* and *BCL2* at early stage of B-cell development (pro-B) gives rise to lymphomas characterized by a variable immunophenotype that – at least based on the two CD95 and CD38 surface markers – points to a different origin of those tumors compared to Cγ1-*Cre*; *lsl-MYC; lsl-BCL2* one.

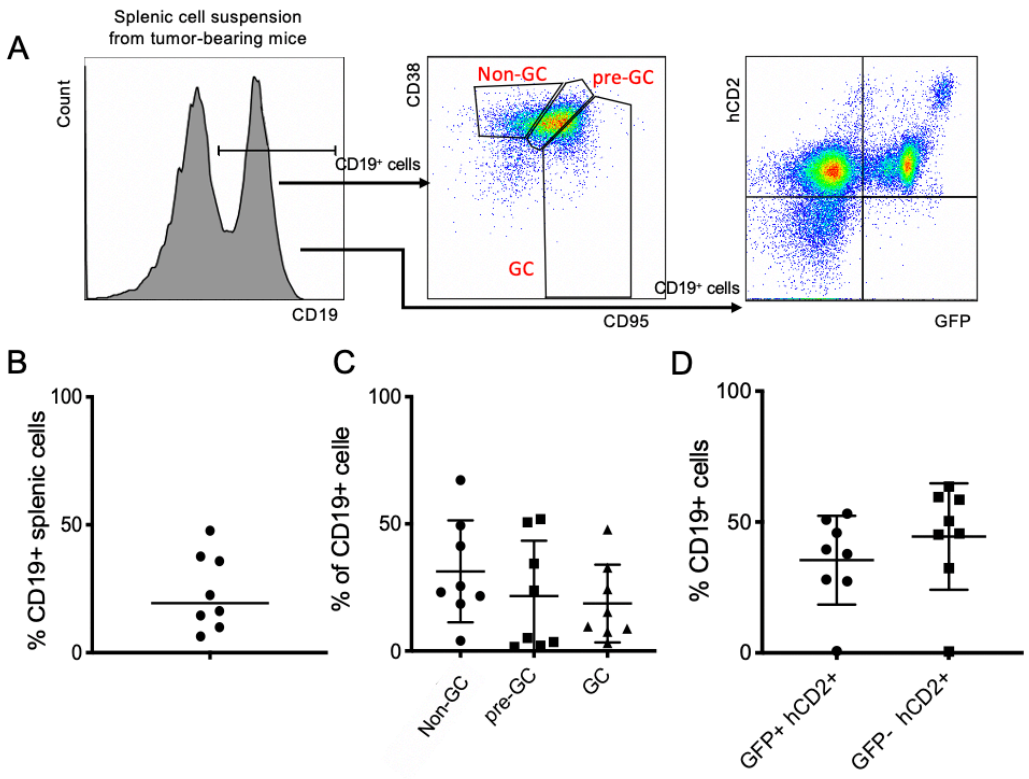

Figure 7.7 NON-GC origin of CD19-*Cre; lsl-MYC; lsl-BCL2* lymphomas.
A: Immune-staining of the splenic cell suspension from tumor-bearing mice performed with B-cell surface marker: CD19, CD95 and CD38 which allowed us to mark non Germinal Center (FO: CD19^{+}, CD38^{hi}, CD95^{low}) , pre-Germinal Center

(pre-GC: $CD19^{+}$, $CD38^{hi}$, $CD95^{hi}$) and Germinal Center (GC: $CD19^{+}$, $CD38^{low}$, $CD95^{hi}$) B cells. hCD2 and GFP activity was measured in GC B cell compartment **B**: summary data of mice analyzed for CD19 marker **C**: summary data of mice analyzed for CD38 and CD95 markers **D**: summary data of mice analyzed for hCD2 and GFP reporter's activity.

7.3 Histo-pathological analysis

In order to classify tumors developed in our Cγ1-*Cre* and CD19-*Cre* driven DHL models, we performed histopathological analysis by Hematoxylin and Eosin (H&E) staining on spleen sections collected upon sacrifice of the diseased animals (Figure 7.8). The pathological evaluation of these sections confirmed morphological alterations of spleen architectures in both cases. In the Cγ1-*Cre*; *lsl-MYC; lsl-BCL2* model, infiltrated spleen section were largely classified as Burkitt-like (8/11-72%), while some tumors were identified as either Lymphoplasmablastic lymphoma (LPL)-like (2/11-18%) or diffuse large B-cells lymphoma (DLBCL)-like tumors (1/11-9%) (Table 6 and Figure 7.8). This morphological variability could reflects the heterogeneity observed among human DHL cases (Aukema et al., 2011). Instead, pathological evaluation of the CD19-*Cre*; *lsl-MYC; lsl-BCL2* model revealed an altered plasmablastic proliferation in 4/5 of the spleen sections evaluated (Table 6 and Figure 7.8): to the best of our knowledge, this is an atypical condition that has not been associated with any type of lymphoma in the clinic. As shown above, flow cytometric analysis confirmed the GC origin of the tumors arising in our Cg1-Cre; lsl-MYC; lsl-BCL2 DHL model (Figure 7.4). To corroborate these results, we stained splenic sections for the GC marker lectin peanut agglutinin (PNA) (Rose et al., 1980), confirming pervasive infiltration of the spleen by PNA-positive cells (Figure 7.10A). Moreover, the tumor samples also showed positivity for another GC marker (Bcl6) and the proliferative marked Ki67 (Figure 7.10B). Regarding BCL6 staining, we still need a wild type control, which is part of the ongoing work (in collaboration with professor Claudio Tripodo, University of Palermo). Beside this, immunohistochemical staining of spleen sections confirmed the over-expression of MYC and BCL2 in Cγ1-Cre; lsl-MYC; lsl-BCL2 tumors, associated with positivity for the proliferation marker Ki67 (Figure 7.10).Altogether, the aforementioned data indicated that activation of *MYC* and *BCL2* at the

GC stage, but not at an early B-cell stage, yielded tumors that most faithfully represent high-grade DLBCL lymphomas as they occur in the clinic. In the remainder of my work, I thus proceeded with a more detailed characterization of the Cγ1-*Cre; lsl-MYC; lsl-BCL2* model.

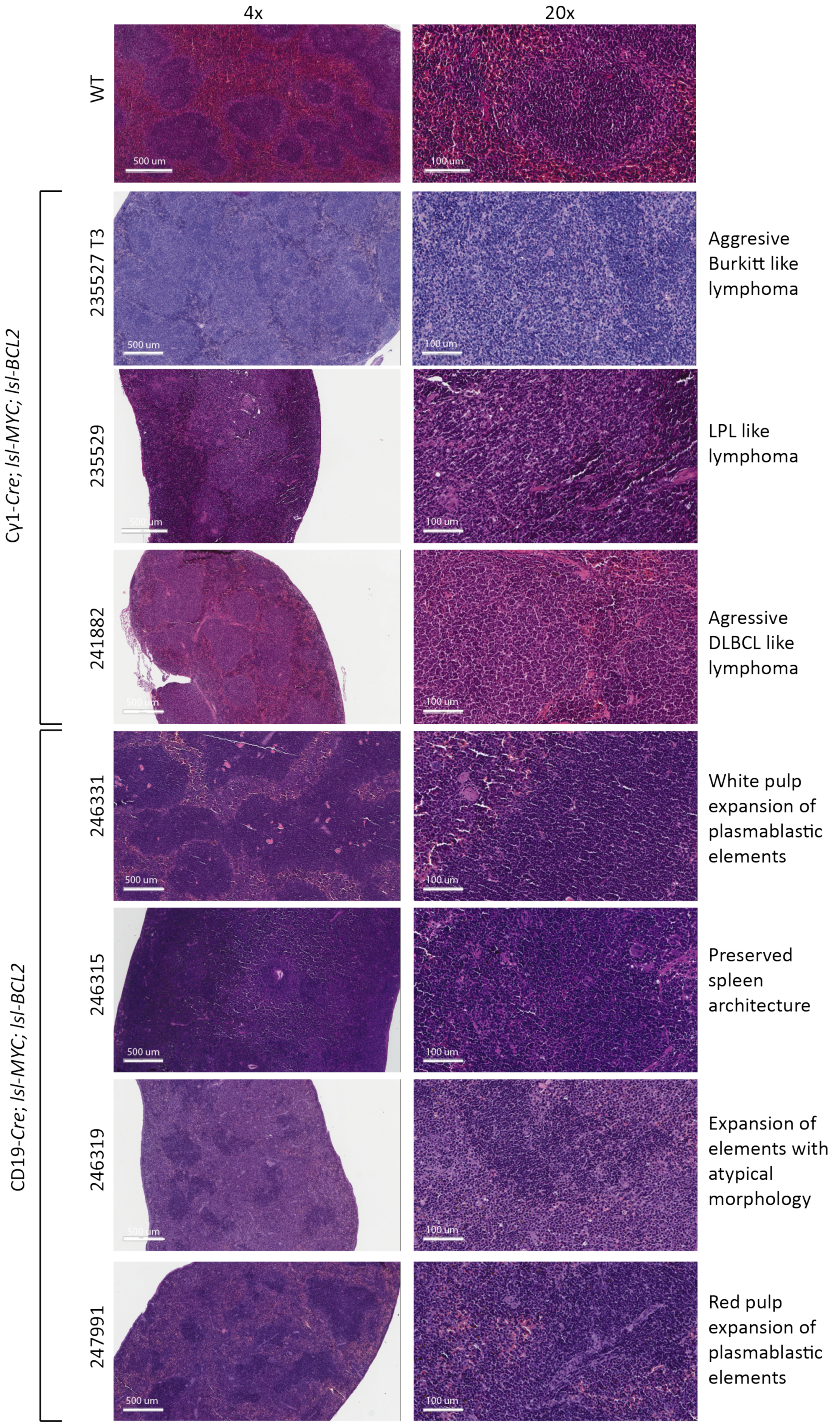

Figure 7.8 Hematoxylin Eosin stain for pathological evaluation.
Representative Hematoxylin Eosin immunohistochemistry stain of Cγ1-*Cre*; *lsl-MYC; lsl-BCL2* and CD19-*Cre*; *lsl-MYC; lsl-BCL2* sick mice. Spleen sections were isolated, and paraffin embedded to perform immunohistochemistry analysis. Scale bar is indicated. A spleen of a wild type mouse 10 days upon SRBC immunization was used as a control. H&E have been evaluated by the Hematopathology director of the European Institute of Oncology.

Experimental group	Lymphoma ID	Pathological evaluation
Cγ1-*Cre; lsl-MYC; lsl- BCL2*	235527 T3	Aggressive Burkitt like lymphoma
	235529	LPL like lymphoma
	237145 T3	Aggressive Burkitt like lymphoma
	237145 T1	Aggressive Burkitt like lymphoma
	237145 T5	Aggressive Burkitt like lymphoma
	237145 T4	Aggressive Burkitt like lymphoma
	241676	Aggressive Burkitt like lymphoma
	91853	LPL like lymphoma
	241882	Aggressive DLBCL like lymphoma
	259614	Aggressive Burkitt like lymphoma
	258059	Aggressive Burkitt like lymphoma
CD19-*Cre; lsl-MYC; lsl- BCL2*	246311	White pulp expansion of plasmablastic elements
	246315	Preserved spleen architecture
	245831	White pulp expansion of plasmablastic elements
	246319	Expansion of elements with atypical morphology not associated with lymphoma
	247911	Red pulp expansion of plasmablastic elements

Table 6 Pathological evaluation.
Spleen tissues from C**γ**1-*Cre*; *lsl-MYC; lsl-BCL2* reconstituted and CD19-*Cre*; *lsl-MYC; lsl-BCL2* tumor-bearing mice have been Hematoxylin-Eosin stained and evaluated for the pathological classification. Experimental group, tumor identification number and pathological evaluation is indicated for each tumor.

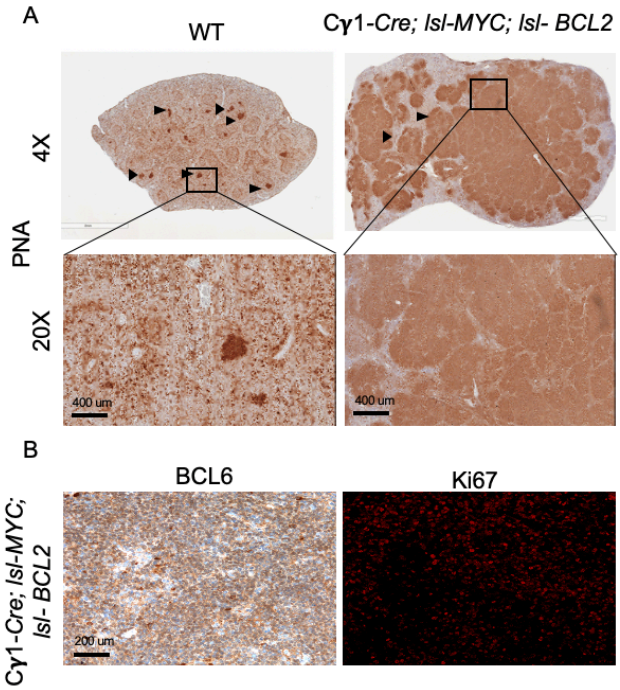

Figure 7.9 Increase number and size of GCs in Cγ**1-*Cre; lsl-MYC; lsl-BCL2* DHL.**
Immunohistochemistry stain of C**γ**1-*Cre*; *lsl-MYC; lsl-BCL2* reconstituted mice. Spleen sections were isolated, and paraffin embedded to perform immunohistochemistry stain of GC markers PNA and BCL6. **A**: Representative staining for control and tumors is shown with arrows indicating PNA+ GCs. This result was observed in 4 different sections of Cγ1-*Cre*; *lsl-MYC; lsl-BCL2* tumor bearing mice derived from independent donors. **B**: Representative BCL6 staining is shown for a C**γ**1-*Cre*; *lsl-MYC; lsl-BCL2* tumor. A representative immunofluorescence Ki67 staining is also shown as a proliferation control. Similar results were observed in 3 independent samples. same result was observed in 3 different spleen sections from independent donors.

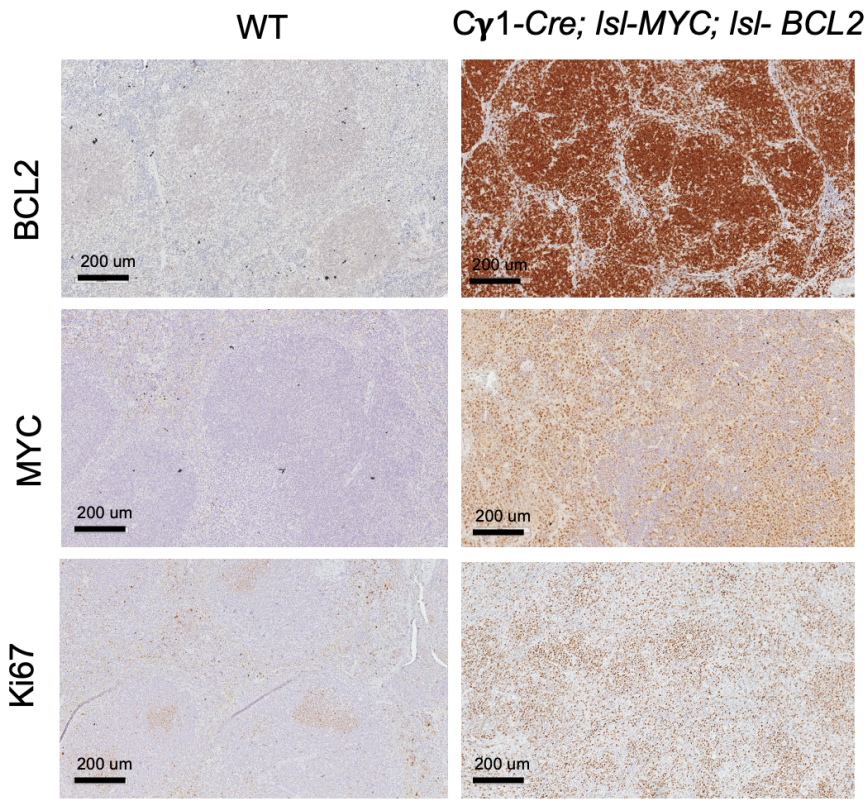

Figure 7.10 *MYC* and *BCL2* are overexpressed in Cγ1-*Cre; lsl-MYC; lsl-BCL2* DHL.
Representative Hematoxylin Eosin immunohistochemistry stain of Cγ1-*Cre*; *lsl-MYC; lsl-BCL2* reconstituted and CD19-*Cre*; *lsl-MYC; lsl-BCL2* sick mice. Spleen sections were isolated, and paraffin embedded to perform immunohistochemistry analysis of MYC, BCL2 and Ki67. Similar results were observed in 3 independent samples. Scale bar is indicated. A spleen of a wild type mouse 10 days upon SRBC immunization was used as a control.

7.4 Cγ1-*Cre*; *lsl-MYC; lsl-BCL2* tumors are transplantable

In order to facilitate the characterization of our Cγ1-*Cre*; *lsl-MYC; lsl-BCL2* DHL model, we sought to establish tumor lines by serial transplantations *in vivo*. Two million cells from the splenic cell suspension isolated from sick mice were injected intravenously (IV) into 6/8-week old NOD scid gamma (NSG) immunodeficient mice. Upon transplantation, mice were monitored for disease onset, through twice-a-week observation and body weight measurement. A total of 24 different Cγ1-*Cre*; *lsl-MYC; lsl-BCL2* lymphomas were transferred in a variable number of NSG recipient mice (**Error! Reference source not found.**A), and 19 of these lymphomas expanded in at least one NSG recipient. On the other hand, none of splenic cells preparations from Cγ1-*Cre*; *lsl-BCL2* tumor-bearing mice expanded in NSG recipients (0/13) (**Error! Reference source not found.**A). Those DHL lymphomas that developed in NSG mice

expanded in both spleen and liver as well as in other organs as described for primary Cγ1-*Cre*; *lsl-MYC; lsl-BCL2* tumors. Most importantly, they recapitulated the main features of the primary tumors, based on flow cytometric analysis of CD19, CD95 and CD38, as well as of the hCD2 and GFP reporters (**Error! Reference source not found.**B: compare with **Error! Reference source not found.**C). These data suggest that tumors developing upon concomitant activation of *MYC* and *BCL2* in the GC compartment are more aggressive than those elicited by *BCL2* alone, allowing them to engraft and expand in NSG recipient mice. Alternatively, GCB precursor cells - that upon concomitant activation of both oncogenes give rise to tumor - are characterized by a different biology and, for example, may be less dependent upon initial T-cell derived stimulation.

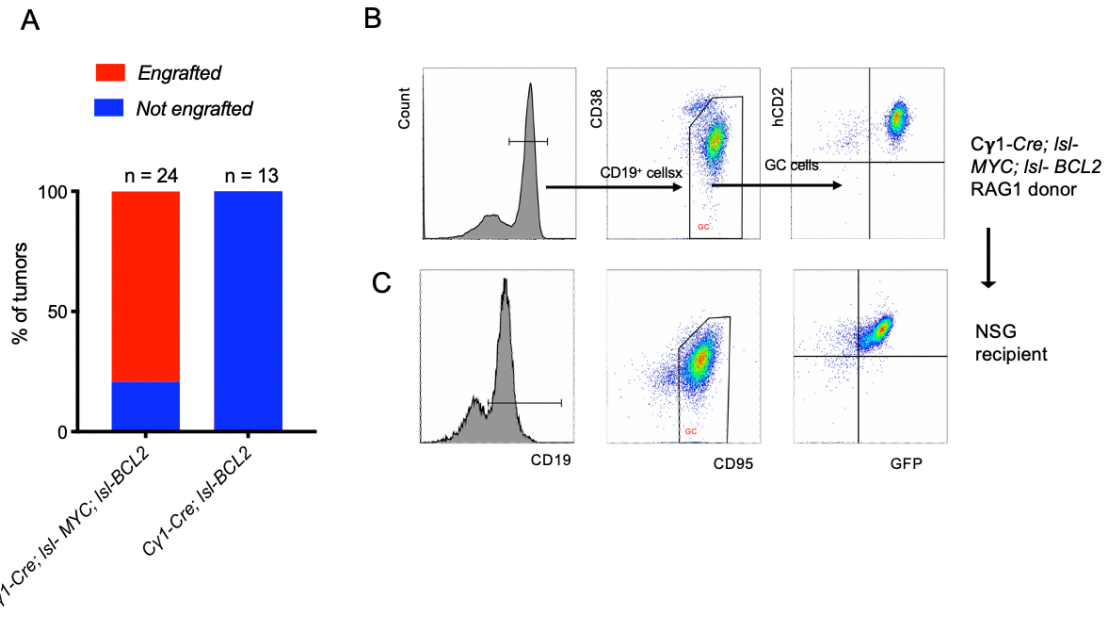

Figure 7.11 DHL are able to propagate in vivo.
Transfer of isolated splenic B cell from sick Cγ1-*Cre*; *lsl-MYC; lsl-BCL2* reconstituted mice induced lymphoma phenotype in NSG recipients. **A**: Bar plot representing the number of NSG mice transplanted for each RAG1 donor (Cγ1-*Cre*; *lsl-MYC; lsl-BCL2* and Cγ1-*Cre*; *lsl-BCL2*) and the relative number of mice where the tumor engrafted; **B**: Representative flow cytometric analysis of isolated splenic B cell from sick Cγ1-*Cre*; *lsl-MYC; lsl-BCL2* reconstituted RAG1 mice showing that the GC phenotype of Splenic B cell of the RAG1 donor is maintained in NSG recipient mice. GC B cells are recombined for the two reporter genes hCD2 and GFP. **C**: Representative flow cytometric analysis of isolated splenic B cell from sick NSG recipient mice showing that the GC phenotype of Splenic B cell of the RAG1 donor is maintained in NSG recipient mice. GC B cells are recombined for the two reporter genes hCD2 and GFP

We then proceeded to expand our tumor lines through serial transplantations *in vivo*, by passaging the same number of splenocyte (99% composed by lymphoma cells) crudely isolated from sick NSG mice into novel NSG recipients. Upon three serial *in vivo* passages in NSG mice, we observed that DHL tumors showed a reduced latency, with recipients reaching a median survival of 15 days at the third passage (**Error! Reference source not found.**A). These data suggest that our DHL tumors may undergo clonal selection upon serial transplantation.

In order to follow tumor expansion in real-time, we modified two previously *in vitro* stabilized mDHLcell lines (see section 7.5) for luciferase expression, coupled with an mCherry reporter gene that allowed us to sort mCherry/luciferase^{+} cells before injection. We then transplanted the same number of cells (2.5 x 10^{6}) from two diffent mDHL cell lines expressing luciferase in both NSG and C57 mice. We transplanted tumor-derived splenocytes in a total of 12 NSG and 20 C57 mice (**Error! Reference source not found.**B). We followed mice for tumor development both by macroscopical observation and whole-body imaging to detect luciferase expression (taking advantage of IVIS *in vivo* imaging technology). 15 days upon transplantation, we detected a positive signal for luciferase expression at the level of the spleen in all NSG mice transplanted while none of C57 mice expressed luciferase (**Error! Reference source not found.**C). Transplanted C57 mice were followed over a period of time of 4 months before deciding to sacrifice them.

Altogether, while readily expanding in NSG recipient animals, our mDHL tumors were not able to propagate in C57 syngeneic mice, implying that they were rejected in immunocompetent animals. While the immunogenic determinants of the tumors remain to be characterized, this features represents a limitation to the use of our mDHL mice as a preclinical model. In particular, we still need a representative, transplantable immuno-competent disease

model of DHL to understand which are the mechanism at the base of disease progression and to develop pre-clinical studies based on immunological therapies.

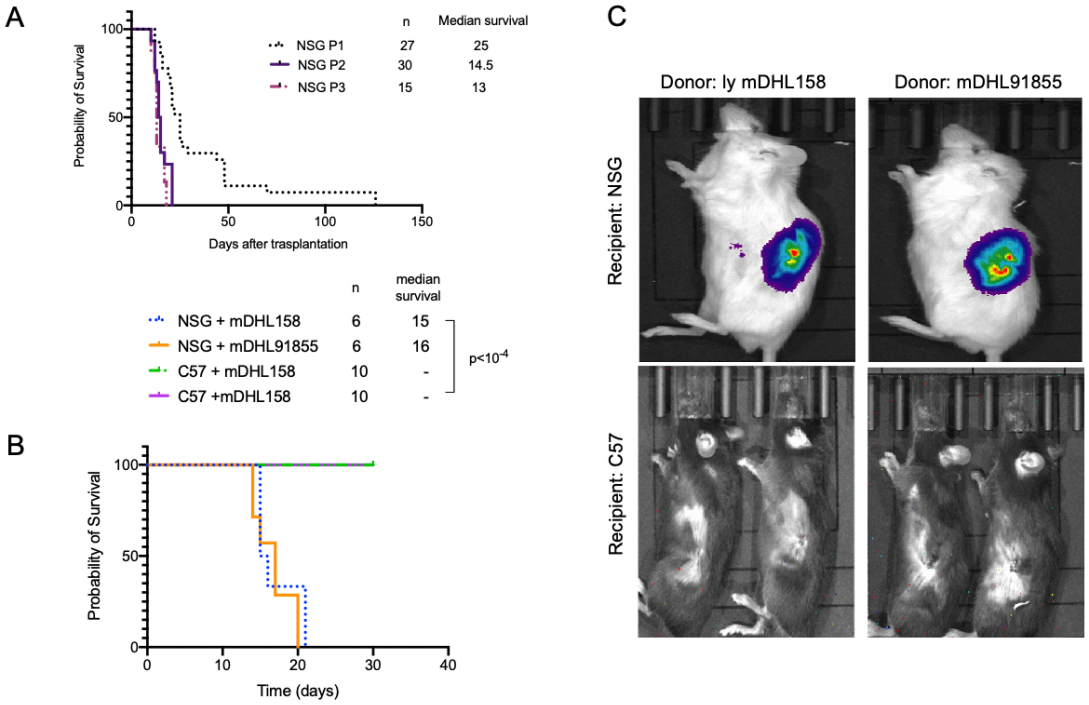

Figure 7.12 Cγ1-*Cre; lsl-MYC; lsl-BCL2* DHL tumors does not expand in immunocompetent syngeneic mice.
A: Kaplan-Meier survival curve of NSG mice upon three serial in vivo passages (P1, P2 and P3) **B**: Kaplan-Meier survival curve of NSG and C57 mice upon IV transplantation of two different Cγ1-Cre; lsl-MYC; lsl-BCL2 DHL (ly #1 and ly #2) which were previously in vivo stabilized by three serial transplantation in NSG mice. C57 mice did not show development of lymphoma while littermates NSG mice developed lymphoma in 15 days. Mice were scored as disease-positive and sacrificed when they developed signs of illness, tumor mass or weight loss. The numbers (n) represent the animals in each group. The median tumor-free survival is indicated (days); **C**: mDHL158 and 91855, tumor development was monitored by whole-body imaging. A representative image of NSG and C57 15 days upon intrasplenic injection is shown. Similar results were observed for all mice analyzed.

7.5 Mouse DHL tumors grow and retain primary tumor characteristics *in vitro*

The ability to address tumor-specific drug responses depends not only on the availability of *in vivo* pre-clinical models, but also of *in vitro*-stabilized cell lines. In order to derive such cell lines from our mouse DHL model, we splenic cell suspensions isolated from NSG sick mice were resuspended in B-Cell Medium (see Material and Methods chapter) and cultures *in vitro*. We were able to grow *in vitro* only mDHL isolated from tumors developed in NSG mice, but not from reconstituted Cγ1-*Cre; lsl-MYC; lsl-BCL2* primary tumors and managed to stabilize a total of 8 mDHL cell lines. In general, we observed that cells underwent an initial crisis that last about six cell passages before immortalization and after which cells

grew regularly with 3 doubling times every 2 days. Cells displayed a homogenous morphology and can grow as single cells suspension or form aggregated cell clumps. Most important here, our mDHL cell lines maintained their GC-specific surface profiles, expressed the hCD2 and GFP reporters (Figure 7.13A,B), as well as the MYC and BCL2 proteins (Figure 7.13C).

As introduced above, DHL is an aggressive disease for which effective targeted therapies are still missing in the clinic. In this regard, compounds that exacerbate MYC-induced apoptosis might cooperate with *BCL2* inhibitors such as Venetoclax (Leverson et al., 2017) in killing DHL cells. In previous work, we validated this concept for Tigecycline (D'Andrea et al., 2016; Rava et al., 2018), an antibiotic that inhibits the mitochondrial ribosome and shows toxicity against a variety of cancer cells (Xu et al., 2016). In particular, we showed that Tigecycline preferentially killed MYC over-expressing cells, providing a therapeutic window against MYC-driven lymphomas (D'Andrea et al., 2016) and strongly synergizing with venetoclax in killing human DHL cells lines (Rava et al., 2018). Based on these observations, two different mDHL (mDHL310 and mDHL158) cell lines were treated with increasing concentrations of Tigecycline and Venetoclax, alone or in combination: as illustrated in Figure 7.13C and Figure 7.13D. When used alone, both of the drugs showed little toxicity, however, when used together showed clear cooperation in killing mDHL cells. Hence, our mDHL cell lines provide an additional tool for the study of drug interactions in pre-clinical development against this aggressive lymphoma subtype.

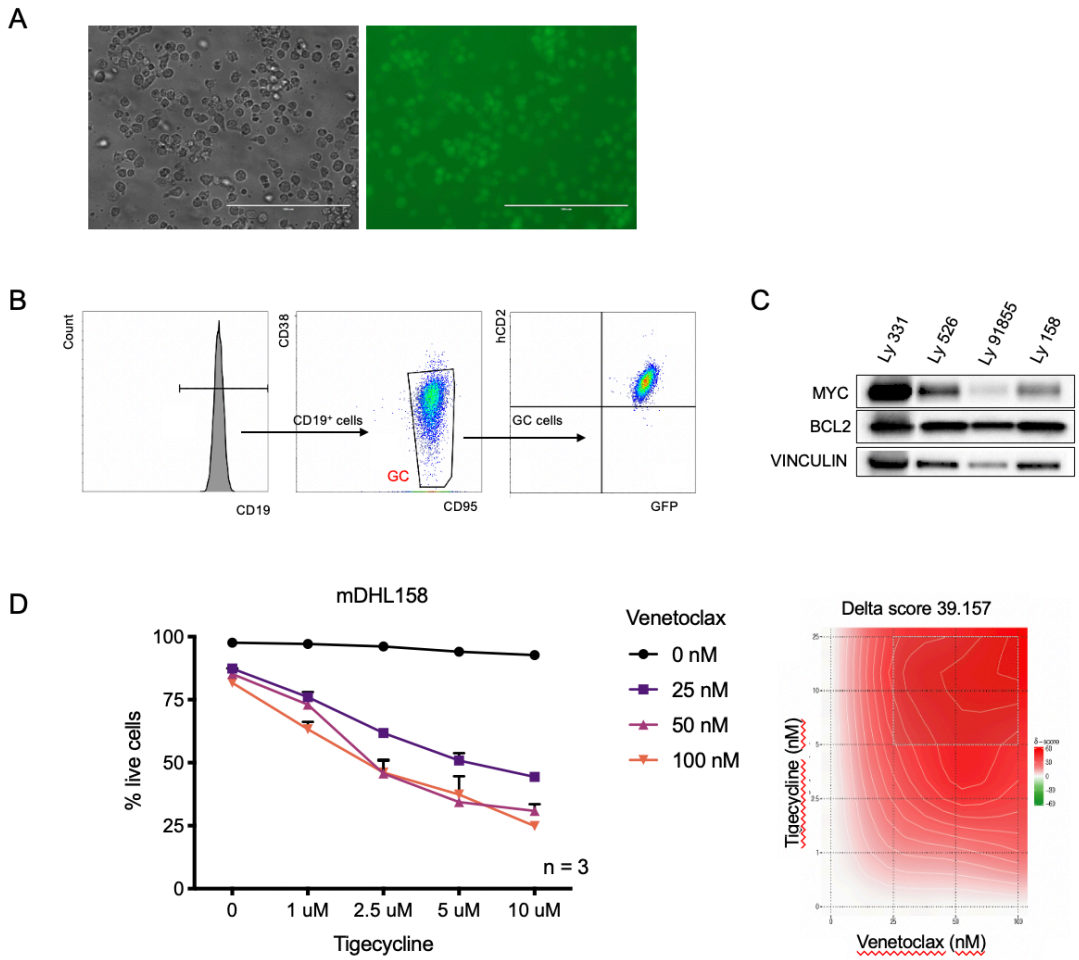

Figure 7.13 DHL ex vivo cultured tumors retain GC characteristics and are sensible to Tigecyclin and Venetoclax. **A**: example of the morphological features of mDHLcell lines (mDHL158). Cells are growing as single cells and as clusters of cells. GFP fluorescence is showed; **B**: Cγ1-*Cre*; *lsl-MYC; lsl-BCL2* DHL cultured in vitro retained GC phenotype, GFP and hCD2 expression; **C**: MYC and BCL2 protein expression level in four different DHL lymphomas was evaluated by Western Blot; **D**: Synergistic effect of Tigecycline and Venetoclax treatment on one of two different mDHL cell lines tested (mDHL158). Mean of three technical replicates is shown. Drug interaction landscapes and delta scores for synergy, based on the ZIP model in SynergyFinder (Ianevski et al., 2017), derived from the data of Figure 7.13 D (left). The landscapes identify the specific dose regions where there is a synergistic (red) or antagonistic (green) drug interaction. Dashed black-and-white squares within the landscapes mark the regions of maximal synergy. A positive delta score signifies a synergistic interaction, while a score near 0 indicates that the drugs are not interactive.

7.6 Stage specific short-term activation of *MYC* and *BCL2* results in expansion of GC B-cells

The aforementioned effects of *MYC* and *BCL2* in accelerating the formation of GC-derived B-cell lymphomas called for a careful characterization of their effects on GC dynamics. In order to evaluate the consequences of the activation of *MYC* and/or *BCL2* in cell undergoing the germinal center reaction, 7-10 weeks old mice were immunized with intraperitoneal onjections of SRBCs. In this instance, the mice were sacrificed after 10 days, and a fraction of the spleen used for histologic analysis, and the remainder for flow cytometric analysis of germinal center B-cell markers. Most importantly, as immunization concomitantly triggers the GC reaction, activation of Cγ1-*Cre* (Casola et al., 2006) and ensuing recombination of the targeted alleles, this provides an ideal model for studying the short-term effects of *MYC* and/or *BCL2* on GC dynamics.

Activation of either *MYC* or *BCL2* alone caused no significant alteration of spleen size compared to the wild type (Figure 7.14). On the contrary, we observed a significant increase in spleen size in Cγ1-*Cre*; *lsl-MYC; lsl-BCL2* mice when compared with wild type, Cγ1-*Cre*; *lsl-MYC;* or Cγ1-*Cre*; *lsl-BCL2* mice (Figure 7.14). Immunohistochemical analysis of MYC and BCL2 in spleen sections confirmed their expression, either when activated alone, or together (Figure 7.15). Ki67 staining indicated increased proliferation upon activation of *MYC,* either alone or with *BCL2,* but not following activation of *BCL2* alone (Figure 7.15). In order to measure the effect of *MYC* and *BCL2* activation on apoptosis in GC B-cells, we monitored caspase activity by Z-VAD-FMK labelling and flow cytometry (Lee et al., 2017). As expected, we observed a reduction in apoptosis upon *BCL2* activation (Smith et al., 2000); *MYC* activation induced a strong increase in apoptosis, which was fully suppressed by *BCL2* (Figure 7.16).

Altogether, the above results showed that *BCL2* blocked the proapoptotic activity of *MYC* in GC B-cells without affecting its proliferative function, fully in line with numerous observations in distinct contexts and/or cell types (Bissonnette et al., 1992; Fanidi et al., 1992), and providing a strong rationale for the cooperative action of both oncogenes (McDonnell and Korsmeyer, 1991; Strasser et al., 1993). Most noteworthy, Cγ1-*Cre*; *lsl-MYC; lsl-BCL2* mice (whether germ-line or BM-reconstituted) lived for several months without apparent signs of disease, before becoming terminally ill with DHL (Figure 7.2 and Figure 7.3), pointing either to a latent phase of the disease, or to the requirement of additional events in the onset of lymphomagenesis.

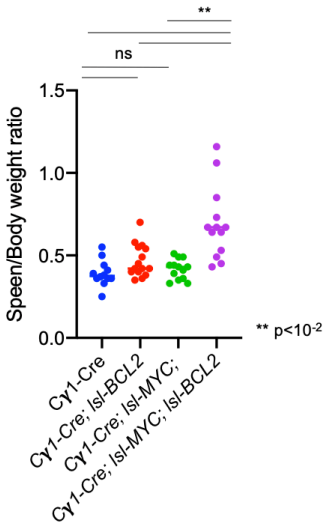

Figure 7.14 Stage specific short-term GC activation of MYC and BCL2 results in spleen enlargement.
Spleen samples were collected from 12 WT, 13 Cγ1-*Cre*; *lsl-MYC; lsl-BCL2* 13 Cγ1-*Cre*; *lsl-MYC;* and 14 Cγ1-*Cre*; *lsl-BCL2* mice 10 days upon SRBC immunization. Summary plot representing the spleen/body weight ratio calculated for each genotype.

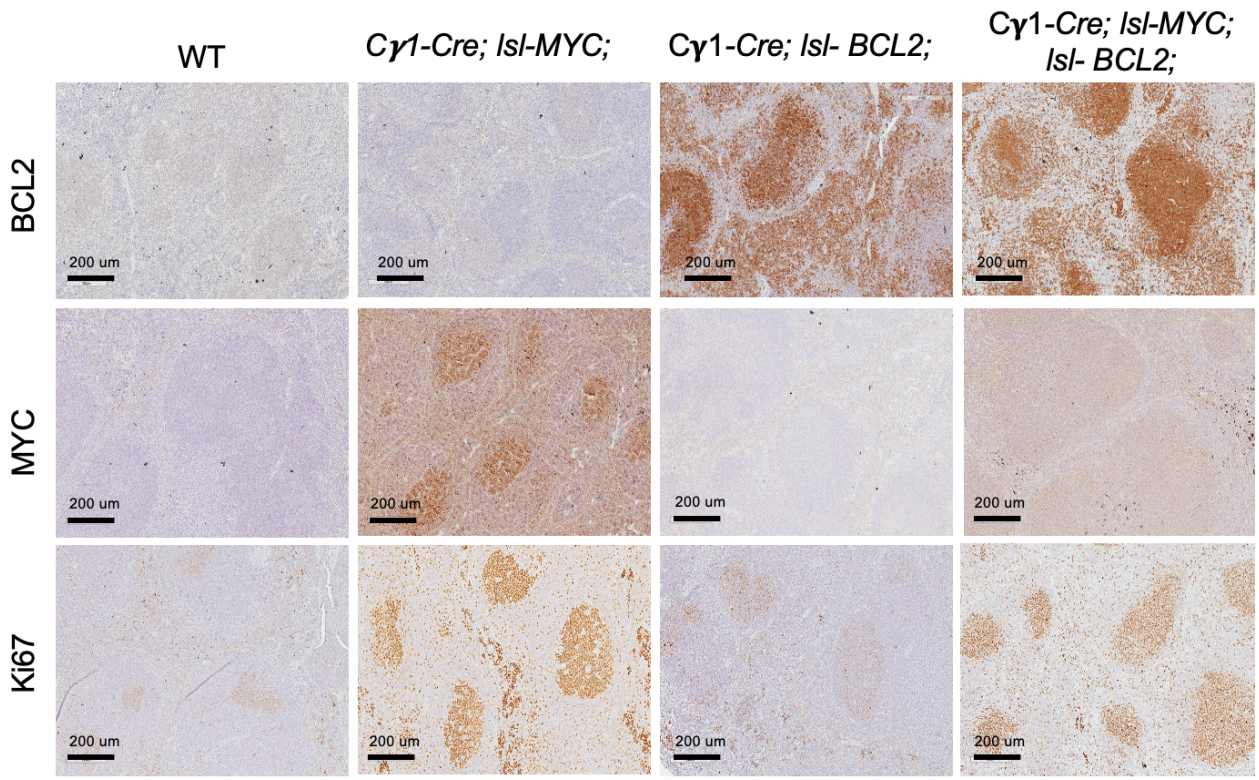

Figure 7.15 IHC staining of MYC, BCL2 and Ki67 upon short-term GC activation.
Spleen samples were collected from Cγ1-*Cre; lsl-MYC; lsl-BCL2*, Cγ1-*Cre; lsl-MYC*; and Cγ1-*Cre; lsl-BCL2* reconstituted mice 10 days upon SRBC immunization. Representative paraffin embedded sections stained with hBCL2 (top), MYC (middle) and Ki67 (bottom) antibodies. Similar results were observed in 3 independent samples for each genotype.

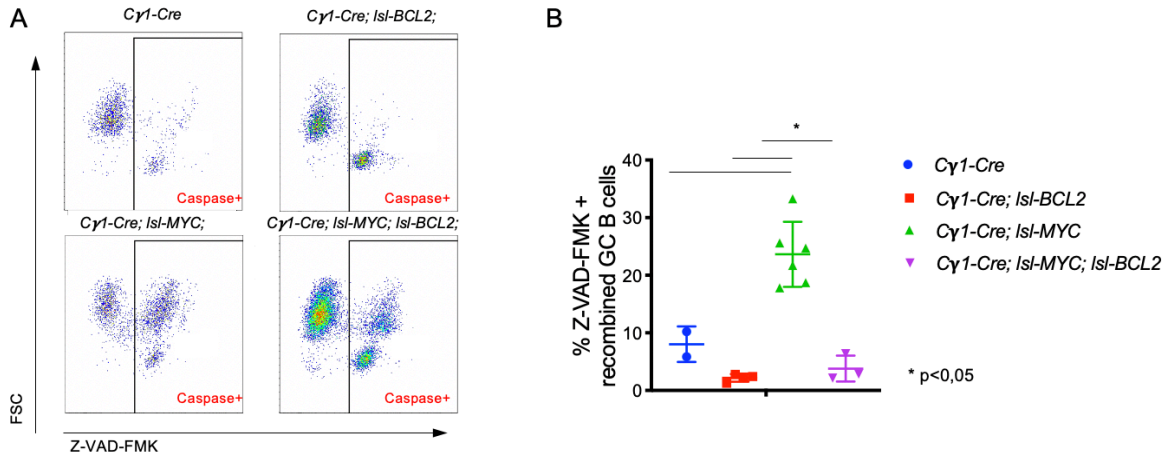

Figure 7.16 Analysis of apoptosis upon stage specific short term MYC and BCL2 activation.
Spleen samples were collected from 12 WT, 13 Cγ1-*Cre*; *lsl-MYC; lsl-BCL2* ,13 Cγ1-*Cre*; *lsl-MYC;* and 14 Cγ1-*Cre*; *lsl-BCL2* mice 10 days upon SRBC immunization. Dot plot showing cells gated on GC B cells positive for GFP (upper right); hCD2 (lower left) or both (lower right). **A**: Flow cytometric analysis of splenic B cells stained with Z-VAD-FMK. **B**: Summary plot of mice analyzed is shown.

In order to follow the progress of GC reaction upon activation of *MYC* and/or *BCL2*, we stained the cells with CD38 and CD95 in order to mark the FO, the putative "pre-GC" (see discussion chapter) and GC compartments, as described above for the profiling of tumors. Most importantly, neither of the oncogene combinations altered the percentage of B-cell in the spleens of SRBC-immunized mice, as judged from the pan B-cell marker CD19 (Figure 7.17A). However, either *MYC* or *BCL2* alone led to increased GC B-cell numbers, as previously observed (Egle et al., 2004; Sander et al., 2012) (Figure 7.17B, C). Remarkably, while co-activation of MYC and *BCL2* showed no significant effect on the conventional GC compartment (CD19+, $CD38^{low}$, $CD95^{hi}$), it caused a major accumulation of "pre-GC" B-cells (CD19+, $CD38^{hi}$, $CD95^{hi}$). Most relevant in this regard, immunohistochemical staining for PNA confirmed the net expansion of a GC-like areas upon activation of the oncogenes (Figure 7.18). Quantification of numbers and areas of GCs (performed by Stefano Freddi, IEO) revealed that while *MYC* had a modest - albeit significant - effect in this regard, the effect of *BCL2* was stronger, with no further change upon co-activation of *MYC*. Finally, staining for CD86 and CXCR4 (Victora et al., 2012)

revealed a strong increase in the DZ/LZ ratio upon the action of BCL2, with no significant contribution of MYC (Figure 7.19). Altogether, we conclude that the concomitant activation of *MYC* and *BCL2* in GC B-cells causes a significant expansion of this compartment but is accompanied by alterations in GC maturation and/or dynamics, the nature of which remains to be addressed.

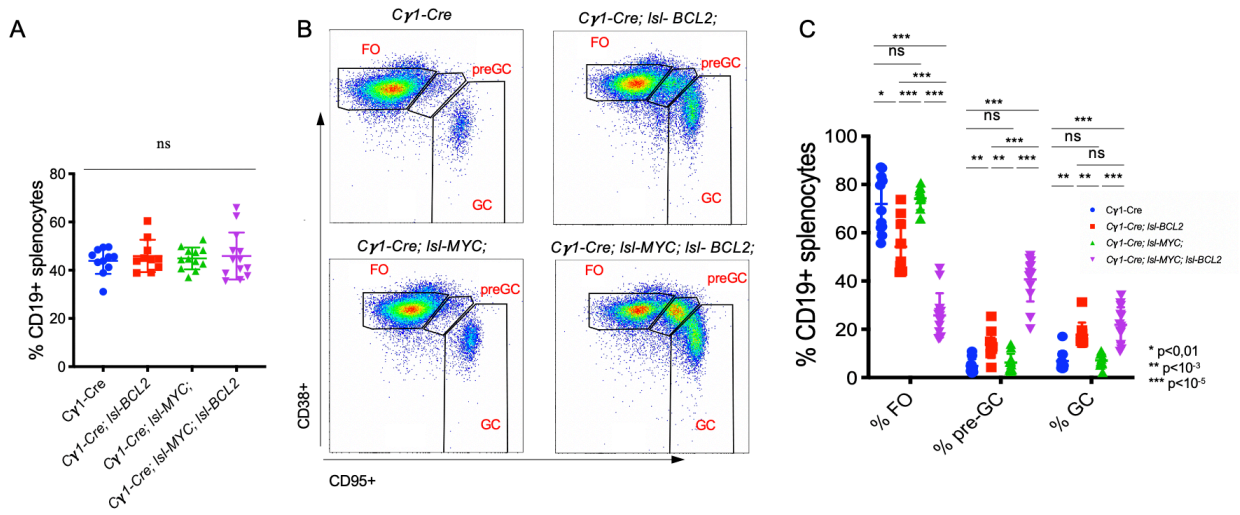

Figure 7.17 GC expansion upon stage specific short-term activation of MYC and BCL2.
Spleen samples were collected from 12 WT, 13 Cγ1-*Cre*; *lsl-MYC; lsl-BCL2* ,13 Cγ1-*Cre*; *lsl-MYC;* and 14 Cγ1-*Cre*; *lsl-BCL2* mice 10 days upon SRBC immunization. **A**: Percentage of CD19+ cells among different experimental groups were calculated by Flowcytometry. **B:** flow cytometric analysis based on CD95 and CD38 surface markers expression. **C**: summary plot of mice analyzed for each genotype is shown

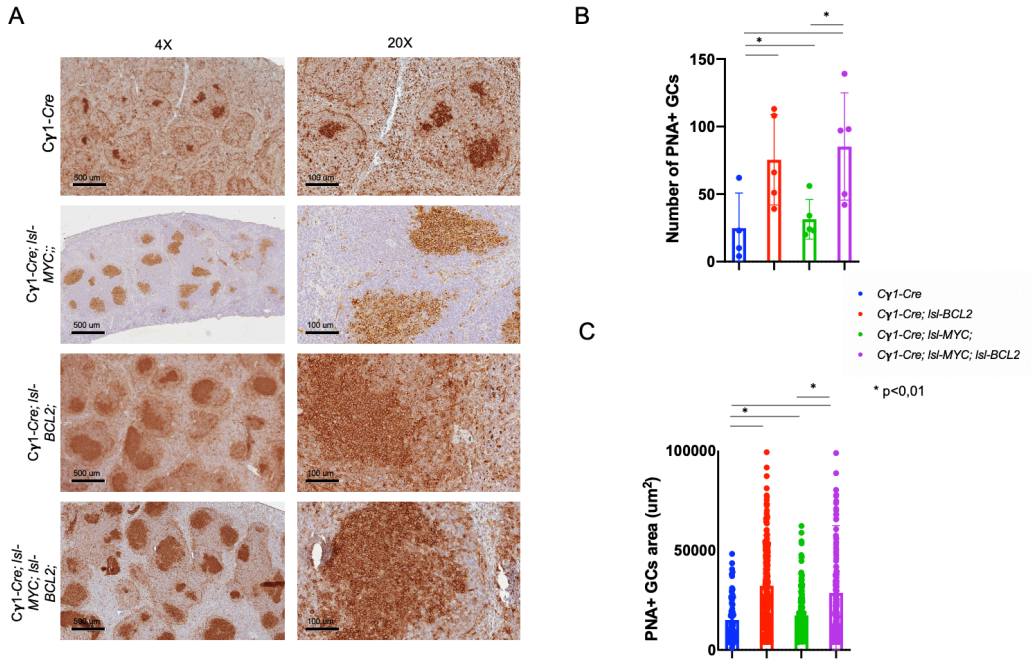

Figure 7.18 Increase number of PNA+ GCs in Cγ1-Cre; lsl-MYC; lsl-BCL2 DHL upon stage specific short-term activation of MYC and BCL2.

Spleen samples were collected from WT, Cγ1-*Cre*; *lsl-MYC; lsl-BCL2*, Cγ1-*Cre*; *lsl-MYC;* and Cγ1-*Cre*; *lsl-BCL2* mice 10 days upon SRBC immunization Paraffin embedded sections were stained with PNA. **A:** Representative PNA staining for controls and DHL; **B:** summary data representing the number of PNA+ GCs among 5 mice analyzed for each experimental group. **C:** summary data representing the size of PNA+ GCs observed in 5 mice analyzed for each experimental group.

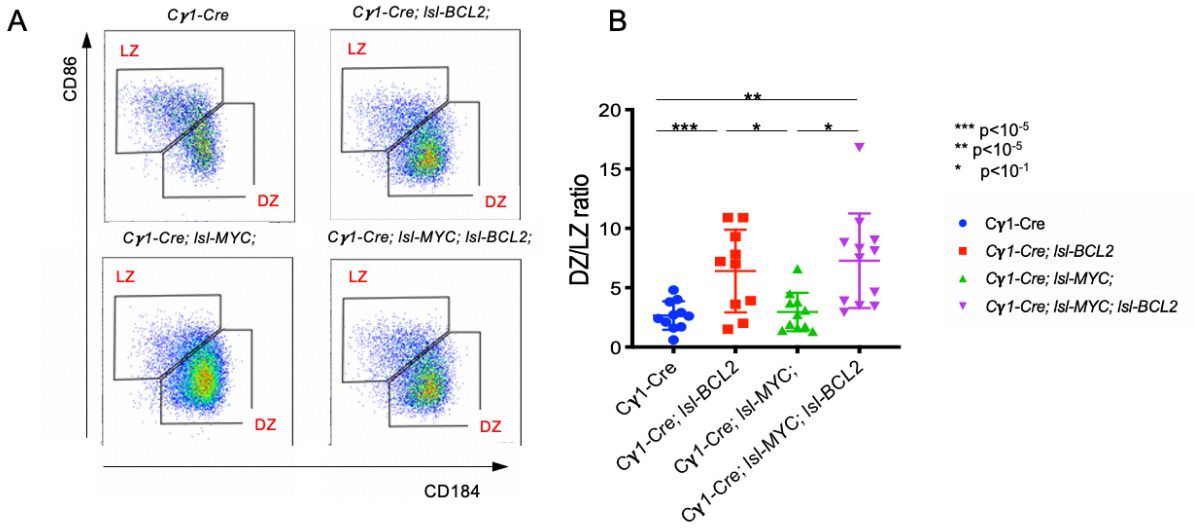

Figure 7.19 BCL2 drive the expansion of DZ present upon concomitant MYC and BCL2 stage specific short-term activation.
Spleen samples were collected from 12 WT, 13 Cγ1-*Cre*; *lsl-MYC; lsl-BCL2* , 13 Cγ1-*Cre*; *lsl-MYC;* and 14 Cγ1-*Cre*; *lsl-BCL2* mice 10 days upon SRBC immunization. **A**: Flow cytometric analysis based on CXCR4 and CD86 surface markers expression (left). Dot plot showing cells gated on GC B cells positive for GFP (upper right); hCD2 (lower left) or both (lower right) **B**: Summary plot of 10 mice analyzed for each genotype is shown (right).

Most noteworthy here, the short-term effects of *MYC* and *BCL2* on GC dynamics described in this section must also initiate the expansion of the cell populations and/or clones that will eventually give rise to DHL tumors, which we have identified based on the signs of terminal illness scored 8/9 months after the initial events (

Figure 7.4). How the initial expansion detected here relates to late-stage DHL lymphomas, and which are the necessary intervening steps in lymphoma development, remains unanswered at this point. Answering these questions is the scope of still-ongoing work, some of which will be described below.

Our current efforts are focusing on three main areas: first, we have profiled gene expression by RNA-seq in our mouse DHL tumors and are currently analyzing those data, with the particular aim to determine their relevance to equivalent profiles in human DLBCL patients: the current state of these analyses will be described below. Second, we have established similar profiles from recombined B-cells following SRBC immunization,

for which we have used either bulk RNA-seq on large numbers of cells (as done for tumor tissue), or single-cell RNA-seq: the analysis of those data is ongoing, and will not be discussed here. Finally, we are completing a series of exome sequencing reactions, aimed at determining whether our mouse DHL tumors acquire consistent patterns of secondary somatic mutations, and how these relate to those described in human tumors. Of these three lines of research, aimed for completion after the defense of my thesis, only the first will developed here.

7.7 Transcriptional profiling of DHL

The aforementioned results show that GC-specific activation of *MYC* and *BCL2* results in the development of a lymphoma that recapitulate the main pathological features of human DHL. In order to further validate this model and assess its similarity to human DLBCL, we analyzed gene expression by RNA-seq in our mouse DHL tumors, with the contribution of Marco Filipuzzi, bioinformatician in our group. In order to obtain a homogeneous cell population for RNA-seq analysis, starting from the cohort of reconstituted Cγ1-*Cre*; *lsl-MYC; lsl-BCL2* mice terminaly ill, we sorted tumor cells crudely isolated from the spleen tacking advantage of the GFP and hCD2 reporters associated with *MYC* and *BCL2* (Fig. 7.6A). On the other hand, to obtain a homogeneous wild type cell population, we used Cγ1-*Cre*; EYFP mice and sorted EYFP+ GC B cells. As shown in Fig. 7.21, the RNA-seq profiles of mDHL tumors showed a high correlation index among all samples (above 90% similarity) (Figure 7.20A). Hierarchical clustering of our profiles alongside those of lymphomas from three other transgenic models (Pascual et al., 2019; Sabò et al., 2014b) further revealed that our mouse DHL tumors formed a uniform cluster, distinct from the other lymphomas (Figure 7.20B).

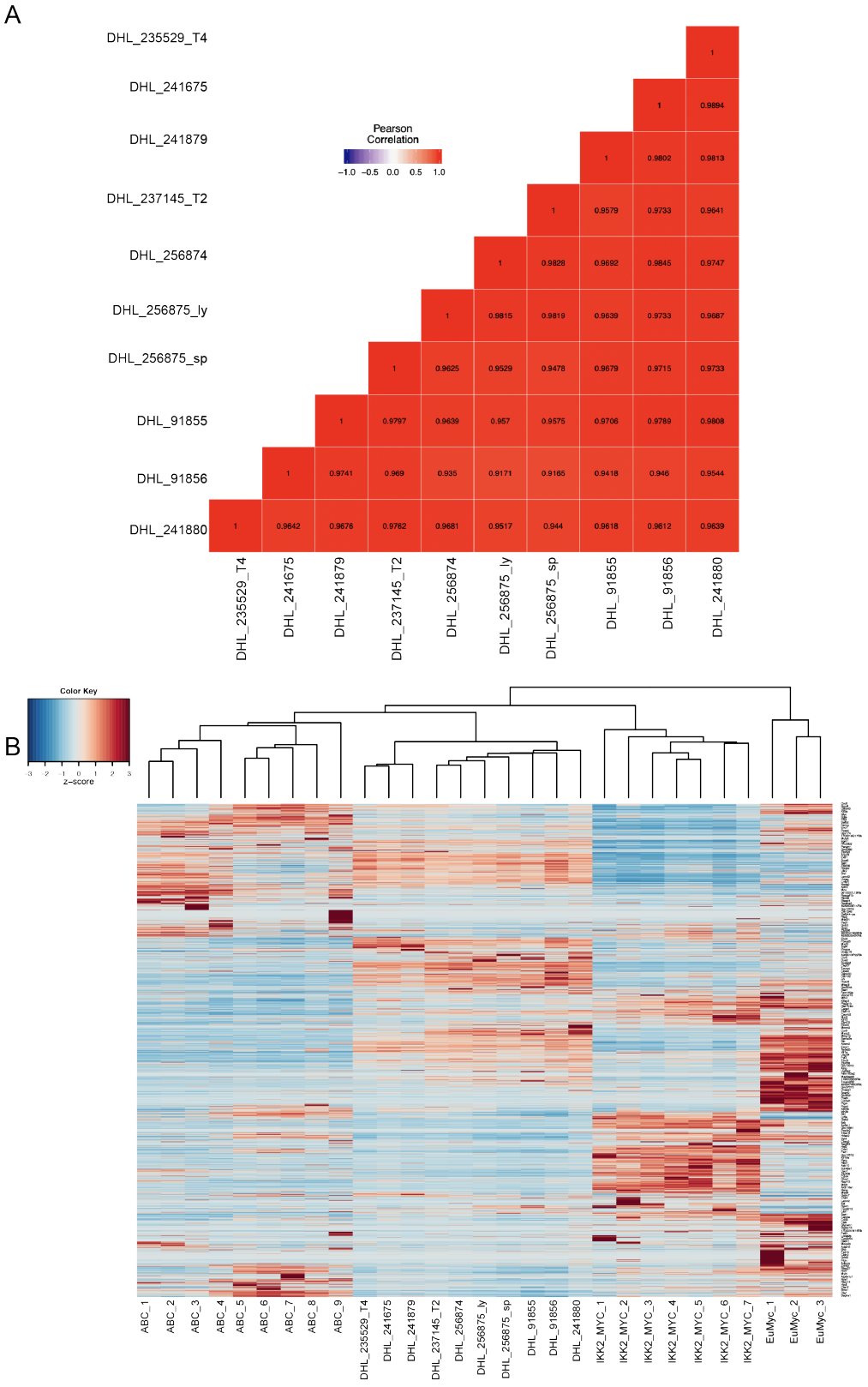

Figure 7.20 DHL tumors are highly correlated between each other.
A: Pearson correlation of reads per kilo base per million mapped reads (RPKM) of each of our 10 DHL samples analyzed; **B**: Unsupervised clustering representing the union of DEG in tumoral samples. From different studies. From left to right, 9 ABC derived lymphomas (Pascual et al., 2019); 10 of our DHL samples; 7 IKK_MYC tumors (Barbosa et al., 2020)and 3 Eμ-*myc* tumors (Sabò et al., 2014b). The color code reports Z-scores value for each gene, colored from the lowest (blue: (-3) to the highest (red: +(3) expression level. Red indicates high relative expression, while blue indicates low relative expression. Informations about analysed lymphomas are in the Materials and methods section.

To further understand the origin of our DHL tumors we took advantage of recently published transcriptomes in various subsets of mature mouse B cells, including GC B cells, bone marrow and splenic plasma cells (PC)**,** peritoneal B1 cells, and FO B cells (Shi et al., 2015), and confronted those with the profiles from our DHL samples, as well as from GC B cells isolated from Cγ1-Cre wild type mice 10 days after SRBC immunization (our controls). We then clustered all those profiles using a reference signature consisting of the 100 most deregulated genes in GC (50 upregulated and 50 downregulated) when comparing the profile of GC B cells (Shi et al., 2015) with all the other B cell subsets mentioned. As shown in Figure 7.21, the samples with the closest similarity to our tumors were GC cells from wild type immunized mice. Furthermore, even if separated in the cluster structure (top), our tumors and the GC B cells profile that we adopted as benchmark (Shi et al., 2015) appear to expressed similar subgroups of genes – albeit with marked difference in expression levels. Noticeably, our DHL tumors showed a transcriptional profile that was highly distinct from those of FO B cells and PC GEPs (Figure 7.21). Altogether, this initial analysis pointed out that our DHL tumors show a GC-like transcriptional profile. We still have to complete this analysis: one example of the ongoing work is to repeat the analysis by excluding genes directy correlated with proliferation in order to exclude the possibility that association of our tumors with GC B cells signature is only a reflection of the proliferative signature.

As introduced above, a fundamental criterion in the classification of DLBCL is the use of gene expression profiling to define the cell of origin, with two main subtypes referred to as germinal center (GCB) or activated B-cell (ABC) (Scott et al., 2015; Scott et al., 2014; Swerdlow et al., 2016; Wright et al., 2020). This subdivision has proven prognostic value and correlates with significant differences in the molecular pathogenesis of the tumors. (Roschewski et al., 2014; Wright et al., 2020). Hence, we interrogated our samples, taking advantage of a 19 genes that define the distinction of human DLBCL into the ABC or GCB

subtypes (Wright et al., 2020). As described in Figure 7.22, our DHL tumors and wild type GC samples were closely clustered in this analysis and enriched for the GCB gene signature. Conversely, the other tumors considered here clustered apart and enriched either for ABC genes such ad “IKK_MYC” samples (even if these tumors are derived from the transformation of plasmablasts) or a different combination of the ABC and GCB genes (”ABC” samples).

Altogether, these initial RNA-seq analyses indicated that MYC and *BCL2* overexpression in GC B cells gave rise to a DHL tumors that transcriptionally differ from three recently published mouse model (Barbosa et al., 2020; Pascual et al., 2019; Sabò et al., 2014b) (Figure 7.20). These preliminary results highlight the need for further in-depth analysis of transcriptional profiles in our DHL model, with the particular aim to determine its relevance and similarity to equivalent profiles in human DLBCL patients. These analyses will be carried on after the discussion of my PhD.

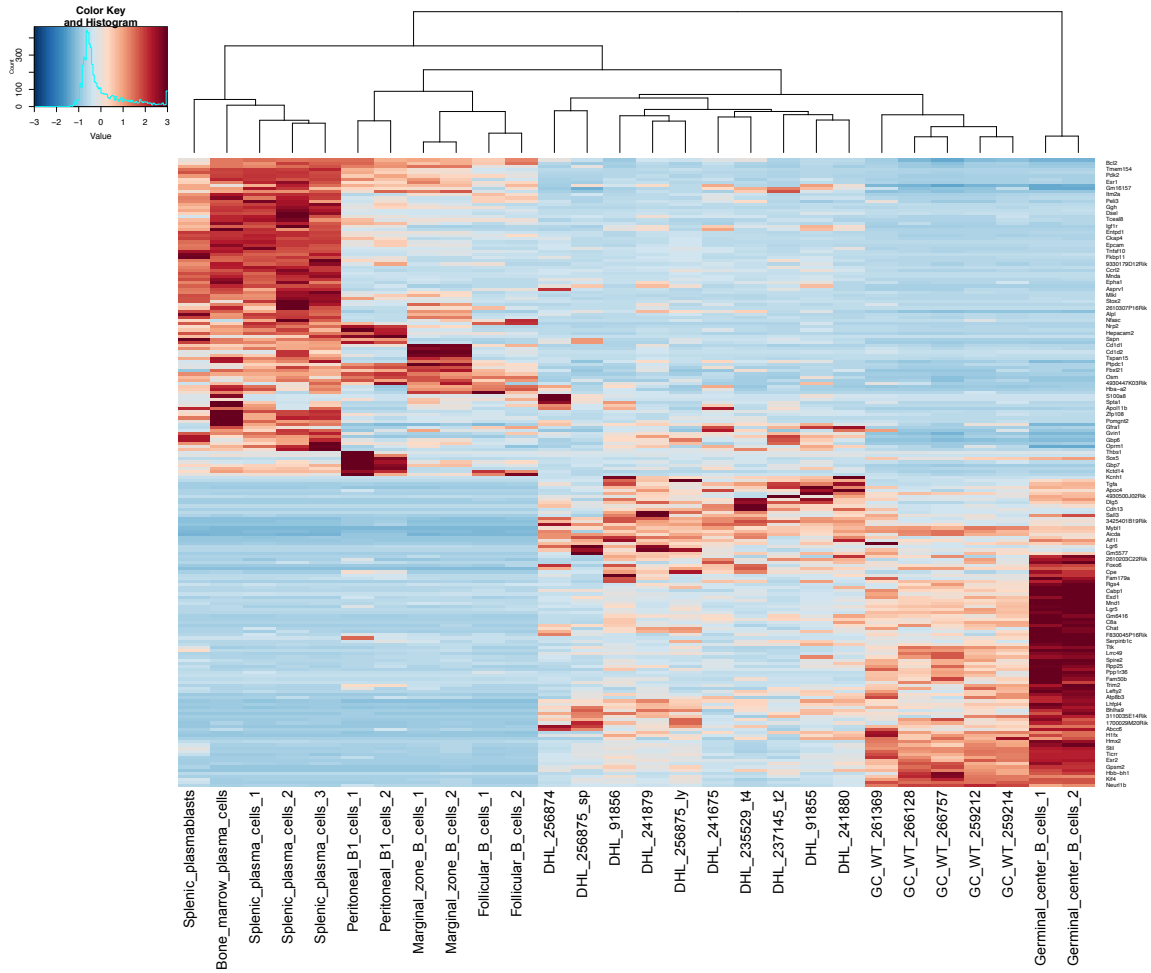

Figure 7.21 DHL tumors are transcriptionally enriched for GC B cell signature.
Unsupervised clustering representing the union of DEG in tumoral samples from different studies. From left to right; bone marrow and splenic plasma cells (PC), peritoneal B1 cells, MZ and FO B cells (Shi et al., 2015); 10 of our DHL samples; 5 of our wild type GC samples; including GC B cells (Shi et al., 2015). The color code reports Z-scores value for each gene, colored from the lowest (blue: (-3) to the highest (red: +(3) expression level. Red indicates high relative expression, while blue indicates low relative expression.

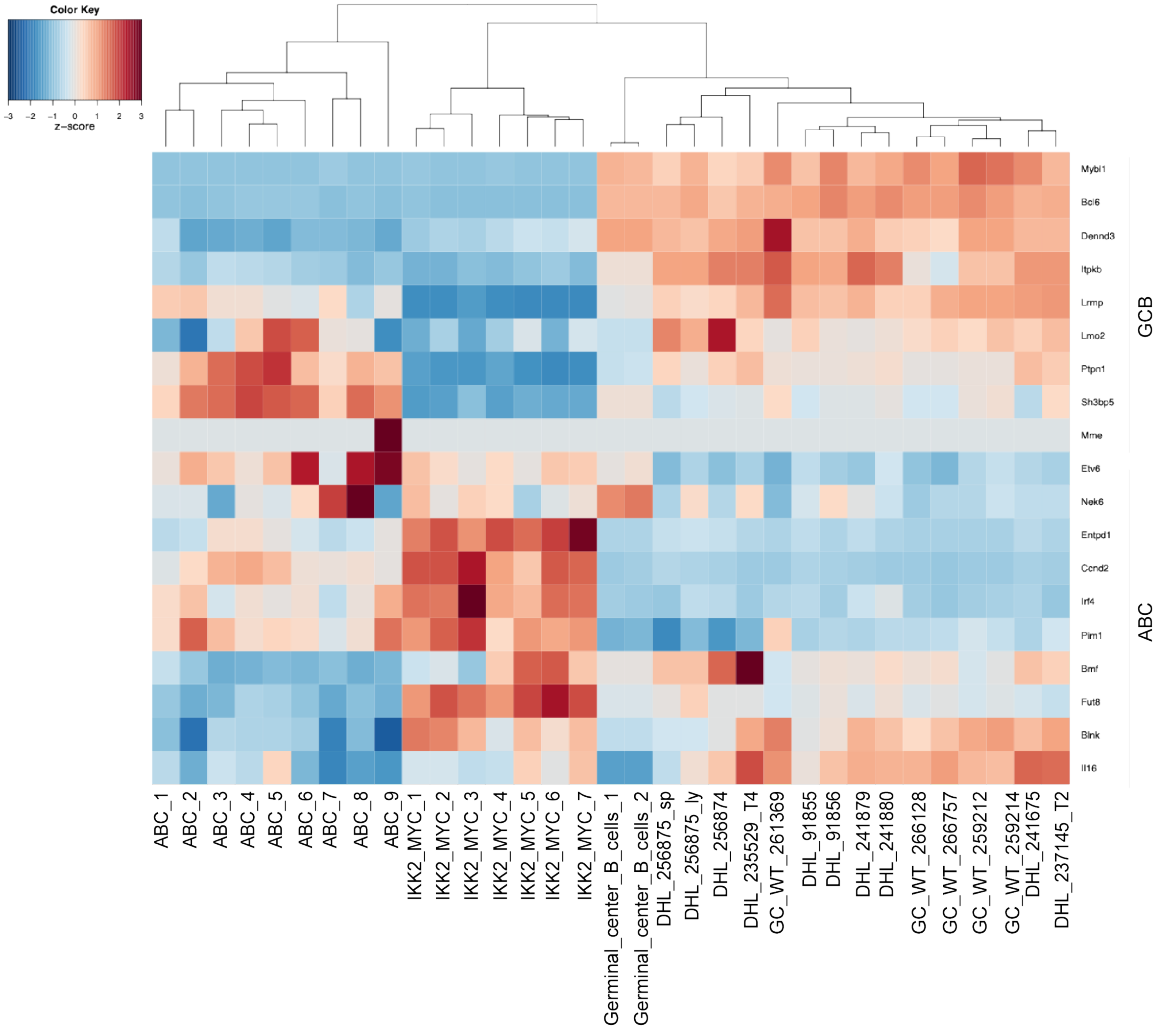

Figure 7.22 DHL tumors have GCB cell of origin.
Hierarchical cluster analysis based on relative transcript levels of 19 genes comprised in a ABC/GCB signature (Wright et al., 2020) of DHL and tumoral samples from different studies: from left to right 9 ABC derived lymphomas (Pascual et al., 2019); 7 IKK_MYC tumors (Barbosa et al., 2020); Germinal Center B cell GEP (Shi et al., 2015); 10 of our DHL tumor and 5 of our wild type GC controls. The color code reports Z-scores value for each gene, colored from the lowest (blue: (-3) to the highest (red: +(3) expression level. Red indicates high relative expression, while blue indicates low relative expression.

8 Discussion

Chromosomal translocations affecting *MYC* and *BCL2* are associated with the occurrence of various B-cell lymphomas. In a subset of DLBCL cases co-ocurrent *MYC* and *BCL2* translocations accumulate, giving rise to particularly aggressive double-hit lymphomas (DHL), which show dismal prognosis in the face of current front-line therapies (Anderson et al., 2016; Basso and Dalla-Favera, 2015; Friedberg, 2017; Karube and Campo, 2015; Rosenquist et al., 2017; Rosenthal and Younes, 2017; Sarkozy et al., 2015; Sesques and Johnson, 2017). In a fraction of DHL, translocations occur at the GC stage of B-cell differentiation (Pasqualucci and Dalla-Favera, 2018), in line with the fact that those DHL generally classifies as GCB in the cell-of-origin classification (Friedberg, 2017; Wright et al., 2020).

Although the cooperativity between *MYC* and *BCL2* has been described in different mouse models (Hemann et al., 2005; Leskov et al., 2013; Letai et al., 2004; Marin et al., 1995; McDonnell and Korsmeyer, 1991; Ortega-Molina et al., 2015; Schuster et al., 2011; Strasser et al., 1990a), none of these reproduces the GC cell of origin of DHL. As a result, we sought to build and characterize a new DHL model that accurately reproduces the human disease, with the initial aim of dissecting the mechanisms of disease progression at the molecular, cellular and organism levels. Having a model that can reproduce human disease in a faithful manner constitutes a fundamental step toward the development of preclinical studies.

We generated a cohort of Cγ1-*Cre; lsl-MYC; lsl-BCL2* mice that have GC specific deregulation of both *MYC* and *BCL2* (Chapter 7.1). These mice were subsequently used for the generation of bone marrow reconstituted RAG1 mice that we followed for lymphoma development. Indeed, Cγ1-*Cre; lsl-MYC; lsl-BCL2* reconstituted animals showed accelerated lymphomagenesis, confirming the

cooperation of two oncogenes in lymphoma development (Hemann et al., 2005; Leskov et al., 2013; Letai et al., 2004; Schuster et al., 2011; Strasser et al., 1990a). The resulting tumors accurately phenocopy their human counterparts, showing similar immunophenotypic profiles that recall DLBCL or BL human lymphomas (Chapter 7.1). Based on the presence of two independent GC markers, PNA and BCL6, together with the expression of the various GC B cell surface markers, such as CD95, CD38, CD86 and CXCR4 that were measured by IHC or flow cytometry, we confirmed that our tumors are derived from GC B cells (Chapter 7.1), with a DZ-like phenotype (Chapter 7.3).

In order to fully characterize our DHL model, its relevance to human DHL and the GC origin of the lymphomas, we profiled tumors by RNA sequencing. As we could expect from the molecular characterization discussed above, these experiments revealed an evident similarity between the transcriptional profile of our DHL tumors and wild type GC B cells - either from our experimental controls, or from publicly available datasets (Shi et al., 2015). In addition, the profiles of our tumors showed no similarities with other mature B cell subsets, such as Follicular B cells or Plasma cells (Shi et al., 2015) (Chapter 7.8). Hence, the mRNA profiles confirmed that our tumors are of GC origin. Furthermore, comparison between a signature of 19 that defines the distinction of human DLBCL into the ABC or GCB subtypes (Wright et al., 2020) (Chapter 7.8) and our tumors confirmed that the latter strongly correlated with the GCB signature, fully recapitulating the cell of origin of human DHL (Roschewski et al., 2014; Wright et al., 2020).

In parallel to the Cγ1-*Cre* driven model, we addressed whether deregulation of *MYC* and *BCL2* under the control of CD19-*Cre*, which drives recombination in the earliest precursors of B cells (Rickert et al., 1997), would also elicit tumor development,

and how this would compare with the above. While confirming the strong cooperativity of *MYC* and *BCL2* in lymphomagenesis, the resulting tumors were not derived from the GC stage, confirming that these oncogenes have the propensity to instruct tumor initiation at various stages of B cell development, if inappropriately activated. More specifically, FACS analysis of tumors arising in CD19-*Cre; lsl-MYC; lsl-BCL2* animals revealed a different phenotype compared to that of their Cγ1-*Cre* counterpart, with a $CD38^{hi}/CD95^{hi}$ surface antigen profile that we refer to as "pre-GC", rather than GC (**Error! Reference source not found.** A, C). The nature and correct assignment of this "pre-GC" stage in our tumors, however, remains to be fully evaluated.

Our tentative classification of the $CD38^{hi}/CD95^{hi}$ profile as "pre-GC" is based on previous studies of physiological GC dynamics, in a non-tumoral context. In particular, a B cell population with similar surface characteristics was described in both mouse and human, and attributed a pre-GC status (Kolar et al., 2007; Roco et al., 2019; Zheng et al., 2004). In particular, the most recent of these studies supports the idea that class switch recombination (CSR) is not an exclusive process that occurs in GCs - as commonly believed in the field - but most largely outside, and prior to entry of B cells into the GC reaction (Roco et al., 2019): according to this model, CSR is initiated early upon immunization (day 1.5) in $CD38^{hi}$, $CD95^{hi}$ pre-GC B cells, and terminates as soon as the cells enter the GC and start somatic hypermutation (SHM) and clonal selection based on the affinity of the B cell receptor (BCR) for the immunizing antigen. Based on these observations, one possible scenario in our model is that activation of *MYC* and *BCL2* under the control of CD19-*Cre* or Cγ1-*Cre* may promote the expansion and/or transformation of different B cell subsets, giving rise to the tumors observed in each model. In the case of CD19-*Cre*, which induces recombination in the whole B-cell lineage, we surmise that these tumor precursors may be stalled at the $CD38^{hi}/CD95^{hi}$

stage (i.e. before entering into the GC reaction): while this remains to be addressed in the CD19-*Cre* driven model, we have initiated the characterization of early steps in Cγ1-*Cre; lsl-MYC; lsl-BCL2* animals, as will be discussed below.

In order to characterize the early stages of tumorigenesis in the Cγ1-*Cre; lsl-MYC; lsl-BCL2* model, we sought to study the effects of *MYC* and/or *BCL2* activation in cells undergoing the germinal center reaction. Toward this aim, we activated the GC reaction through SRBC immunization, and followed the short-term effects of *MYC* and *BCL2* by measuring the expansion of GC B-cells by IHC and FACS analysis (Chapter 7.7). *BCL2* blocked the proapoptotic activity of *MYC* in GC B-cell which was accompanied by an increase in DZ GC B cells compartment upon *BCL2* overexpression. This result is fully in line with other contexts and/or cell types, where *BCL2* blocked the proapoptotic activity of *MYC*, without affecting its proliferative function (Bissonnette et al., 1992; Fanidi et al., 1992). As a matter of fact, Ki67 staining upon short term SRBC immunization suggested an increased proliferation upon activation of *MYC,* either alone or with *BCL2,* but not following activation of *BCL2* alone. However, at this stage, we still need a direct assay to quantify GC B cell proliferation (for example EdU proliferation assay) (Buck et al., 2008) upon SRBC immunization. Finally, in parallel with the characterization of cellular phenotypes, we established RNA-seq profiles from recombined GC B-cells upon short-term activation of the GC reaction, with and without the concomitant activation *MYC* and/or *BCL2*: in this instance, we used either bulk RNA-seq (as done for tumor tissue) or single-cell RNA-seq: the analysis of those data is ongoing. Together with the accurate characterization of cellular phenotypes, these experiments shall instruct us on the early impact of the oncogenes on GC dynamics, and hopefully allow us to narrow down on the cells that give origin to the resulting tumors.

Altogether, our studies of short term GC activation provided a strong rationale for the cooperation between *MYC* and *BCL2* in the GC, generally confirming the synergistic action of the oncogenes when activated in diverse cellular compartment, owing to their differential activities in proliferation and survival (Bissonnette et al., 1992; Fanidi et al., 1992). Most noteworthy however, this did not lead to rapid tumor development, as the mice survived for several months without apparent signs of disease before becoming terminally ill with DHL (Chapter 7.1), suggesting a latent phase of the disease or the requirement of additional events in the onset of lymphomagenesis. This aspect revealed the necessity to determine whether our mouse DHL tumors acquire consistent patterns of secondary somatic mutations, and how these relate to those described in human tumors. This part of the work is ongoing, with a series of exome sequencing reactions that shall help us answer two fundamental questions: how the initial expansion detected here relates to late-stage DHL lymphomas, and which are the necessary intervening steps in lymphoma development.

Another fundamental aspect in the progression of our work is the stabilization of mDHL cell lines isolated from sick mice for *in vitro* expansion and characterization (Chapter 7.5), which is important for two main reasons. First, having the possibility to work *in vitro* can allow us to test the effects of different drug combination in a more feasible manner. Accordingly, following from a recent study in our group, we tested the effect of two targeted drugs - Tigecycline and Venetoclax - and observed a strong synergistic effect in the killing of mDHA cells, as previously reported in human DHL cell lines (Rava et al., 2018): this confirms that our mDHL lines provide an additional tool for the study of drug interactions in pre-clinical development against this aggressive lymphoma subtype (Chapter 7.5).

Second, having mDHL cells growing *in vitro* gave us the possibility to modify them and build a tracking system (based on luciferase expression) to follow their expansion upon *in vivo* transplantation (Chapter 7.6). Remarkably, our mDHL tumors successfully expanded in immunodeficient NSG recipients, but not in syngeneic, immun-competent C57/J animals. This result, made us hypothesize that our DHL could need a specific microenvironment to prevent rejection and develop in C57/J mice, which could conceivably be overcome by transplanting DHL cells directly in a less immunologically exposed compartment, such as the spleen: while the experiment is still ongoing, out initial observations suggest that this is not sufficient to bypass rejections and allow tumor growth. Altogether, our data suggest that our mDHL clones are strongly immunogenic, thus provoking T-cell dependent tumor rejection in immunocompetent mice. One possible cause of rejection might be that our mDHL tumors express exogenous antigens, such as the the *MYC- and BCL2*-associated reporters hCD2 and GFP, which elicit their rejection in non-transgenic recipients. Since we worked before with GFP+ lymphoma models, which were transplantable in C57/J recipients analogous to those used here, we tend to exclude an immunogenic potential of GFP. On the other hand, we are still investigating whether rejection might be due to the presence of hCD2: in particular, we are trying to obtain immunocompetent recipient mice that activate hCD2 in the germline and should thus recognize this antigen as self. Alternatively, and most relevant to the biology of our model, the mDHL cells might be immunogenic based on endogenous, tumor-associated antigens, the nature of which remains to be understood. Unraveling this issue would not only be informative in terms of the molecular and systemic mechanisms underlying disease development but would also be strategic toward development of a fully representative pre-clinical

model, taking into account the effects of the immune system in the responses to pharmacological intervention, and allowing to address immunological therapies.

Altogether, we set up a novel mouse model of DHL that faithfully recapitulates the cellular GC origin of the human disease, as confirmed at the histological, molecular and transcriptional levels. Ongoing work will allow us to fully understand the dynamics and mechanisms of disease, as well as the early impact of Myc and Bcl2 on the dynamics of the GC reaction. A comprehensive characterization of our DHL model shall provide an advanced, tractable experimental platform for the extension of pre-clinical studies toward novel therapeutic combinations, hopefully allowing us to account for the full complexity of host-disease interactions.

9 References

Adams, J.M., and Cory, S. (2018). The BCL-2 arbiters of apoptosis and their growing role as cancer targets. Cell Death Differ *25*, 27-36.

Akhtar, R.S., Klocke, B.J., Strasser, A., and Roth, K.A. (2008). Loss of BH3-only protein Bim inhibits apoptosis of hemopoietic cells in the fetal liver and male germ cells but not neuronal cells in bcl-x-deficient mice. J Histochem Cytochem *56*, 921-927.

Alevizopoulos, K., Vlach, J., Hennecke, S., and Amati, B. (1997). Cyclin E and c-Myc promote cell proliferation in the presence of p16INK4a and of hypophosphorylated retinoblastoma family proteins. EMBO J *16*, 5322-5333.

Allen, C.D., Ansel, K.M., Low, C., Lesley, R., Tamamura, H., Fujii, N., and Cyster, J.G. (2004). Germinal center dark and light zone organization is mediated by CXCR4 and CXCR5. Nat Immunol *5*, 943-952.

Allen, C.D., Okada, T., and Cyster, J.G. (2007). Germinal-center organization and cellular dynamics. Immunity *27*, 190-202.

Amati, B., Brooks, M.W., Levy, N., Littlewood, T.D., Evan, G.I., and Land, H. (1993a). Oncogenic activity of the c-Myc protein requires dimerization with Max. Cell *72*, 233-245.

Amati, B., Dalton, S., Brooks, M.W., Littlewood, T.D., Evan, G.I., and Land, H. (1992). Transcriptional activation by the human c-Myc oncoprotein in yeast requires interaction with Max. Nature *359*, 423-426.

Amati, B., and Land, H. (1994). Myc-Max-Mad: a transcription factor network controlling cell cycle progression, differentiation and death. Curr Opin Genet Dev *4*, 102-108.

Amati, B., Littlewood, T.D., Evan, G.I., and Land, H. (1993b). The c-Myc protein induces cell cycle progression and apoptosis through dimerization with Max. EMBO J *12*, 5083-5087.

Anderson, M.A., Tsui, A., Wall, M., Huang, D.C., and Roberts, A.W. (2016). Current challenges and novel treatment strategies in double hit lymphomas. Ther Adv Hematol *7*, 52-64.

Arabi, A., Wu, S., Ridderstrale, K., Bierhoff, H., Shiue, C., Fatyol, K., Fahlen, S., Hydbring, P., Soderberg, O., Grummt, I.*, et al.* (2005). c-Myc associates with ribosomal DNA and activates RNA polymerase I transcription. Nat Cell Biol *7*, 303-310.

Arbour, N., Vanderluit, J.L., Le Grand, J.N., Jahani-Asl, A., Ruzhynsky, V.A., Cheung, E.C., Kelly, M.A., MacKenzie, A.E., Park, D.S., Opferman, J.T.*, et al.* (2008). Mcl-1 is a key regulator of apoptosis during CNS development and after DNA damage. J Neurosci *28*, 6068-6078.

Arnold, H.K., and Sears, R.C. (2006). Protein phosphatase 2A regulatory subunit b56 alpha associates with c-Myc and negatively regulates c-Myc accumulation. Molecular and Cellular Biology *26*, 2832-2844.

Aukema, S.M., Siebert, R., Schuuring, E., van Imhoff, G.W., Kluin-Nelemans, H.C., Boerma, E.J., and Kluin, P.M. (2011). Double-hit B-cell lymphomas. Blood *117*, 2319-2331.

Bakhshi, A., Jensen, J.P., Goldman, P., Wright, J.J., McBride, O.W., Epstein, A.L., and Korsmeyer, S.J. (1985). Cloning the chromosomal breakpoint of t(14;18) human lymphomas: clustering around JH on chromosome 14 and near a transcriptional unit on 18. Cell *41*, 899-906.

Barbosa, R., Xu, A., D'Andrea, D., Copley, F., Patel, H., Chakravarty, P., Clear, A., Calaminici, M., Janz, M., Zhang, B.*, et al.* (2020). Co-activation of NF-kB and MYC renders cancer cells addicted to IL6 for survival and phenotypic stability
. bioRxiv.

Barrans, S., Crouch, S., Smith, A., Turner, K., Owen, R., Patmore, R., Roman, E., and Jack, A. (2010). Rearrangement of MYC is associated with poor prognosis in patients with diffuse large B-cell lymphoma treated in the era of rituximab. J Clin Oncol *28*, 3360-3365.

Basso, K., and Dalla-Favera, R. (2015). Germinal centres and B cell lymphomagenesis. Nat Rev Immunol *15*, 172-184.

Beier, R., Burgin, A., Kiermaier, A., Fero, M., Karsunky, H., Saffrich, R., Moroy, T., Ansorge, W., Roberts, J., and Eilers, M. (2000). Induction of cyclin E-cdk2 kinase activity, E2F-dependent transcription and cell growth by Myc are genetically separable events. EMBO J *19*, 5813-5823.

Bemark, M., and Neuberger, M.S. (2000). The c-MYC allele that is translocated into the IgH locus undergoes constitutive hypermutation in a Burkitt's lymphoma line. Oncogene *19*, 3404-3410.

Bentley, D.L., and Groudine, M. (1986). A block to elongation is largely responsible for decreased transcription of c-myc in differentiated HL60 cells. Nature *321*, 702-706.

Bereshchenko, O.R., Gu, W., and Dalla-Favera, R. (2002). Acetylation inactivates the transcriptional repressor BCL6. Nat Genet *32*, 606-613.

Bergman, Y. (1999). Allelic exclusion in B and T lymphopoiesis. Semin Immunol *11*, 319-328.

Beroukhim, R., Mermel, C.H., Porter, D., Wei, G., Raychaudhuri, S., Donovan, J., Barretina, J., Boehm, J.S., Dobson, J., Urashima, M.*, et al.* (2010). The landscape of somatic copy-number alteration across human cancers. Nature *463*, 899-905.

Beverly, L.J., and Varmus, H.E. (2009). MYC-induced myeloid leukemogenesis is accelerated by all six members of the antiapoptotic BCL family. Oncogene *28*, 1274-1279.

Bhatia, K., Huppi, K., Spangler, G., Siwarski, D., Iyer, R., and Magrath, I. (1993). Point mutations in the c-Myc transactivation domain are common in Burkitt's lymphoma and mouse plasmacytomas. Nat Genet *5*, 56-61.

Bhatia, K., Spangler, G., Gaidano, G., Hamdy, N., Dalla-Favera, R., and Magrath, I. (1994). Mutations in the coding region of c-myc occur frequently in acquired immunodeficiency syndrome-associated lymphomas. Blood *84*, 883-888.

Bianchi, V., Ceol, A., Ogier, A.G., de Pretis, S., Galeota, E., Kishore, K., Bora, P., Croci, O., Campaner, S., Amati, B.*, et al.* (2016). Integrated Systems for NGS Data Management and Analysis: Open Issues and Available Solutions. Front Genet *7*, 75.

Bisso, A., Sabo, A., and Amati, B. (2019). MYC in Germinal Center-derived lymphomas: Mechanisms and therapeutic opportunities. Immunol Rev *288*, 178-197.

Bissonnette, R.P., Echeverri, F., Mahboubi, A., and Green, D.R. (1992). Apoptotic cell death induced by c-myc is inhibited by bcl-2. Nature *359*, 552-554.

Blackwood, E.M., and Eisenman, R.N. (1991). Max: a helix-loop-helix zipper protein that forms a sequence-specific DNA-binding complex with Myc. Science *251*, 1211-1217.

Bouchard, C., Marquardt, J., Bras, A., Medema, R.H., and Eilers, M. (2004). Myc-induced proliferation and transformation require Akt-mediated phosphorylation of FoxO proteins. EMBO J *23*, 2830-2840.

Bouillet, P., Cory, S., Zhang, L.C., Strasser, A., and Adams, J.M. (2001). Degenerative disorders caused by Bcl-2 deficiency prevented by loss of its BH3-only antagonist Bim. Dev Cell *1*, 645-653.

Bouillet, P., Metcalf, D., Huang, D.C., Tarlinton, D.M., Kay, T.W., Kontgen, F., Adams, J.M., and Strasser, A. (1999). Proapoptotic Bcl-2 relative Bim required for certain apoptotic responses, leukocyte homeostasis, and to preclude autoimmunity. Science *286*, 1735-1738.

Bouillet, P., Purton, J.F., Godfrey, D.I., Zhang, L.C., Coultas, L., Puthalakath, H., Pellegrini, M., Cory, S., Adams, J.M., and Strasser, A. (2002). BH3-only Bcl-2 family member Bim is required for apoptosis of autoreactive thymocytes. Nature *415*, 922-926.

Boylan, K.L., Gosse, M.A., Staggs, S.E., Janz, S., Grindle, S., Kansas, G.S., and Van Ness, B.G. (2007). A transgenic mouse model of plasma cell malignancy shows phenotypic, cytogenetic, and gene expression heterogeneity similar to human multiple myeloma. Cancer Res *67*, 4069-4078.

Bredesen, D.E., Mehlen, P., and Rabizadeh, S. (2004). Apoptosis and dependence receptors: a molecular basis for cellular addiction. Physiol Rev *84*, 411-430.

Bromberg, J.F., Wrzeszczynska, M.H., Devgan, G., Zhao, Y., Pestell, R.G., Albanese, C., and Darnell, J.E., Jr. (1999). Stat3 as an oncogene. Cell *98*, 295-303.

Buck, S.B., Bradford, J., Gee, K.R., Agnew, B.J., Clarke, S.T., and Salic, A. (2008). Detection of S-phase cell cycle progression using 5-ethynyl-2'-deoxyuridine incorporation with click chemistry, an alternative to using 5-bromo-2'-deoxyuridine antibodies. Biotechniques *44*, 927-929.

Burotto, M., Berkovits, A., and Dunleavy, K. (2016). Double hit lymphoma: from biology to therapeutic implications. Expert Rev Hematol *9*, 669-678.

Caeser, R., Di Re, M., Krupka, J.A., Gao, J., Lara-Chica, M., Dias, J.M.L., Cooke, S.L., Fenner, R., Usheva, Z., Runge, H.F.P., *et al.* (2019). Genetic modification of primary human B cells to model high-grade lymphoma. Nat Commun *10*, 4543.

Calado, D.P., Sasaki, Y., Godinho, S.A., Pellerin, A., Kochert, K., Sleckman, B.P., de Alboran, I.M., Janz, M., Rodig, S., and Rajewsky, K. (2012). The cell-cycle regulator c-Myc is essential for the formation and maintenance of germinal centers. Nat Immunol *13*, 1092-1100.

Campaner, S., Doni, M., Hydbring, P., Verrecchia, A., Bianchi, L., Sardella, D., Schleker, T., Perna, D., Tronnersjo, S., Murga, M., *et al.* (2010). Cdk2 suppresses cellular senescence induced by the c-myc oncogene. Nat Cell Biol *12*, 54-59; sup pp 51-14.

Campbell, K.J., Bath, M.L., Turner, M.L., Vandenberg, C.J., Bouillet, P., Metcalf, D., Scott, C.L., and Cory, S. (2010). Elevated Mcl-1 perturbs lymphopoiesis, promotes transformation of hematopoietic stem/progenitor cells, and enhances drug resistance. Blood *116*, 3197-3207.

Caron, G., Le Gallou, S., Lamy, T., Tarte, K., and Fest, T. (2009). CXCR4 expression functionally discriminates centroblasts versus centrocytes within human germinal center B cells. J Immunol *182*, 7595-7602.

Carsetti, R., Kohler, G., and Lamers, M.C. (1995). Transitional B cells are the target of negative selection in the B cell compartment. J Exp Med *181*, 2129-2140.

Casola, S., Cattoretti, G., Uyttersprot, N., Koralov, S.B., Seagal, J., Hao, Z., Waisman, A., Egert, A., Ghitza, D., and Rajewsky, K. (2006). Tracking germinal center B cells expressing germ-line immunoglobulin gamma1 transcripts by conditional gene targeting. Proc Natl Acad Sci U S A *103*, 7396-7401.

Cedar, H., and Bergman, Y. (2008). Choreography of Ig allelic exclusion. Curr Opin Immunol *20*, 308-317.

Chappell, S.A., LeQuesne, J.P., Paulin, F.E., deSchoolmeester, M.L., Stoneley, M., Soutar, R.L., Ralston, S.H., Helfrich, M.H., and Willis, A.E. (2000). A mutation in the c-myc-IRES leads to enhanced internal ribosome entry in multiple myeloma: a novel mechanism of oncogene de-regulation. Oncogene *19*, 4437-4440.

Chapuy, B., Stewart, C., Dunford, A.J., Kim, J., Kamburov, A., Redd, R.A., Lawrence, M.S., Roemer, M.G.M., Li, A.J., Ziepert, M.*, et al.* (2018). Molecular subtypes of diffuse large B cell lymphoma are associated with distinct pathogenic mechanisms and outcomes. Nat Med *24*, 679-690.

Charron, J., Malynn, B.A., Fisher, P., Stewart, V., Jeannotte, L., Goff, S.P., Robertson, E.J., and Alt, F.W. (1992). Embryonic lethality in mice homozygous for a targeted disruption of the N-myc gene. Genes Dev *6*, 2248-2257.

Chaudhuri, J., and Alt, F.W. (2004). Class-switch recombination: interplay of transcription, DNA deamination and DNA repair. Nat Rev Immunol *4*, 541-552.

Chen, L., Willis, S.N., Wei, A., Smith, B.J., Fletcher, J.I., Hinds, M.G., Colman, P.M., Day, C.L., Adams, J.M., and Huang, D.C. (2005). Differential targeting of prosurvival Bcl-2 proteins by their BH3-only ligands allows complementary apoptotic function. Mol Cell *17*, 393-403.

Chen-Levy, Z., and Cleary, M.L. (1990). Membrane topology of the Bcl-2 proto-oncogenic protein demonstrated in vitro. J Biol Chem *265*, 4929-4933.

Cheng, E.H., Wei, M.C., Weiler, S., Flavell, R.A., Mak, T.W., Lindsten, T., and Korsmeyer, S.J. (2001). BCL-2, BCL-X(L) sequester BH3 domain-only molecules preventing BAX- and BAK-mediated mitochondrial apoptosis. Mol Cell *8*, 705-711.

Cheng, S.W., Davies, K.P., Yung, E., Beltran, R.J., Yu, J., and Kalpana, G.V. (1999). c-MYC interacts with INI1/hSNF5 and requires the SWI/SNF complex for transactivation function. Nat Genet *22*, 102-105.

Cheung, T.H., and Rando, T.A. (2013). Molecular regulation of stem cell quiescence. Nat Rev Mol Cell Biol *14*, 329-340.

Cheung, W.C., Kim, J.S., Linden, M., Peng, L., Van Ness, B., Polakiewicz, R.D., and Janz, S. (2004). Novel targeted deregulation of c-Myc cooperates with Bcl-X(L) to cause plasma cell neoplasms in mice. J Clin Invest *113*, 1763-1773.

Chipuk, J.E., Bouchier-Hayes, L., and Green, D.R. (2006). Mitochondrial outer membrane permeabilization during apoptosis: the innocent bystander scenario. Cell Death Differ *13*, 1396-1402.

Chipuk, J.E., Kuwana, T., Bouchier-Hayes, L., Droin, N.M., Newmeyer, D., Schuler, M., and Green, D.R. (2004). Direct activation of Bax by p53 mediates mitochondrial membrane permeabilization and apoptosis. Science *303*, 1010-1014.

Chuang, P.I., Morefield, S., Liu, C.Y., Chen, S., Harlan, J.M., and Willerford, D.M. (2002). Perturbation of B-cell development in mice overexpressing the Bcl-2 homolog A1. Blood *99*, 3350-3359.

Cleary, M.L., Haynes, J.R., Schon, E.A., and Lingrel, J.B. (1980). Identification by nucleotide sequence analysis of a goat pseudoglobin gene. Nucleic Acids Res *8*, 4791-4802.

Clegg, N.J., Couto, S.S., Wongvipat, J., Hieronymus, H., Carver, B.S., Taylor, B.S., Ellwood-Yen, K., Gerald, W.L., Sander, C., and Sawyers, C.L. (2011). MYC cooperates with AKT in prostate tumorigenesis and alters sensitivity to mTOR inhibitors. PLoS One *6*, e17449.

Cobaleda, C., Jochum, W., and Busslinger, M. (2007). Conversion of mature B cells into T cells by dedifferentiation to uncommitted progenitors. Nature *449*, 473-477.

Conacci-Sorrell, M., McFerrin, L., and Eisenman, R.N. (2014). An overview of MYC and its interactome. Cold Spring Harb Perspect Med *4*, a014357.

Cory, S., Roberts, A.W., Colman, P.M., and Adams, J.M. (2016). Targeting BCL-2-like Proteins to Kill Cancer Cells. Trends Cancer *2*, 443-460.

Coultas, L., Bouillet, P., Loveland, K.L., Meachem, S., Perlman, H., Adams, J.M., and Strasser, A. (2005). Concomitant loss of proapoptotic BH3-only Bcl-2 antagonists Bik and Bim arrests spermatogenesis. EMBO J *24*, 3963-3973.

Coultas, L., Bouillet, P., Stanley, E.G., Brodnicki, T.C., Adams, J.M., and Strasser, A. (2004). Proapoptotic BH3-only Bcl-2 family member Bik/Blk/Nbk is expressed in hemopoietic and endothelial cells but is redundant for their programmed death. Mol Cell Biol *24*, 1570-1581.

Cowling, V.H., Chandriani, S., Whitfield, M.L., and Cole, M.D. (2006). A conserved Myc protein domain, MBIV, regulates DNA binding, apoptosis, transformation, and G2 arrest. Mol Cell Biol *26*, 4226-4239.

Crouch, D.H., Fisher, F., Clark, W., Jayaraman, P.S., Goding, C.R., and Gillespie, D.A. (1993). Gene-regulatory properties of Myc helix-loop-helix/leucine zipper mutants: Max-dependent DNA binding and transcriptional activation in yeast correlates with transforming capacity. Oncogene *8*, 1849-1855.

Csibi, A., Lee, G., Yoon, S.O., Tong, H., Ilter, D., Elia, I., Fendt, S.M., Roberts, T.M., and Blenis, J. (2014). The mTORC1/S6K1 pathway regulates glutamine metabolism through the eIF4B-dependent control of c-Myc translation. Curr Biol *24*, 2274-2280.

Culjkovic, B., Topisirovic, I., Skrabanek, L., Ruiz-Gutierrez, M., and Borden, K.L. (2006). eIF4E is a central node of an RNA regulon that governs cellular proliferation. J Cell Biol *175*, 415-426.

Cutrona, G., Dono, M., Pastorino, S., Ulivi, M., Burgio, V.L., Zupo, S., Roncella, S., and Ferrarini, M. (1997a). c-myc proto-oncogene expression by germinal center B cells isolated from human tonsils. Ann N Y Acad Sci *815*, 436-439.

Cutrona, G., Dono, M., Pastorino, S., Ulivi, M., Burgio, V.L., Zupo, S., Roncella, S., and Ferrarini, M. (1997b). The propensity to apoptosis of centrocytes and centroblasts correlates with elevated levels of intracellular myc protein. Eur J Immunol *27*, 234-238.

Czabotar, P.E., Lessene, G., Strasser, A., and Adams, J.M. (2014). Control of apoptosis by the BCL-2 protein family: implications for physiology and therapy. Nat Rev Mol Cell Biol *15*, 49-63.

D'Andrea, A., Gritti, I., Nicoli, P., Giorgio, M., Doni, M., Conti, A., Bianchi, V., Casoli, L., Sabo, A., Mironov, A.*, et al.* (2016). The mitochondrial translation machinery as a therapeutic target in Myc-driven lymphomas. Oncotarget *7*, 72415-72430.

Dang, C.V. (2012). MYC on the path to cancer. Cell *149*, 22-35.

Dang, C.V. (2013). MYC, metabolism, cell growth, and tumorigenesis. Cold Spring Harb Perspect Med *3*.

Dang, C.V., Barrett, J., Villa-Garcia, M., Resar, L.M., Kato, G.J., and Fearon, E.R. (1991). Intracellular leucine zipper interactions suggest c-Myc hetero-oligomerization. Mol Cell Biol *11*, 954-962.

Dang, C.V., and Lee, W.M. (1988). Identification of the human c-myc protein nuclear translocation signal. Mol Cell Biol *8*, 4048-4054.

Dani, C., Blanchard, J.M., Piechaczyk, M., El Sabouty, S., Marty, L., and Jeanteur, P. (1984). Extreme instability of myc mRNA in normal and transformed human cells. Proc Natl Acad Sci U S A *81*, 7046-7050.

Darzynkiewicz, Z., Traganos, F., and Melamed, M.R. (1980). New cell cycle compartments identified by multiparameter flow cytometry. Cytometry *1*, 98-108.

Davis, A.C., Wims, M., Spotts, G.D., Hann, S.R., and Bradley, A. (1993). A null c-myc mutation causes lethality before 10.5 days of gestation in homozygotes and reduced fertility in heterozygous female mice. Genes Dev *7*, 671-682.

de Alboran, I.M., Baena, E., and Martinez, A.C. (2004). c-Myc-deficient B lymphocytes are resistant to spontaneous and induced cell death. Cell Death Differ *11*, 61-68.

de Alboran, I.M., O'Hagan, R.C., Gartner, F., Malynn, B., Davidson, L., Rickert, R., Rajewsky, K., DePinho, R.A., and Alt, F.W. (2001). Analysis of C-MYC function in normal cells via conditional gene-targeted mutation. Immunity *14*, 45-55.

de Pretis, S., Kress, T.R., Morelli, M.J., Sabò, A., Locarno, C., Verrecchia, A., Doni, M., Campaner, S., Amati, B., and Pelizzola, M. (2017). Integrative analysis of RNA polymerase II and transcriptional dynamics upon MYC activation. Genome Res *27*, 1658-1664.

De Silva, N.S., and Klein, U. (2015). Dynamics of B cells in germinal centres. Nat Rev Immunol *15*, 137-148.

Dejure, F.R., and Eilers, M. (2017). MYC and tumor metabolism: chicken and egg. EMBO J *36*, 3409-3420.

DeKoter, R.P., and Singh, H. (2000). Regulation of B lymphocyte and macrophage development by graded expression of PU.1. Science *288*, 1439-1441.

DeoCampo, N.D., Wilson, M.R., and Trosko, J.E. (2000). Cooperation of bcl-2 and myc in the neoplastic transformation of normal rat liver epithelial cells is related to the down-regulation of gap junction-mediated intercellular communication. Carcinogenesis *21*, 1501-1506.

Dominguez-Sola, D., and Gautier, J. (2014). MYC and the control of DNA replication. Cold Spring Harb Perspect Med *4*.

Dominguez-Sola, D., Kung, J., Holmes, A.B., Wells, V.A., Mo, T., Basso, K., and Dalla-Favera, R. (2015). The FOXO1 Transcription Factor Instructs the Germinal Center Dark Zone Program. Immunity *43*, 1064-1074.

Dominguez-Sola, D., Victora, G.D., Ying, C.Y., Phan, R.T., Saito, M., Nussenzweig, M.C., and Dalla-Favera, R. (2012). The proto-oncogene MYC is required for selection in the germinal center and cyclic reentry. Nat Immunol *13*, 1083-1091.

Dominguez-Sola, D., Ying, C.Y., Grandori, C., Ruggiero, L., Chen, B., Li, M., Galloway, D.A., Gu, W., Gautier, J., and Dalla-Favera, R. (2007). Non-transcriptional control of DNA replication by c-Myc. Nature *448*, 445-451.

Dreyer, W.J., and Bennett, J.C. (1965). The molecular basis of antibody formation: a paradox. Proc Natl Acad Sci U S A *54*, 864-869.

Dyer, M.J., Lillington, D.M., Bastard, C., Tilly, H., Lens, D., Heward, J.M., Stranks, G., Morilla, R., Monrad, S., Guglielmi, P.*, et al.* (1996). Concurrent activation of MYC and BCL2 in B cell non-Hodgkin lymphoma cell lines by translocation of both oncogenes to the same immunoglobulin heavy chain locus. Leukemia *10*, 1198-1208.

Eberhardy, S.R., and Farnham, P.J. (2002). Myc recruits P-TEFb to mediate the final step in the transcriptional activation of the cad promoter. J Biol Chem *277*, 40156-40162.

Egle, A., Harris, A.W., Bath, M.L., O'Reilly, L., and Cory, S. (2004). VavP-Bcl2 transgenic mice develop follicular lymphoma preceded by germinal center hyperplasia. Blood *103*, 2276-2283.

Ehninger, A., Boch, T., Uckelmann, H., Essers, M.A., Mudder, K., Sleckman, B.P., and Trumpp, A. (2014). Posttranscriptional regulation of c-Myc expression in adult murine HSCs during homeostasis and interferon-alpha-induced stress response. Blood *123*, 3909-3913.

Eick, D., and Bornkamm, G.W. (1986). Transcriptional arrest within the first exon is a fast control mechanism in c-myc gene expression. Nucleic Acids Res *14*, 8331-8346.

Eischen, C.M., Roussel, M.F., Korsmeyer, S.J., and Cleveland, J.L. (2001a). Bax loss impairs Myc-induced apoptosis and circumvents the selection of p53 mutations during Myc-mediated lymphomagenesis. Mol Cell Biol *21*, 7653-7662.

Eischen, C.M., Woo, D., Roussel, M.F., and Cleveland, J.L. (2001b). Apoptosis triggered by Myc-induced suppression of Bcl-X(L) or Bcl-2 is bypassed during lymphomagenesis. Mol Cell Biol *21*, 5063-5070.

Enders, A., Bouillet, P., Puthalakath, H., Xu, Y., Tarlinton, D.M., and Strasser, A. (2003). Loss of the pro-apoptotic BH3-only Bcl-2 family member Bim inhibits BCR stimulation-induced apoptosis and deletion of autoreactive B cells. J Exp Med *198*, 1119-1126.

Era, T., Ogawa, M., Nishikawa, S., Okamoto, M., Honjo, T., Akagi, K., Miyazaki, J., and Yamamura, K. (1991). Differentiation of growth signal requirement of B lymphocyte precursor is directed by expression of immunoglobulin. EMBO J *10*, 337-342.

Erlacher, M., Labi, V., Manzl, C., Bock, G., Tzankov, A., Hacker, G., Michalak, E., Strasser, A., and Villunger, A. (2006). Puma cooperates with Bim, the rate-limiting BH3-only protein in cell death during lymphocyte development, in apoptosis induction. J Exp Med *203*, 2939-2951.

Evan, G.I., Wyllie, A.H., Gilbert, C.S., Littlewood, T.D., Land, H., Brooks, M., Waters, C.M., Penn, L.Z., and Hancock, D.C. (1992). Induction of apoptosis in fibroblasts by c-myc protein. Cell *69*, 119-128.

Faiola, F., Liu, X., Lo, S., Pan, S., Zhang, K., Lymar, E., Farina, A., and Martinez, E. (2005). Dual regulation of c-Myc by p300 via acetylation-dependent control of Myc protein turnover and coactivation of Myc-induced transcription. Mol Cell Biol *25*, 10220-10234.

Fanidi, A., Harrington, E.A., and Evan, G.I. (1992). Cooperative interaction between c-myc and bcl-2 proto-oncogenes. Nature *359*, 554-556.

Farrell, A.S., and Sears, R.C. (2014). MYC degradation. Cold Spring Harb Perspect Med *4*.

Felsher, D.W., and Bishop, J.M. (1999). Reversible tumorigenesis by MYC in hematopoietic lineages. Mol Cell *4*, 199-207.

Felsher, D.W., Zetterberg, A., Zhu, J., Tlsty, T., and Bishop, J.M. (2000). Overexpression of MYC causes p53-dependent G2 arrest of normal fibroblasts. Proc Natl Acad Sci U S A *97*, 10544-10548.

Fernandez, P.C., Frank, S.R., Wang, L., Schroeder, M., Liu, S., Greene, J., Cocito, A., and Amati, B. (2003). Genomic targets of the human c-Myc protein. Genes Dev *17*, 1115-1129.

Frank, S.R., Parisi, T., Taubert, S., Fernandez, P., Fuchs, M., Chan, H.M., Livingston, D.M., and Amati, B. (2003). MYC recruits the TIP60 histone acetyltransferase complex to chromatin. EMBO Rep *4*, 575-580.

Frenzel, A., Labi, V., Chmelewskij, W., Ploner, C., Geley, S., Fiegl, H., Tzankov, A., and Villunger, A. (2010). Suppression of B-cell lymphomagenesis by the BH3-only proteins Bmf and Bad. Blood *115*, 995-1005.

Friedberg, J.W. (2017). How I treat double-hit lymphoma. Blood *130*, 590-596.

Fuchs, Y., and Steller, H. (2011). Programmed cell death in animal development and disease. Cell *147*, 742-758.

Gabay, M., Li, Y., and Felsher, D.W. (2014). MYC activation is a hallmark of cancer initiation and maintenance. Cold Spring Harb Perspect Med *4*.

Garrison, S.P., Jeffers, J.R., Yang, C., Nilsson, J.A., Hall, M.A., Rehg, J.E., Yue, W., Yu, J., Zhang, L., Onciu, M.*, et al.* (2008). Selection against PUMA gene expression in Myc-driven B-cell lymphomagenesis. Mol Cell Biol *28*, 5391-5402.

Gartel, A.L., Ye, X., Goufman, E., Shianov, P., Hay, N., Najmabadi, F., and Tyner, A.L. (2001). Myc represses the p21(WAF1/CIP1) promoter and interacts with Sp1/Sp3. Proc Natl Acad Sci U S A *98*, 4510-4515.

Gitlin, A.D., Shulman, Z., and Nussenzweig, M.C. (2014). Clonal selection in the germinal centre by regulated proliferation and hypermutation. Nature *509*, 637-640.

Giulino-Roth, L., Wang, K., MacDonald, T.Y., Mathew, S., Tam, Y., Cronin, M.T., Palmer, G., Lucena-Silva, N., Pedrosa, F., Pedrosa, M.*, et al.* (2012). Targeted genomic sequencing of pediatric Burkitt lymphoma identifies recurrent alterations in antiapoptotic and chromatin-remodeling genes. Blood *120*, 5181-5184.

Gonzalez-Prieto, R., Cuijpers, S.A., Kumar, R., Hendriks, I.A., and Vertegaal, A.C. (2015). c-Myc is targeted to the proteasome for degradation in a SUMOylation-dependent manner, regulated by PIAS1, SENP7 and RNF4. Cell Cycle *14*, 1859-1872.

Grande, B.M., Gerhard, D.S., Jiang, A., Griner, N.B., Abramson, J.S., Alexander, T.B., Allen, H., Ayers, L.W., Bethony, J.M., Bhatia, K.*, et al.* (2019). Genome-wide discovery of somatic coding and noncoding mutations in pediatric endemic and sporadic Burkitt lymphoma. Blood *133*, 1313-1324.

Grandori, C., Gomez-Roman, N., Felton-Edkins, Z.A., Ngouenet, C., Galloway, D.A., Eisenman, R.N., and White, R.J. (2005). c-Myc binds to human ribosomal DNA and stimulates transcription of rRNA genes by RNA polymerase I. Nat Cell Biol *7*, 311-318.

Grandori, C., Wu, K.J., Fernandez, P., Ngouenet, C., Grim, J., Clurman, B.E., Moser, M.J., Oshima, J., Russell, D.W., Swisshelm, K.*, et al.* (2003). Werner syndrome protein limits MYC-induced cellular senescence. Genes Dev *17*, 1569-1574.

Greasley, P.J., Bonnard, C., and Amati, B. (2000). Myc induces the nucleolin and BN51 genes: possible implications in ribosome biogenesis. Nucleic Acids Res *28*, 446-453.

Grewal, S.S., Li, L., Orian, A., Eisenman, R.N., and Edgar, B.A. (2005). Myc-dependent regulation of ribosomal RNA synthesis during Drosophila development. Nat Cell Biol *7*, 295-302.

Grillot, D.A., Merino, R., and Nunez, G. (1995). Bcl-XL displays restricted distribution during T cell development and inhibits multiple forms of apoptosis but not clonal deletion in transgenic mice. J Exp Med *182*, 1973-1983.

Guccione, E., Martinato, F., Finocchiaro, G., Luzi, L., Tizzoni, L., Dall' Olio, V., Zardo, G., Nervi, C., Bernard, L., and Amati, B. (2006). Myc-binding-site recognition in the human genome is determined by chromatin context. Nat Cell Biol *8*, 764-770.

Hagman, J., Belanger, C., Travis, A., Turck, C.W., and Grosschedl, R. (1993). Cloning and functional characterization of early B-cell factor, a regulator of lymphocyte-specific gene expression. Genes Dev *7*, 760-773.

Hamasaki, A., Sendo, F., Nakayama, K., Ishida, N., Negishi, I., Nakayama, K., and Hatakeyama, S. (1998). Accelerated neutrophil apoptosis in mice lacking A1-a, a subtype of the bcl-2-related A1 gene. J Exp Med *188*, 1985-1992.

Hardwick, J.M., and Youle, R.J. (2009). SnapShot: BCL-2 proteins. Cell *138*, 404, 404 e401.

Hardy, R.R., Carmack, C.E., Shinton, S.A., Kemp, J.D., and Hayakawa, K. (1991). Resolution and characterization of pro-B and pre-pro-B cell stages in normal mouse bone marrow. J Exp Med *173*, 1213-1225.

Hardy, R.R., and Hayakawa, K. (1991). A developmental switch in B lymphopoiesis. Proc Natl Acad Sci U S A *88*, 11550-11554.

Hatton, K.S., Mahon, K., Chin, L., Chiu, F.C., Lee, H.W., Peng, D., Morgenbesser, S.D., Horner, J., and DePinho, R.A. (1996). Expression and activity of L-Myc in normal mouse development. Mol Cell Biol *16*, 1794-1804.

Hatzi, K., and Melnick, A. (2014). Breaking bad in the germinal center: how deregulation of BCL6 contributes to lymphomagenesis. Trends Mol Med *20*, 343-352.

He, T.C., Sparks, A.B., Rago, C., Hermeking, H., Zawel, L., da Costa, L.T., Morin, P.J., Vogelstein, B., and Kinzler, K.W. (1998). Identification of c-MYC as a target of the APC pathway. Science *281*, 1509-1512.

Hemann, M.T., Bric, A., Teruya-Feldstein, J., Herbst, A., Nilsson, J.A., Cordon-Cardo, C., Cleveland, J.L., Tansey, W.P., and Lowe, S.W. (2005). Evasion of the p53 tumour surveillance network by tumour-derived MYC mutants. Nature *436*, 807-811.

Hengartner, M.O., Ellis, R.E., and Horvitz, H.R. (1992). Caenorhabditis elegans gene ced-9 protects cells from programmed cell death. Nature *356*, 494-499.

Hengartner, M.O., and Horvitz, H.R. (1994). C. elegans cell survival gene ced-9 encodes a functional homolog of the mammalian proto-oncogene bcl-2. Cell *76*, 665-676.

Herbst, A., Hemann, M.T., Tworkowski, K.A., Salghetti, S.E., Lowe, S.W., and Tansey, W.P. (2005). A conserved element in Myc that negatively regulates its proapoptotic activity. EMBO Rep *6*, 177-183.

Herold, S., Wanzel, M., Beuger, V., Frohme, C., Beul, D., Hillukkala, T., Syvaoja, J., Saluz, H.P., Haenel, F., and Eilers, M. (2002). Negative regulation of the mammalian UV response by Myc through association with Miz-1. Mol Cell *10*, 509-521.

Hofmann, J.W., Zhao, X., De Cecco, M., Peterson, A.L., Pagliaroli, L., Manivannan, J., Hubbard, G.B., Ikeno, Y., Zhang, Y., Feng, B.*, et al.* (2015). Reduced expression of MYC increases longevity and enhances healthspan. Cell *160*, 477-488.

Hua, C., Zorn, S., Jensen, J.P., Coupland, R.W., Ko, H.S., Wright, J.J., and Bakhshi, A. (1988). Consequences of the t(14;18) chromosomal translocation in follicular lymphoma: deregulated expression of a chimeric and mutated BCL-2 gene. Oncogene Res *2*, 263-275.

Huang, C.Y., Bredemeyer, A.L., Walker, L.M., Bassing, C.H., and Sleckman, B.P. (2008). Dynamic regulation of c-Myc proto-oncogene expression during lymphocyte development revealed by a GFP-c-Myc knock-in mouse. Eur J Immunol *38*, 342-349.

Huang, D.C., and Strasser, A. (2000). BH3-Only proteins-essential initiators of apoptotic cell death. Cell *103*, 839-842.

Huh, Y.O., Lin, K.I., Vega, F., Schlette, E., Yin, C.C., Keating, M.J., Luthra, R., Medeiros, L.J., and Abruzzo, L.V. (2008). MYC translocation in chronic lymphocytic leukaemia is associated with increased prolymphocytes and a poor prognosis. Br J Haematol *142*, 36-44.

Ianevski, A., He, L., Aittokallio, T., and Tang, J. (2017). SynergyFinder: a web application for analyzing drug combination dose-response matrix data. Bioinformatics *33*, 2413-2415.

Ikuta, K., and Weissman, I.L. (1992). Evidence that hematopoietic stem cells express mouse c-kit but do not depend on steel factor for their generation. Proc Natl Acad Sci U S A *89*, 1502-1506.

Iorio, M.V., and Croce, C.M. (2009). MicroRNAs in cancer: small molecules with a huge impact. J Clin Oncol *27*, 5848-5856.

Iqbal, J., Sanger, W.G., Horsman, D.E., Rosenwald, A., Pickering, D.L., Dave, B., Dave, S., Xiao, L., Cao, K., Zhu, Q.*, et al.* (2004). BCL2 translocation defines a unique tumor subset within the germinal center B-cell-like diffuse large B-cell lymphoma. Am J Pathol *165*, 159-166.

Iritani, B.M., and Eisenman, R.N. (1999). c-Myc enhances protein synthesis and cell size during B lymphocyte development. Proc Natl Acad Sci U S A *96*, 13180-13185.

Jain, M., Arvanitis, C., Chu, K., Dewey, W., Leonhardt, E., Trinh, M., Sundberg, C.D., Bishop, J.M., and Felsher, D.W. (2002). Sustained loss of a neoplastic phenotype by brief inactivation of MYC. Science *297*, 102-104.

Jeffers, J.R., Parganas, E., Lee, Y., Yang, C., Wang, J., Brennan, J., MacLean, K.H., Han, J., Chittenden, T., Ihle, J.N.*, et al.* (2003). Puma is an essential mediator of p53-dependent and -independent apoptotic pathways. Cancer Cell *4*, 321-328.

Kalkat, M., Chan, P.K., Wasylishen, A.R., Srikumar, T., Kim, S.S., Ponzielli, R., Bazett-Jones, D.P., Raught, B., and Penn, L.Z. (2014). Identification of c-MYC SUMOylation by mass spectrometry. PLoS One *9*, e115337.

Kalkat, M., Resetca, D., Lourenco, C., Chan, P.K., Wei, Y., Shiah, Y.J., Vitkin, N., Tong, Y., Sunnerhagen, M., Done, S.J.*, et al.* (2018). MYC Protein Interactome Profiling Reveals Functionally Distinct Regions that Cooperate to Drive Tumorigenesis. Mol Cell *72*, 836-848 e837.

Kang, R., Zeh, H.J., Lotze, M.T., and Tang, D. (2011). The Beclin 1 network regulates autophagy and apoptosis. Cell Death Differ *18*, 571-580.

Karube, K., and Campo, E. (2015). MYC alterations in diffuse large B-cell lymphomas. Semin Hematol *52*, 97-106.

Kasai, S., Chuma, S., Motoyama, N., and Nakatsuji, N. (2003). Haploinsufficiency of Bcl-x leads to male-specific defects in fetal germ cells: differential regulation of germ cell apoptosis between the sexes. Dev Biol *264*, 202-216.

Kato, G.J., Barrett, J., Villa-Garcia, M., and Dang, C.V. (1990). An amino-terminal c-myc domain required for neoplastic transformation activates transcription. Mol Cell Biol *10*, 5914-5920.

Kelly, K., Cochran, B.H., Stiles, C.D., and Leder, P. (1983). Cell-specific regulation of the c-myc gene by lymphocyte mitogens and platelet-derived growth factor. Cell *35*, 603-610.

Kelly, P.N., White, M.J., Goschnick, M.W., Fairfax, K.A., Tarlinton, D.M., Kinkel, S.A., Bouillet, P., Adams, J.M., Kile, B.T., and Strasser, A. (2010). Individual and overlapping roles of BH3-only proteins Bim and Bad in apoptosis of lymphocytes and platelets and in suppression of thymic lymphoma development. Cell Death Differ *17*, 1655-1664.

Kennedy, D.E., Okoreeh, M.K., Maienschein-Cline, M., Ai, J., Veselits, M., McLean, K.C., Dhungana, Y., Wang, H., Peng, J., Chi, H.*, et al.* (2020). Novel specialized cell state and spatial compartments within the germinal center. Nat Immunol *21*, 660-670.

Kepler, T.B., and Perelson, A.S. (1993). Somatic hypermutation in B cells: an optimal control treatment. J Theor Biol *164*, 37-64.

Kerr, J.F., Wyllie, A.H., and Currie, A.R. (1972). Apoptosis: a basic biological phenomenon with wide-ranging implications in tissue kinetics. Br J Cancer *26*, 239-257.

Kieffer-Kwon, K.R., Nimura, K., Rao, S.S.P., Xu, J., Jung, S., Pekowska, A., Dose, M., Stevens, E., Mathe, E., Dong, P.*, et al.* (2017). Myc Regulates Chromatin Decompaction and Nuclear Architecture during B Cell Activation. Mol Cell *67*, 566-578 e510.

Kim, D., Pertea, G., Trapnell, C., Pimentel, H., Kelley, R., and Salzberg, S.L. (2013). TopHat2: accurate alignment of transcriptomes in the presence of insertions, deletions and gene fusions. Genome Biol *14*, R36.

Kim, H.H., Kuwano, Y., Srikantan, S., Lee, E.K., Martindale, J.L., and Gorospe, M. (2009). HuR recruits let-7/RISC to repress c-Myc expression. Genes Dev *23*, 1743-1748.

Kim, J.W., Gao, P., Liu, Y.C., Semenza, G.L., and Dang, C.V. (2007). Hypoxia-inducible factor 1 and dysregulated c-Myc cooperatively induce vascular endothelial growth factor and metabolic switches hexokinase 2 and pyruvate dehydrogenase kinase 1. Mol Cell Biol *27*, 7381-7393.

Kim, S.Y., Herbst, A., Tworkowski, K.A., Salghetti, S.E., and Tansey, W.P. (2003). Skp2 regulates Myc protein stability and activity. Mol Cell *11*, 1177-1188.

Kiuchi, N., Nakajima, K., Ichiba, M., Fukada, T., Narimatsu, M., Mizuno, K., Hibi, M., and Hirano, T. (1999). STAT3 is required for the gp130-mediated full activation of the c-myc gene. J Exp Med *189*, 63-73.

Klein, U., Tu, Y., Stolovitzky, G.A., Keller, J.L., Haddad, J., Jr., Miljkovic, V., Cattoretti, G., Califano, A., and Dalla-Favera, R. (2003). Transcriptional analysis of the B cell germinal center reaction. Proc Natl Acad Sci U S A *100*, 2639-2644.

Knittel, G., Liedgens, P., Korovkina, D., Seeger, J.M., Al-Baldawi, Y., Al-Maarri, M., Fritz, C., Vlantis, K., Bezhanova, S., Scheel, A.H.*, et al.* (2016). B-cell-specific conditional expression of Myd88p.L252P leads to the development of diffuse large B-cell lymphoma in mice. Blood *127*, 2732-2741.

Kolar, G.R., Mehta, D., Pelayo, R., and Capra, J.D. (2007). A novel human B cell subpopulation representing the initial germinal center population to express AID. Blood *109*, 2545-2552.

Korsmeyer, S.J., McDonnell, T.J., Nunez, G., Hockenbery, D., and Young, R. (1990). Bcl-2: B cell life, death and neoplasia. Curr Top Microbiol Immunol *166*, 203-207.

Kortlever, R.M., Sodir, N.M., Wilson, C.H., Burkhart, D.L., Pellegrinet, L., Brown Swigart, L., Littlewood, T.D., and Evan, G.I. (2017). Myc Cooperates with Ras by Programming Inflammation and Immune Suppression. Cell *171*, 1301-1315 e1314.

Kozak, M. (1989). The scanning model for translation: an update. J Cell Biol *108*, 229-241.

Kress, T.R., Pellanda, P., Pellegrinet, L., Bianchi, V., Nicoli, P., Doni, M., Recordati, C., Bianchi, S., Rotta, L., Capra, T.*, et al.* (2016). Identification of MYC-Dependent Transcriptional Programs in Oncogene-Addicted Liver Tumors. Cancer Res *76*, 3463-3472.

Kress, T.R., Sabo, A., and Amati, B. (2015a). MYC: connecting selective transcriptional control to global RNA production. Nat Rev Cancer *15*, 593-607.

Kress, T.R., Sabò, A., and Amati, B. (2015b). MYC: connecting selective transcriptional control to global RNA production. Nat Rev Cancer *15*, 593-607.

Kretzner, L., Blackwood, E.M., and Eisenman, R.N. (1992). Myc and Max proteins possess distinct transcriptional activities. Nature *359*, 426-429.

Krystal, G., Birrer, M., Way, J., Nau, M., Sausville, E., Thompson, C., Minna, J., and Battey, J. (1988). Multiple mechanisms for transcriptional regulation of the myc gene family in small-cell lung cancer. Mol Cell Biol *8*, 3373-3381.

Kuppers, R., and Dalla-Favera, R. (2001). Mechanisms of chromosomal translocations in B cell lymphomas. Oncogene *20*, 5580-5594.

Kuwana, T., Bouchier-Hayes, L., Chipuk, J.E., Bonzon, C., Sullivan, B.A., Green, D.R., and Newmeyer, D.D. (2005). BH3 domains of BH3-only proteins differentially regulate Bax-mediated mitochondrial membrane permeabilization both directly and indirectly. Mol Cell *17*, 525-535.

Kwon, K., Hutter, C., Sun, Q., Bilic, I., Cobaleda, C., Malin, S., and Busslinger, M. (2008). Instructive role of the transcription factor E2A in early B lymphopoiesis and germinal center B cell development. Immunity *28*, 751-762.

Labi, V., Erlacher, M., Kiessling, S., Manzl, C., Frenzel, A., O'Reilly, L., Strasser, A., and Villunger, A. (2008). Loss of the BH3-only protein Bmf impairs B cell homeostasis and accelerates gamma irradiation-induced thymic lymphoma development. J Exp Med *205*, 641-655.

Land, H., Parada, L.F., and Weinberg, R.A. (1983). Tumorigenic conversion of primary embryo fibroblasts requires at least two cooperating oncogenes. Nature *304*, 596-602.

Latil, M., Rocheteau, P., Chatre, L., Sanulli, S., Memet, S., Ricchetti, M., Tajbakhsh, S., and Chretien, F. (2012). Skeletal muscle stem cells adopt a dormant cell state post mortem and retain regenerative capacity. Nat Commun *3*, 903.

Laurenti, E., Varnum-Finney, B., Wilson, A., Ferrero, I., Blanco-Bose, W.E., Ehninger, A., Knoepfler, P.S., Cheng, P.F., MacDonald, H.R., Eisenman, R.N.*, et al.* (2008). Hematopoietic stem cell function and survival depend on c-Myc and N-Myc activity. Cell Stem Cell *3*, 611-624.

Le Gouill, S., Talmant, P., Touzeau, C., Moreau, A., Garand, R., Juge-Morineau, N., Gaillard, F., Gastinne, T., Milpied, N., Moreau, P.*, et al.* (2007). The clinical presentation and prognosis of diffuse large B-cell lymphoma with t(14;18) and 8q24/c-MYC rearrangement. Haematologica *92*, 1335-1342.

Lee, J.Y., Jun, D.Y., Park, J.E., Kwon, G.H., Kim, J.S., and Kim, Y.H. (2017). Pro-Apoptotic Role of the Human YPEL5 Gene Identified by Functional Complementation of a Yeast moh1Delta Mutation. J Microbiol Biotechnol *27*, 633-643.

Leskov, I., Pallasch, C.P., Drake, A., Iliopoulou, B.P., Souza, A., Shen, C.H., Schweighofer, C.D., Abruzzo, L., Frenzel, L.P., Wendtner, C.M.*, et al.* (2013). Rapid generation of human B-cell lymphomas via combined expression of Myc and Bcl2 and their use as a preclinical model for biological therapies. Oncogene *32*, 1066-1072.

Letai, A., Sorcinelli, M.D., Beard, C., and Korsmeyer, S.J. (2004). Antiapoptotic BCL-2 is required for maintenance of a model leukemia. Cancer Cell *6*, 241-249.

Leverson, J.D., Sampath, D., Souers, A.J., Rosenberg, S.H., Fairbrother, W.J., Amiot, M., Konopleva, M., and Letai, A. (2017). Found in Translation: How Preclinical Research Is Guiding the Clinical Development of the BCL2-Selective Inhibitor Venetoclax. Cancer Discov *7*, 1376-1393.

Li, C.L., and Johnson, G.R. (1995). Murine hematopoietic stem and progenitor cells: I. Enrichment and biologic characterization. Blood *85*, 1472-1479.

Li, F., Wang, Y., Zeller, K.I., Potter, J.J., Wonsey, D.R., O'Donnell, K.A., Kim, J.W., Yustein, J.T., Lee, L.A., and Dang, C.V. (2005). Myc stimulates nuclearly encoded mitochondrial genes and mitochondrial biogenesis. Mol Cell Biol *25*, 6225-6234.

Liao, B., Hu, Y., and Brewer, G. (2007). Competitive binding of AUF1 and TIAR to MYC mRNA controls its translation. Nat Struct Mol Biol *14*, 511-518.

Liao, Y., Smyth, G.K., and Shi, W. (2014). featureCounts: an efficient general purpose program for assigning sequence reads to genomic features. Bioinformatics *30*, 923-930.

Lin, C.Y., Loven, J., Rahl, P.B., Paranal, R.M., Burge, C.B., Bradner, J.E., Lee, T.I., and Young, R.A. (2012). Transcriptional amplification in tumor cells with elevated c-Myc. Cell *151*, 56-67.

Lindsten, T., Ross, A.J., King, A., Zong, W.X., Rathmell, J.C., Shiels, H.A., Ulrich, E., Waymire, K.G., Mahar, P., Frauwirth, K.*, et al.* (2000). The combined functions of proapoptotic Bcl-2 family members bak and bax are essential for normal development of multiple tissues. Mol Cell *6*, 1389-1399.

Lithgow, T., van Driel, R., Bertram, J.F., and Strasser, A. (1994). The protein product of the oncogene bcl-2 is a component of the nuclear envelope, the endoplasmic reticulum, and the outer mitochondrial membrane. Cell Growth Differ *5*, 411-417.

Littlewood, T.D., and Evan, G.I. (1995). Transcription factors 2: helix-loop-helix. Protein Profile *2*, 621-702.

Liu, Y.J., Joshua, D.E., Williams, G.T., Smith, C.A., Gordon, J., and MacLennan, I.C. (1989). Mechanism of antigen-driven selection in germinal centres. Nature *342*, 929-931.

Lomonosova, E., and Chinnadurai, G. (2008). BH3-only proteins in apoptosis and beyond: an overview. Oncogene *27 Suppl 1*, S2-19.

Love, M.I., Huber, W., and Anders, S. (2014). Moderated estimation of fold change and dispersion for RNA-seq data with DESeq2. Genome Biol *15*, 550.

Luscher, B., and Larsson, L.G. (1999). The basic region/helix-loop-helix/leucine zipper domain of Myc proto-oncoproteins: function and regulation. Oncogene *18*, 2955-2966.

Luscher, B., and Vervoorts, J. (2012). Regulation of gene transcription by the oncoprotein MYC. Gene *494*, 145-160.

Maclean, K.H., Keller, U.B., Rodriguez-Galindo, C., Nilsson, J.A., and Cleveland, J.L. (2003). c-Myc augments gamma irradiation-induced apoptosis by suppressing Bcl-X-L. Molecular and Cellular Biology *23*, 7256-7270.

MacLennan, I.C. (1994). Somatic mutation. From the dark zone to the light. Curr Biol *4*, 70-72.

Maggi, L.B., Jr., Kuchenruether, M., Dadey, D.Y., Schwope, R.M., Grisendi, S., Townsend, R.R., Pandolfi, P.P., and Weber, J.D. (2008). Nucleophosmin serves as a rate-limiting nuclear export chaperone for the Mammalian ribosome. Mol Cell Biol *28*, 7050-7065.

Maiuri, M.C., Le Toumelin, G., Criollo, A., Rain, J.C., Gautier, F., Juin, P., Tasdemir, E., Pierron, G., Troulinaki, K., Tavernarakis, N.*, et al.* (2007). Functional and physical interaction between Bcl-X(L) and a BH3-like domain in Beclin-1. EMBO J *26*, 2527-2539.

Malynn, B.A., de Alboran, I.M., O'Hagan, R.C., Bronson, R., Davidson, L., DePinho, R.A., and Alt, F.W. (2000). N-myc can functionally replace c-myc in murine development, cellular growth, and differentiation. Genes Dev *14*, 1390-1399.

Mao, D.Y., Watson, J.D., Yan, P.S., Barsyte-Lovejoy, D., Khosravi, F., Wong, W.W., Farnham, P.J., Huang, T.H., and Penn, L.Z. (2003). Analysis of Myc bound loci identified by CpG island arrays shows that Max is essential for Myc-dependent repression. Curr Biol *13*, 882-886.

Marin, M.C., Hsu, B., Stephens, L.C., Brisbay, S., and McDonnell, T.J. (1995). The functional basis of c-myc and bcl-2 complementation during multistep lymphomagenesis in vivo. Exp Cell Res *217*, 240-247.

Martinez-Valdez, H., Guret, C., de Bouteiller, O., Fugier, I., Banchereau, J., and Liu, Y.J. (1996). Human germinal center B cells express the apoptosis-inducing genes Fas, c-myc, P53, and Bax but not the survival gene bcl-2. J Exp Med *183*, 971-977.

Mason, K.D., Carpinelli, M.R., Fletcher, J.I., Collinge, J.E., Hilton, A.A., Ellis, S., Kelly, P.N., Ekert, P.G., Metcalf, D., Roberts, A.W.*, et al.* (2007). Programmed anuclear cell death delimits platelet life span. Cell *128*, 1173-1186.

Mathsyaraja, H., Freie, B., Cheng, P.-F., Babaeva, E., Janssens, D., Henikoff, S., and Eisenman, R.N. (2019). *Max* deletion destabilizes MYC protein and abrogates Eμ-*Myc* lymphomagenesis. BioRxiv.

Matsuoka, Y., Fukamachi, K., Uehara, N., Tsuda, H., and Tsubura, A. (2008). Induction of a novel histone deacetylase 1/c-Myc/Mnt/Max complex formation is implicated in parity-induced refractoriness to mammary carcinogenesis. Cancer Sci *99*, 309-315.

Matthias, P., and Rolink, A.G. (2005). Transcriptional networks in developing and mature B cells. Nat Rev Immunol *5*, 497-508.

Mazan-Mamczarz, K., Lal, A., Martindale, J.L., Kawai, T., and Gorospe, M. (2006). Translational repression by RNA-binding protein TIAR. Mol Cell Biol *26*, 2716-2727.

McDonnell, T.J., Deane, N., Platt, F.M., Nunez, G., Jaeger, U., McKearn, J.P., and Korsmeyer, S.J. (1989). bcl-2-immunoglobulin transgenic mice demonstrate extended B cell survival and follicular lymphoproliferation. Cell *57*, 79-88.

McDonnell, T.J., and Korsmeyer, S.J. (1991). Progression from lymphoid hyperplasia to high-grade malignant lymphoma in mice transgenic for the t(14; 18). Nature *349*, 254-256.

McHeyzer-Williams, L.J., Pelletier, N., Mark, L., Fazilleau, N., and McHeyzer-Williams, M.G. (2009). Follicular helper T cells as cognate regulators of B cell immunity. Curr Opin Immunol *21*, 266-273.

McMahon, S.B., Van Buskirk, H.A., Dugan, K.A., Copeland, T.D., and Cole, M.D. (1998). The novel ATM-related protein TRRAP is an essential cofactor for the c-Myc and E2F oncoproteins. Cell *94*, 363-374.

McMahon, S.B., Wood, M.A., and Cole, M.D. (2000). The essential cofactor TRRAP recruits the histone acetyltransferase hGCN5 to c-Myc. Mol Cell Biol *20*, 556-562.

Menendez, P., Vargas, A., Bueno, C., Barrena, S., Almeida, J., De Santiago, M., Lopez, A., Roa, S., San Miguel, J.F., and Orfao, A. (2004). Quantitative analysis of bcl-2 expression in normal and leukemic human B-cell differentiation. Leukemia *18*, 491-498.

Meyer, N., and Penn, L.Z. (2008). Reflecting on 25 years with MYC. Nat Rev Cancer *8*, 976-990.

Michalak, E.M., Jansen, E.S., Happo, L., Cragg, M.S., Tai, L., Smyth, G.K., Strasser, A., Adams, J.M., and Scott, C.L. (2009). Puma and to a lesser extent Noxa are suppressors of Myc-induced lymphomagenesis. Cell Death Differ *16*, 684-696.

Milpied, P., Cervera-Marzal, I., Mollichella, M.L., Tesson, B., Brisou, G., Traverse-Glehen, A., Salles, G., Spinelli, L., and Nadel, B. (2018). Human germinal center transcriptional programs are de-synchronized in B cell lymphoma. Nat Immunol *19*, 1013-1024.

Mitchell, K.O., Ricci, M.S., Miyashita, T., Dicker, D.T., Jin, Z., Reed, J.C., and El-Deiry, W.S. (2000). Bax is a transcriptional target and mediator of c-myc-induced apoptosis. Cancer Res *60*, 6318-6325.

Momose, S., Weissbach, S., Pischimarov, J., Nedeva, T., Bach, E., Rudelius, M., Geissinger, E., Staiger, A.M., Ott, G., and Rosenwald, A. (2015). The diagnostic gray zone between Burkitt lymphoma and diffuse large B-cell lymphoma is also a gray zone of the mutational spectrum. Leukemia *29*, 1789-1791.

Monzon-Casanova, E., Screen, M., Diaz-Munoz, M.D., Coulson, R.M.R., Bell, S.E., Lamers, G., Solimena, M., Smith, C.W.J., and Turner, M. (2018). The RNA-binding protein PTBP1 is necessary for B cell selection in germinal centers. Nat Immunol *19*, 267-278.

Motoyama, N., Wang, F., Roth, K.A., Sawa, H., Nakayama, K., Nakayama, K., Negishi, I., Senju, S., Zhang, Q., Fujii, S.*, et al.* (1995). Massive cell death of immature hematopoietic cells and neurons in Bcl-x-deficient mice. Science *267*, 1506-1510.

Murn, J., Mlinaric-Rascan, I., Vaigot, P., Alibert, O., Frouin, V., and Gidrol, X. (2009). A Myc-regulated transcriptional network controls B-cell fate in response to BCR triggering. BMC Genomics *10*, 323.

Muthalagu, N., Junttila, M.R., Wiese, K.E., Wolf, E., Morton, J., Bauer, B., Evan, G.I., Eilers, M., and Murphy, D.J. (2014). BIM is the primary mediator of MYC-induced apoptosis in multiple solid tissues. Cell Rep *8*, 1347-1353.

Nagasawa, T. (2006). Microenvironmental niches in the bone marrow required for B-cell development. Nat Rev Immunol *6*, 107-116.

Ng, S.Y., Yoshida, T., Zhang, J., and Georgopoulos, K. (2009). Genome-wide lineage-specific transcriptional networks underscore Ikaros-dependent lymphoid priming in hematopoietic stem cells. Immunity *30*, 493-507.

Nie, Z., Hu, G., Wei, G., Cui, K., Yamane, A., Resch, W., Wang, R., Green, D.R., Tessarollo, L., Casellas, R.*, et al.* (2012). c-Myc is a universal amplifier of expressed genes in lymphocytes and embryonic stem cells. Cell *151*, 68-79.

Nunez, G., London, L., Hockenbery, D., Alexander, M., McKearn, J.P., and Korsmeyer, S.J. (1990). Deregulated Bcl-2 gene expression selectively prolongs survival of growth factor-deprived hemopoietic cell lines. J Immunol *144*, 3602-3610.

Nutt, S.L., Rolink, A.G., and Busslinger, M. (1999). The molecular basis of B-cell lineage commitment. Cold Spring Harb Symp Quant Biol *64*, 51-59.

Oda, E., Ohki, R., Murasawa, H., Nemoto, J., Shibue, T., Yamashita, T., Tokino, T., Taniguchi, T., and Tanaka, N. (2000). Nora, a BH3-only member of the Bcl-2 family and candidate mediator of p53-induced apoptosis. Science *288*, 1053-1058.

Ogilvy, S., Metcalf, D., Print, C.G., Bath, M.L., Harris, A.W., and Adams, J.M. (1999). Constitutive Bcl-2 expression throughout the hematopoietic compartment affects multiple lineages and enhances progenitor cell survival. Proc Natl Acad Sci U S A *96*, 14943-14948.

Opferman, J.T., Iwasaki, H., Ong, C.C., Suh, H., Mizuno, S., Akashi, K., and Korsmeyer, S.J. (2005). Obligate role of anti-apoptotic MCL-1 in the survival of hematopoietic stem cells. Science *307*, 1101-1104.

Opferman, J.T., Letai, A., Beard, C., Sorcinelli, M.D., Ong, C.C., and Korsmeyer, S.J. (2003). Development and maintenance of B and T lymphocytes requires antiapoptotic MCL-1. Nature *426*, 671-676.

Oprea, M., and Perelson, A.S. (1997). Somatic mutation leads to efficient affinity maturation when centrocytes recycle back to centroblasts. J Immunol *158*, 5155-5162.

Ortega-Molina, A., Boss, I.W., Canela, A., Pan, H., Jiang, Y., Zhao, C., Jiang, M., Hu, D., Agirre, X., Niesvizky, I.*, et al.* (2015). The histone lysine methyltransferase KMT2D sustains a gene expression program that represses B cell lymphoma development. Nat Med *21*, 1199-1208.

Oster, S.K., Ho, C.S., Soucie, E.L., and Penn, L.Z. (2002). The myc oncogene: MarvelouslY Complex. Adv Cancer Res *84*, 81-154.

Pal, S., Yun, R., Datta, A., Lacomis, L., Erdjument-Bromage, H., Kumar, J., Tempst, P., and Sif, S. (2003). mSin3A/histone deacetylase 2- and PRMT5-containing Brg1 complex is involved in transcriptional repression of the Myc target gene cad. Mol Cell Biol *23*, 7475-7487.

Palomero, T., Lim, W.K., Odom, D.T., Sulis, M.L., Real, P.J., Margolin, A., Barnes, K.C., O'Neil, J., Neuberg, D., Weng, A.P.*, et al.* (2006). NOTCH1 directly regulates c-MYC and activates a feed-forward-loop transcriptional network promoting leukemic cell growth. Proc Natl Acad Sci U S A *103*, 18261-18266.

Papathanasiou, P., Attema, J.L., Karsunky, H., Hosen, N., Sontani, Y., Hoyne, G.F., Tunningley, R., Smale, S.T., and Weissman, I.L. (2009). Self-renewal of the long-term reconstituting subset of hematopoietic stem cells is regulated by Ikaros. Stem Cells *27*, 3082-3092.

Park, J., Wood, M.A., and Cole, M.D. (2002). BAF53 forms distinct nuclear complexes and functions as a critical c-Myc-interacting nuclear cofactor for oncogenic transformation. Mol Cell Biol *22*, 1307-1316.

Pascual, M., Mena-Varas, M., Robles, E.F., Garcia-Barchino, M.J., Panizo, C., Hervas-Stubbs, S., Alignani, D., Sagardoy, A., Martinez-Ferrandis, J.I., Bunting, K.L.*, et al.* (2019). PD-1/PD-L1 immune checkpoint and p53 loss facilitate tumor progression in activated B-cell diffuse large B-cell lymphomas. Blood *133*, 2401-2412.

Pasqualucci, L., and Dalla-Favera, R. (2018). Genetics of diffuse large B-cell lymphoma. Blood *131*, 2307-2319.

Pasqualucci, L., Khiabanian, H., Fangazio, M., Vasishtha, M., Messina, M., Holmes, A.B., Ouillette, P., Trifonov, V., Rossi, D., Tabbo, F.*, et al.* (2014). Genetics of follicular lymphoma transformation. Cell Rep *6*, 130-140.

Pattingre, S., Tassa, A., Qu, X., Garuti, R., Liang, X.H., Mizushima, N., Packer, M., Schneider, M.D., and Levine, B. (2005). Bcl-2 antiapoptotic proteins inhibit Beclin 1-dependent autophagy. Cell *122*, 927-939.

Paulin, F.E., Chappell, S.A., and Willis, A.E. (1998). A single nucleotide change in the c-myc internal ribosome entry segment leads to enhanced binding of a group of protein factors. Nucleic Acids Res *26*, 3097-3103.

Pellanda, P., Dalsass, M., Filippuzzzi, M., Loffreda, A., Verrecchia, A., Castillo Cano, V., Doni, M., Morelli, M., Beaulieu, M., Soucek, L.*, et al.* (2020). Integrated requirement of non-specific and sequence-specific DNA binding in MYC-driven transcription.

Perez-Olivares, M., Trento, A., Rodriguez-Acebes, S., Gonzalez-Acosta, D., Fernandez-Antoran, D., Roman-Garcia, S., Martinez, D., Lopez-Briones, T., Torroja, C., Carrasco, Y.R., *et al.* (2018). Functional interplay between c-Myc and Max in B lymphocyte differentiation. EMBO Rep *19*.

Perez-Roger, I., Kim, S.H., Griffiths, B., Sewing, A., and Land, H. (1999). Cyclins D1 and D2 mediate myc-induced proliferation via sequestration of p27(Kip1) and p21(Cip1). EMBO J *18*, 5310-5320.

Perna, D., Faga, G., Verrecchia, A., Gorski, M.M., Barozzi, I., Narang, V., Khng, J., Lim, K.C., Sung, W.K., Sanges, R., *et al.* (2012). Genome-wide mapping of Myc binding and gene regulation in serum-stimulated fibroblasts. Oncogene *31*, 1695-1709.

Pezzella, F., Tse, A.G., Cordell, J.L., Pulford, K.A., Gatter, K.C., and Mason, D.Y. (1990). Expression of the bcl-2 oncogene protein is not specific for the 14;18 chromosomal translocation. Am J Pathol *137*, 225-232.

Pillai, S., Cariappa, A., and Moran, S.T. (2004). Positive selection and lineage commitment during peripheral B-lymphocyte development. Immunol Rev *197*, 206-218.

Pistoni, M., Verrecchia, A., Doni, M., Guccione, E., and Amati, B. (2010). Chromatin association and regulation of rDNA transcription by the Ras-family protein RasL11a. EMBO J *29*, 1215-1224.

Poortinga, G., Hannan, K.M., Snelling, H., Walkley, C.R., Jenkins, A., Sharkey, K., Wall, M., Brandenburger, Y., Palatsides, M., Pearson, R.B., *et al.* (2004). MAD1 and c-MYC regulate UBF and rDNA transcription during granulocyte differentiation. EMBO J *23*, 3325-3335.

Popov, N., Schulein, C., Jaenicke, L.A., and Eilers, M. (2010). Ubiquitylation of the amino terminus of Myc by SCF(beta-TrCP) antagonizes SCF(Fbw7)-mediated turnover. Nat Cell Biol *12*, 973-981.

Prendergast, G.C., Lawe, D., and Ziff, E.B. (1991). Association of Myn, the murine homolog of max, with c-Myc stimulates methylation-sensitive DNA binding and ras cotransformation. Cell *65*, 395-407.

Print, C.G., Loveland, K.L., Gibson, L., Meehan, T., Stylianou, A., Wreford, N., de Kretser, D., Metcalf, D., Kontgen, F., Adams, J.M.*, et al.* (1998). Apoptosis regulator bcl-w is essential for spermatogenesis but appears otherwise redundant. Proc Natl Acad Sci U S A *95*, 12424-12431.

Pritchard, D.M., Print, C., O'Reilly, L., Adams, J.M., Potten, C.S., and Hickman, J.A. (2000). Bcl-w is an important determinant of damage-induced apoptosis in epithelia of small and large intestine. Oncogene *19*, 3955-3959.

Pulverer, B.J., Fisher, C., Vousden, K., Littlewood, T., Evan, G., and Woodgett, J.R. (1994). Site-specific modulation of c-Myc cotransformation by residues phosphorylated in vivo. Oncogene *9*, 59-70.

Rabellino, A., Melegari, M., Tompkins, V.S., Chen, W., Van Ness, B.G., Teruya-Feldstein, J., Conacci-Sorrell, M., Janz, S., and Scaglioni, P.P. (2016). PIAS1 Promotes Lymphomagenesis through MYC Upregulation. Cell Rep *15*, 2266-2278.

Radbruch, A., Muehlinghaus, G., Luger, E.O., Inamine, A., Smith, K.G., Dorner, T., and Hiepe, F. (2006). Competence and competition: the challenge of becoming a long-lived plasma cell. Nat Rev Immunol *6*, 741-750.

Raff, M.C. (1992). Social controls on cell survival and cell death. Nature *356*, 397-400.

Rahl, P.B., Lin, C.Y., Seila, A.C., Flynn, R.A., McCuine, S., Burge, C.B., Sharp, P.A., and Young, R.A. (2010). c-Myc regulates transcriptional pause release. Cell *141*, 432-445.

Ramezani-Rad, P., Chen, C., Zhu, Z., and Rickert, R.C. (2020). Cyclin D3 Governs Clonal Expansion of Dark Zone Germinal Center B Cells. Cell Rep *33*, 108403.

Rampino, N., Yamamoto, H., Ionov, Y., Li, Y., Sawai, H., Reed, J.C., and Perucho, M. (1997). Somatic frameshift mutations in the BAX gene in colon cancers of the microsatellite mutator phenotype. Science *275*, 967-969.

Rava, M., D'Andrea, A., Nicoli, P., Gritti, I., Donati, G., Doni, M., Giorgio, M., Olivero, D., and Amati, B. (2018). Therapeutic synergy between tigecycline and venetoclax in a preclinical model of MYC/BCL2 double-hit B cell lymphoma. Sci Transl Med *10*.

Reddy, A., Zhang, J., Davis, N.S., Moffitt, A.B., Love, C.L., Waldrop, A., Leppa, S., Pasanen, A., Meriranta, L., Karjalainen-Lindsberg, M.L.*, et al.* (2017). Genetic and Functional Drivers of Diffuse Large B Cell Lymphoma. Cell *171*, 481-494 e415.

Reddy, C.D., Dasgupta, P., Saikumar, P., Dudek, H., Rauscher, F.J., 3rd, and Reddy, E.P. (1992). Mutational analysis of Max: role of basic, helix-loop-helix/leucine zipper domains in DNA binding, dimerization and regulation of Myc-mediated transcriptional activation. Oncogene *7*, 2085-2092.

Richart, L., Carrillo-de Santa Pau, E., Rio-Machin, A., de Andres, M.P., Cigudosa, J.C., Lobo, V.J.S., and Real, F.X. (2016). BPTF is required for c-MYC transcriptional activity and in vivo tumorigenesis. Nat Commun *7*, 10153.

Richter-Larrea, J.A., Robles, E.F., Fresquet, V., Beltran, E., Rullan, A.J., Agirre, X., Calasanz, M.J., Panizo, C., Richter, J.A., Hernandez, J.M.*, et al.* (2010). Reversion of epigenetically mediated BIM silencing overcomes chemoresistance in Burkitt lymphoma. Blood *116*, 2531-2542.

Rinkenberger, J.L., Horning, S., Klocke, B., Roth, K., and Korsmeyer, S.J. (2000). Mcl-1 deficiency results in peri-implantation embryonic lethality. Genes Dev *14*, 23-27.

Roco, J.A., Mesin, L., Binder, S.C., Nefzger, C., Gonzalez-Figueroa, P., Canete, P.F., Ellyard, J., Shen, Q., Robert, P.A., Cappello, J.*, et al.* (2019). Class-Switch Recombination Occurs Infrequently in Germinal Centers. Immunity *51*, 337-350 e337.

Roschewski, M., Staudt, L.M., and Wilson, W.H. (2014). Diffuse large B-cell lymphoma-treatment approaches in the molecular era. Nat Rev Clin Oncol *11*, 12-23.

Rosenquist, R., Bea, S., Du, M.Q., Nadel, B., and Pan-Hammarstrom, Q. (2017). Genetic landscape and deregulated pathways in B-cell lymphoid malignancies. J Intern Med *282*, 371-394.

Rosenthal, A., and Younes, A. (2017). High grade B-cell lymphoma with rearrangements of MYC and BCL2 and/or BCL6: Double hit and triple hit lymphomas and double expressing lymphoma. Blood Rev *31*, 37-42.

Ross, A.J., Waymire, K.G., Moss, J.E., Parlow, A.F., Skinner, M.K., Russell, L.D., and MacGregor, G.R. (1998). Testicular degeneration in Bclw-deficient mice. Nat Genet *18*, 251-256.

Roulland, S., Faroudi, M., Mamessier, E., Sungalee, S., Salles, G., and Nadel, B. (2011). Early steps of follicular lymphoma pathogenesis. Adv Immunol *111*, 1-46.

Roussel, M., Saule, S., Lagrou, C., Rommens, C., Beug, H., Graf, T., and Stehelin, D. (1979). Three new types of viral oncogene of cellular origin specific for haematopoietic cell transformation. Nature *281*, 452-455.

Sabò, A., and Amati, B. (2014). Genome recognition by MYC. Cold Spring Harb Perspect Med *4*.

Sabo, A., Doni, M., and Amati, B. (2014a). SUMOylation of Myc-family proteins. PLoS One *9*, e91072.

Sabò, A., Doni, M., and Amati, B. (2014a). SUMOylation of Myc-family proteins. PLoS One *9*, e91072.

Sabo, A., Kress, T.R., Pelizzola, M., de Pretis, S., Gorski, M.M., Tesi, A., Morelli, M.J., Bora, P., Doni, M., Verrecchia, A.*, et al.* (2014b). Selective transcriptional regulation by Myc in cellular growth control and lymphomagenesis. Nature *511*, 488-492.

Sabò, A., Kress, T.R., Pelizzola, M., de Pretis, S., Gorski, M.M., Tesi, A., Morelli, M.J., Bora, P., Doni, M., Verrecchia, A.*, et al.* (2014b). Selective transcriptional regulation by Myc in cellular growth control and lymphomagenesis. Nature *511*, 488-492.

Sander, S., Calado, D.P., Srinivasan, L., Kochert, K., Zhang, B., Rosolowski, M., Rodig, S.J., Holzmann, K., Stilgenbauer, S., Siebert, R.*, et al.* (2012). Synergy between PI3K signaling and MYC in Burkitt lymphomagenesis. Cancer Cell *22*, 167-179.

Sander, S., Chu, V.T., Yasuda, T., Franklin, A., Graf, R., Calado, D.P., Li, S., Imami, K., Selbach, M., Di Virgilio, M.*, et al.* (2015). PI3 Kinase and FOXO1 Transcription Factor Activity Differentially Control B Cells in the Germinal Center Light and Dark Zones. Immunity *43*, 1075-1086.

Sansom, O.J., Meniel, V.S., Muncan, V., Phesse, T.J., Wilkins, J.A., Reed, K.R., Vass, J.K., Athineos, D., Clevers, H., and Clarke, A.R. (2007). Myc deletion rescues Apc deficiency in the small intestine. Nature *446*, 676-679.

Sant, M., Allemani, C., Tereanu, C., De Angelis, R., Capocaccia, R., Visser, O., Marcos-Gragera, R., Maynadie, M., Simonetti, A., Lutz, J.M.*, et al.* (2010). Incidence of hematologic malignancies in Europe by morphologic subtype: results of the HAEMACARE project. Blood *116*, 3724-3734.

Sarkozy, C., Traverse-Glehen, A., and Coiffier, B. (2015). Double-hit and double-protein-expression lymphomas: aggressive and refractory lymphomas. Lancet Oncol *16*, e555-e567.

Sattler, M., Liang, H., Nettesheim, D., Meadows, R.P., Harlan, J.E., Eberstadt, M., Yoon, H.S., Shuker, S.B., Chang, B.S., Minn, A.J.*, et al.* (1997). Structure of Bcl-xL-Bak peptide complex: recognition between regulators of apoptosis. Science *275*, 983-986.

Schlosser, I., Holzel, M., Murnseer, M., Burtscher, H., Weidle, U.H., and Eick, D. (2003). A role for c-Myc in the regulation of ribosomal RNA processing. Nucleic Acids Res *31*, 6148-6156.

Schmidt, E.V. (2004). The role of c-myc in regulation of translation initiation. Oncogene *23*, 3217-3221.

Schmitt, C.A., Fridman, J.S., Yang, M., Baranov, E., Hoffman, R.M., and Lowe, S.W. (2002). Dissecting p53 tumor suppressor functions in vivo. Cancer Cell *1*, 289-298.

Schmitz, R., Wright, G.W., Huang, D.W., Johnson, C.A., Phelan, J.D., Wang, J.Q., Roulland, S., Kasbekar, M., Young, R.M., Shaffer, A.L.*, et al.* (2018). Genetics and Pathogenesis of Diffuse Large B-Cell Lymphoma. N Engl J Med *378*, 1396-1407.

Schulze-Osthoff, K., Ferrari, D., Los, M., Wesselborg, S., and Peter, M.E. (1998). Apoptosis signaling by death receptors. Eur J Biochem *254*, 439-459.

Schuster, C., Berger, A., Hoelzl, M.A., Putz, E.M., Frenzel, A., Simma, O., Moritz, N., Hoelbl, A., Kovacic, B., Freissmuth, M.*, et al.* (2011). The cooperating mutation or "second hit" determines the immunologic visibility toward MYC-induced murine lymphomas. Blood *118*, 4635-4645.

Schwickert, T.A., Lindquist, R.L., Shakhar, G., Livshits, G., Skokos, D., Kosco-Vilbois, M.H., Dustin, M.L., and Nussenzweig, M.C. (2007). In vivo imaging of germinal centres reveals a dynamic open structure. Nature *446*, 83-87.

Scognamiglio, R., Cabezas-Wallscheid, N., Thier, M.C., Altamura, S., Reyes, A., Prendergast, A.M., Baumgartner, D., Carnevalli, L.S., Atzberger, A., Haas, S.*, et al.* (2016). Myc Depletion Induces a Pluripotent Dormant State Mimicking Diapause. Cell *164*, 668-680.

Scott, D.W., King, R.L., Staiger, A.M., Ben-Neriah, S., Jiang, A., Horn, H., Mottok, A., Farinha, P., Slack, G.W., Ennishi, D.*, et al.* (2018). High-grade B-cell lymphoma with MYC and BCL2 and/or BCL6 rearrangements with diffuse large B-cell lymphoma morphology. Blood *131*, 2060-2064.

Scott, D.W., Mottok, A., Ennishi, D., Wright, G.W., Farinha, P., Ben-Neriah, S., Kridel, R., Barry, G.S., Hother, C., Abrisqueta, P.*, et al.* (2015). Prognostic Significance of Diffuse Large B-Cell Lymphoma Cell of Origin Determined by Digital Gene Expression in Formalin-Fixed Paraffin-Embedded Tissue Biopsies. J Clin Oncol *33*, 2848-2856.

Scott, D.W., Wright, G.W., Williams, P.M., Lih, C.J., Walsh, W., Jaffe, E.S., Rosenwald, A., Campo, E., Chan, W.C., Connors, J.M.*, et al.* (2014). Determining cell-of-origin subtypes of diffuse large B-cell lymphoma using gene expression in formalin-fixed paraffin-embedded tissue. Blood *123*, 1214-1217.

Sears, R., Nuckolls, F., Haura, E., Taya, Y., Tamai, K., and Nevins, J.R. (2000). Multiple Ras-dependent phosphorylation pathways regulate Myc protein stability. Genes Dev *14*, 2501-2514.

Secombe, J., and Eisenman, R.N. (2007). The function and regulation of the JARID1 family of histone H3 lysine 4 demethylases: the Myc connection. Cell Cycle *6*, 1324-1328.

Sentman, C.L., Shutter, J.R., Hockenbery, D., Kanagawa, O., and Korsmeyer, S.J. (1991). bcl-2 inhibits multiple forms of apoptosis but not negative selection in thymocytes. Cell *67*, 879-888.

Seoane, J., Pouponnot, C., Staller, P., Schader, M., Eilers, M., and Massague, J. (2001). TGFbeta influences Myc, Miz-1 and Smad to control the CDK inhibitor p15INK4b. Nat Cell Biol *3*, 400-408.

Sesques, P., and Johnson, N.A. (2017). Approach to the diagnosis and treatment of high-grade B-cell lymphomas with MYC and BCL2 and/or BCL6 rearrangements. Blood *129*, 280-288.

Shachaf, C.M., Kopelman, A.M., Arvanitis, C., Karlsson, A., Beer, S., Mandl, S., Bachmann, M.H., Borowsky, A.D., Ruebner, B., Cardiff, R.D.*, et al.* (2004). MYC inactivation uncovers pluripotent differentiation and tumour dormancy in hepatocellular cancer. Nature *431*, 1112-1117.

Shaffer, A.L., Rosenwald, A., Hurt, E.M., Giltnane, J.M., Lam, L.T., Pickeral, O.K., and Staudt, L.M. (2001). Signatures of the immune response. Immunity *15*, 375-385.

Shi, W., Liao, Y., Willis, S.N., Taubenheim, N., Inouye, M., Tarlinton, D.M., Smyth, G.K., Hodgkin, P.D., Nutt, S.L., and Corcoran, L.M. (2015). Transcriptional profiling of mouse B cell terminal differentiation defines a signature for antibody-secreting plasma cells. Nat Immunol *16*, 663-673.

Shiue, C.N., Berkson, R.G., and Wright, A.P. (2009). c-Myc induces changes in higher order rDNA structure on stimulation of quiescent cells. Oncogene *28*, 1833-1842.

Shou, Y., Martelli, M.L., Gabrea, A., Qi, Y., Brents, L.A., Roschke, A., Dewald, G., Kirsch, I.R., Bergsagel, P.L., and Kuehl, W.M. (2000). Diverse karyotypic abnormalities of the c-myc locus associated with c-myc dysregulation and tumor progression in multiple myeloma. Proc Natl Acad Sci U S A *97*, 228-233.

Singh, R., Letai, A., and Sarosiek, K. (2019). Regulation of apoptosis in health and disease: the balancing act of BCL-2 family proteins. Nat Rev Mol Cell Biol *20*, 175-193.

Smith, K.G., Light, A., O'Reilly, L.A., Ang, S.M., Strasser, A., and Tarlinton, D. (2000). bcl-2 transgene expression inhibits apoptosis in the germinal center and reveals differences in the selection of memory B cells and bone marrow antibody-forming cells. J Exp Med *191*, 475-484.

Smith, M.J., Charron-Prochownik, D.C., and Prochownik, E.V. (1990). The leucine zipper of c-Myc is required for full inhibition of erythroleukemia differentiation. Mol Cell Biol *10*, 5333-5339.

Sodir, N.M., Kortlever, R.M., Barthet, V.J.A., Campos, T., Pellegrinet, L., Kupczak, S., Anastasiou, P., Swigart, L.B., Soucek, L., Arends, M.J.*, et al.* (2020). MYC Instructs and Maintains Pancreatic Adenocarcinoma Phenotype. Cancer Discov *10*, 588-607.

Song, H., and Cerny, J. (2003). Functional heterogeneity of marginal zone B cells revealed by their ability to generate both early antibody-forming cells and germinal centers with hypermutation and memory in response to a T-dependent antigen. J Exp Med *198*, 1923-1935.

Sosa, M.S., Bragado, P., and Aguirre-Ghiso, J.A. (2014). Mechanisms of disseminated cancer cell dormancy: an awakening field. Nat Rev Cancer *14*, 611-622.

Soucek, L., Whitfield, J.R., Sodir, N.M., Masso-Valles, D., Serrano, E., Karnezis, A.N., Swigart, L.B., and Evan, G.I. (2013). Inhibition of Myc family proteins eradicates KRas-driven lung cancer in mice. Genes Dev *27*, 504-513.

Staller, P., Peukert, K., Kiermaier, A., Seoane, J., Lukas, J., Karsunky, H., Moroy, T., Bartek, J., Massague, J., Hanel, F.*, et al.* (2001). Repression of p15INK4b expression by Myc through association with Miz-1. Nat Cell Biol *3*, 392-399.

Stanton, B.R., Perkins, A.S., Tessarollo, L., Sassoon, D.A., and Parada, L.F. (1992). Loss of N-myc function results in embryonic lethality and failure of the epithelial component of the embryo to develop. Genes Dev *6*, 2235-2247.

Stavnezer, J., and Amemiya, C.T. (2004). Evolution of isotype switching. Semin Immunol *16*, 257-275.

Steimer, D.A., Boyd, K., Takeuchi, O., Fisher, J.K., Zambetti, G.P., and Opferman, J.T. (2009). Selective roles for antiapoptotic MCL-1 during granulocyte development and macrophage effector function. Blood *113*, 2805-2815.

Stoneley, M., Paulin, F.E., Le Quesne, J.P., Chappell, S.A., and Willis, A.E. (1998). C-Myc 5' untranslated region contains an internal ribosome entry segment. Oncogene *16*, 423-428.

Strasser, A., Harris, A.W., Bath, M.L., and Cory, S. (1990a). Novel primitive lymphoid tumours induced in transgenic mice by cooperation between myc and bcl-2. Nature *348*, 331-333.

Strasser, A., Harris, A.W., and Cory, S. (1991). bcl-2 transgene inhibits T cell death and perturbs thymic self-censorship. Cell *67*, 889-899.

Strasser, A., Harris, A.W., and Cory, S. (1993). E mu-bcl-2 transgene facilitates spontaneous transformation of early pre-B and immunoglobulin-secreting cells but not T cells. Oncogene *8*, 1-9.

Strasser, A., Harris, A.W., Vaux, D.L., Webb, E., Bath, M.L., Adams, J.M., and Cory, S. (1990b). Abnormalities of the immune system induced by dysregulated bcl-2 expression in transgenic mice. Curr Top Microbiol Immunol *166*, 175-181.

Su, Y., Pelz, C., Huang, T., Torkenczy, K., Wang, X., Cherry, A., Daniel, C.J., Liang, J., Nan, X., Dai, M.S.*, et al.* (2018). Post-translational modification localizes MYC to the nuclear pore basket to regulate a subset of target genes involved in cellular responses to environmental signals. Genes Dev *32*, 1398-1419.

Swanson, P.J., Kuslak, S.L., Fang, W., Tze, L., Gaffney, P., Selby, S., Hippen, K.L., Nunez, G., Sidman, C.L., and Behrens, T.W. (2004). Fatal acute lymphoblastic leukemia in mice transgenic for B cell-restricted bcl-xL and c-myc. J Immunol *172*, 6684-6691.

Swerdlow, S.H., Campo, E., Pileri, S.A., Harris, N.L., Stein, H., Siebert, R., Advani, R., Ghielmini, M., Salles, G.A., Zelenetz, A.D.*, et al.* (2016). The 2016 revision of the World Health Organization classification of lymphoid neoplasms. Blood *127*, 2375-2390.

Tagawa, H., Karnan, S., Suzuki, R., Matsuo, K., Zhang, X., Ota, A., Morishima, Y., Nakamura, S., and Seto, M. (2005). Genome-wide array-based CGH for mantle cell lymphoma: identification of homozygous deletions of the proapoptotic gene BIM. Oncogene *24*, 1348-1358.

Takayama, M., Taira, T., Iguchi-Ariga, S.M., and Ariga, H. (2000a). CDC6 interacts with c-Myc to inhibit E-box-dependent transcription by abrogating c-Myc/Max complex. FEBS Lett *477*, 43-48.

Takayama, M.A., Taira, T., Tamai, K., Iguchi-Ariga, S.M., and Ariga, H. (2000b). ORC1 interacts with c-Myc to inhibit E-box-dependent transcription by abrogating c-Myc-SNF5/INI1 interaction. Genes Cells *5*, 481-490.

Tang, D., Kang, R., Berghe, T.V., Vandenabeele, P., and Kroemer, G. (2019). The molecular machinery of regulated cell death. Cell Res *29*, 347-364.

Tansey, W.P. (2014). Mammalian MYC proteins in cancer. Hindawi Publishing Corporation New Journal of Science *2014*, 27.

Tesi, A., de Pretis, S., Furlan, M., Filipuzzi, M., Morelli, M.J., Andronache, A., Doni, M., Verrecchia, A., Pelizzola, M., Amati, B.*, et al.* (2019a). An early Myc-dependent transcriptional program orchestrates cell growth during B-cell activation. EMBO Rep *20*, e47987.

Tesi, A., de Pretis, S., Furlan, M., Filipuzzi, M., Morelli, M.J., Andronache, A., Doni, M., Verrecchia, A., Pelizzola, M., Amati, B.*, et al.* (2019b). An early Myc-dependent transcriptional program orchestrates cell growth during B-cell activation. EMBO Rep, e47987.

Thomas, L.R., Adams, C.M., Wang, J., Weissmiller, A.M., Creighton, J., Lorey, S.L., Liu, Q., Fesik, S.W., Eischen, C.M., and Tansey, W.P. (2019). Interaction of the oncoprotein transcription factor MYC with its chromatin cofactor WDR5 is essential for tumor maintenance. Proc Natl Acad Sci U S A *116*, 25260-25268.

Thomas, L.R., Foshage, A.M., Weissmiller, A.M., and Tansey, W.P. (2015a). The MYC-WDR5 Nexus and Cancer. Cancer Res *75*, 4012-4015.

Thomas, L.R., and Tansey, W.P. (2011). Proteolytic control of the oncoprotein transcription factor Myc. Adv Cancer Res *110*, 77-106.

Thomas, L.R., Wang, Q., Grieb, B.C., Phan, J., Foshage, A.M., Sun, Q., Olejniczak, E.T., Clark, T., Dey, S., Lorey, S.*, et al.* (2015b). Interaction with WDR5 promotes target gene recognition and tumorigenesis by MYC. Mol Cell *58*, 440-452.

Tonegawa, S. (1983). Somatic generation of antibody diversity. Nature *302*, 575-581.

Trumpp, A., Refaeli, Y., Oskarsson, T., Gasser, S., Murphy, M., Martin, G.R., and Bishop, J.M. (2001). c-Myc regulates mammalian body size by controlling cell number but not cell size. Nature *414*, 768-773.

Tsujimoto, Y., Finger, L.R., Yunis, J., Nowell, P.C., and Croce, C.M. (1984). Cloning of the chromosome breakpoint of neoplastic B cells with the t(14;18) chromosome translocation. Science *226*, 1097-1099.

Tu, W.B., Helander, S., Pilstal, R., Hickman, K.A., Lourenco, C., Jurisica, I., Raught, B., Wallner, B., Sunnerhagen, M., and Penn, L.Z. (2015). Myc and its interactors take shape. Biochim Biophys Acta *1849*, 469-483.

Vallespinos, M., Fernandez, D., Rodriguez, L., Alvaro-Blanco, J., Baena, E., Ortiz, M., Dukovska, D., Martinez, D., Rojas, A., Campanero, M.R.*, et al.* (2011). B Lymphocyte commitment program is driven by the proto-oncogene c-Myc. J Immunol *186*, 6726-6736.

Valovka, T., Schonfeld, M., Raffeiner, P., Breuker, K., Dunzendorfer-Matt, T., Hartl, M., and Bister, K. (2013). Transcriptional control of DNA replication licensing by Myc. Sci Rep-Uk *3*.

Vaux, D.L., Cory, S., and Adams, J.M. (1988). Bcl-2 gene promotes haemopoietic cell survival and cooperates with c-myc to immortalize pre-B cells. Nature *335*, 440-442.

Veis, D.J., Sorenson, C.M., Shutter, J.R., and Korsmeyer, S.J. (1993). Bcl-2-deficient mice demonstrate fulminant lymphoid apoptosis, polycystic kidneys, and hypopigmented hair. Cell *75*, 229-240.

Vennstrom, B., Sheiness, D., Zabielski, J., and Bishop, J.M. (1982). Isolation and characterization of c-myc, a cellular homolog of the oncogene (v-myc) of avian myelocytomatosis virus strain 29. J Virol *42*, 773-779.

Verbeke, C.S., Wenthe, U., and Zentgraf, H. (1999). Fas ligand expression in the germinal centre. J Pathol *189*, 155-160.

Vervoorts, J., Luscher-Firzlaff, J., and Luscher, B. (2006). The ins and outs of MYC regulation by posttranslational mechanisms. J Biol Chem *281*, 34725-34729.

Vervoorts, J., Luscher-Firzlaff, J.M., Rottmann, S., Lilischkis, R., Walsemann, G., Dohmann, K., Austen, M., and Luscher, B. (2003). Stimulation of c-MYC transcriptional activity and acetylation by recruitment of the cofactor CBP. EMBO Rep *4*, 484-490.

Vick, B., Weber, A., Urbanik, T., Maass, T., Teufel, A., Krammer, P.H., Opferman, J.T., Schuchmann, M., Galle, P.R., and Schulze-Bergkamen, H. (2009). Knockout of myeloid cell

leukemia-1 induces liver damage and increases apoptosis susceptibility of murine hepatocytes. Hepatology *49*, 627-636.

Victora, G.D., Dominguez-Sola, D., Holmes, A.B., Deroubaix, S., Dalla-Favera, R., and Nussenzweig, M.C. (2012). Identification of human germinal center light and dark zone cells and their relationship to human B-cell lymphomas. Blood *120*, 2240-2248.

Victora, G.D., and Nussenzweig, M.C. (2012). Germinal centers. Annu Rev Immunol *30*, 429-457.

Victora, G.D., Schwickert, T.A., Fooksman, D.R., Kamphorst, A.O., Meyer-Hermann, M., Dustin, M.L., and Nussenzweig, M.C. (2010). Germinal center dynamics revealed by multiphoton microscopy with a photoactivatable fluorescent reporter. Cell *143*, 592-605.

Vikstrom, I., Carotta, S., Luthje, K., Peperzak, V., Jost, P.J., Glaser, S., Busslinger, M., Bouillet, P., Strasser, A., Nutt, S.L.*, et al.* (2010). Mcl-1 is essential for germinal center formation and B cell memory. Science *330*, 1095-1099.

Villunger, A., Michalak, E.M., Coultas, L., Mullauer, F., Bock, G., Ausserlechner, M.J., Adams, J.M., and Strasser, A. (2003). p53- and drug-induced apoptotic responses mediated by BH3-only proteins puma and noxa. Science *302*, 1036-1038.

Vlach, J., Hennecke, S., Alevizopoulos, K., Conti, D., and Amati, B. (1996). Growth arrest by the cyclin-dependent kinase inhibitor p27Kip1 is abrogated by c-Myc. EMBO J *15*, 6595-6604.

Von Ahsen, O., Waterhouse, N.J., Kuwana, T., Newmeyer, D.D., and Green, D.R. (2000). The 'harmless' release of cytochrome c. Cell Death Differ *7*, 1192-1199.

Vousden, K.H., and Lane, D.P. (2007). p53 in health and disease. Nat Rev Mol Cell Biol *8*, 275-283.

Wagner, A.J., Meyers, C., Laimins, L.A., and Hay, N. (1993). c-Myc induces the expression and activity of ornithine decarboxylase. Cell Growth Differ *4*, 879-883.

Wagner, S.D., and Neuberger, M.S. (1996). Somatic hypermutation of immunoglobulin genes. Annual review of immunology *14*, 441-457.

Walz, S., Lorenzin, F., Morton, J., Wiese, K.E., von Eyss, B., Herold, S., Rycak, L., Dumay-Odelot, H., Karim, S., Bartkuhn, M.*, et al.* (2014). Activation and repression by oncogenic MYC shape tumour-specific gene expression profiles. Nature *511*, 483-487.

Wang, M.L., Walsh, R., Robinson, K.L., Burchard, J., Bartz, S.R., Cleary, M., Galloway, D.A., and Grandori, C. (2011a). Gene expression signature of c-MYC-immortalized human fibroblasts reveals loss of growth inhibitory response to TGFbeta. Cell Cycle *10*, 2540-2548.

Wang, R., Dillon, C.P., Shi, L.Z., Milasta, S., Carter, R., Finkelstein, D., McCormick, L.L., Fitzgerald, P., Chi, H., Munger, J.*, et al.* (2011b). The transcription factor Myc controls metabolic reprogramming upon T lymphocyte activation. Immunity *35*, 871-882.

Weber, J.D., Taylor, L.J., Roussel, M.F., Sherr, C.J., and Bar-Sagi, D. (1999). Nucleolar Arf sequesters Mdm2 and activates p53. Nat Cell Biol *1*, 20-26.

Welcker, M., Orian, A., Jin, J., Grim, J.E., Harper, J.W., Eisenman, R.N., and Clurman, B.E. (2004). The Fbw7 tumor suppressor regulates glycogen synthase kinase 3 phosphorylation-dependent c-Myc protein degradation. Proc Natl Acad Sci U S A *101*, 9085-9090.

Welm, A.L., Kim, S., Welm, B.E., and Bishop, J.M. (2005). MET and MYC cooperate in mammary tumorigenesis. Proc Natl Acad Sci U S A *102*, 4324-4329.

Weng, A.P., Millholland, J.M., Yashiro-Ohtani, Y., Arcangeli, M.L., Lau, A., Wai, C., Del Bianco, C., Rodriguez, C.G., Sai, H., Tobias, J.*, et al.* (2006). c-Myc is an important direct target of Notch1 in T-cell acute lymphoblastic leukemia/lymphoma. Genes Dev *20*, 2096-2109.

Willis, S.N., Chen, L., Dewson, G., Wei, A., Naik, E., Fletcher, J.I., Adams, J.M., and Huang, D.C. (2005). Proapoptotic Bak is sequestered by Mcl-1 and Bcl-xL, but not Bcl-2, until displaced by BH3-only proteins. Genes Dev *19*, 1294-1305.

Willis, S.N., Fletcher, J.I., Kaufmann, T., van Delft, M.F., Chen, L., Czabotar, P.E., Ierino, H., Lee, E.F., Fairlie, W.D., Bouillet, P.*, et al.* (2007). Apoptosis initiated when BH3 ligands engage multiple Bcl-2 homologs, not Bax or Bak. Science *315*, 856-859.

Willis, T.G., and Dyer, M.J. (2000). The role of immunoglobulin translocations in the pathogenesis of B-cell malignancies. Blood *96*, 808-822.

Wilson, A., Laurenti, E., Oser, G., van der Wath, R.C., Blanco-Bose, W., Jaworski, M., Offner, S., Dunant, C.F., Eshkind, L., Bockamp, E.*, et al.* (2008). Hematopoietic stem cells reversibly switch from dormancy to self-renewal during homeostasis and repair. Cell *135*, 1118-1129.

Winkles, J.A. (1998). Serum- and polypeptide growth factor-inducible gene expression in mouse fibroblasts. Prog Nucleic Acid Res Mol Biol *58*, 41-78.

Wright, G.W., Huang, D.W., Phelan, J.D., Coulibaly, Z.A., Roulland, S., Young, R.M., Wang, J.Q., Schmitz, R., Morin, R.D., Tang, J.*, et al.* (2020). A Probabilistic Classification Tool for Genetic Subtypes of Diffuse Large B Cell Lymphoma with Therapeutic Implications. Cancer Cell *37*, 551-568 e514.

Wu, C.H., Sahoo, D., Arvanitis, C., Bradon, N., Dill, D.L., and Felsher, D.W. (2008). Combined analysis of murine and human microarrays and ChIP analysis reveals genes associated with the ability of MYC to maintain tumorigenesis. PLoS Genet *4*, e1000090.

Xiang, Z., Ahmed, A.A., Moller, C., Nakayama, K., Hatakeyama, S., and Nilsson, G. (2001). Essential role of the prosurvival bcl-2 homologue A1 in mast cell survival after allergic activation. J Exp Med *194*, 1561-1569.

Xu, L., Morgenbesser, S.D., and DePinho, R.A. (1991). Complex transcriptional regulation of myc family gene expression in the developing mouse brain and liver. Mol Cell Biol *11*, 6007-6015.

Xu, Y., Poggio, M., Jin, H.Y., Shi, Z., Forester, C.M., Wang, Y., Stumpf, C.R., Xue, L., Devericks, E., So, L.*, et al.* (2019). Translation control of the immune checkpoint in cancer and its therapeutic targeting. Nat Med *25*, 301-311.

Xu, Z., Yan, Y., Li, Z., Qian, L., and Gong, Z. (2016). The Antibiotic Drug Tigecycline: A Focus on its Promising Anticancer Properties. Front Pharmacol *7*, 473.

Yada, M., Hatakeyama, S., Kamura, T., Nishiyama, M., Tsunematsu, R., Imaki, H., Ishida, N., Okumura, F., Nakayama, K., and Nakayama, K.I. (2004). Phosphorylation-dependent degradation of c-Myc is mediated by the F-box protein Fbw7. EMBO J *23*, 2116-2125.

Yeh, E., Cunningham, M., Arnold, H., Chasse, D., Monteith, T., Ivaldi, G., Hahn, W.C., Stukenberg, P.T., Shenolikar, S., Uchida, T.*, et al.* (2004). A signalling pathway controlling c-

Myc degradation that impacts oncogenic transformation of human cells. Nat Cell Biol *6*, 308-318.

Yin, C., Knudson, C.M., Korsmeyer, S.J., and Van Dyke, T. (1997). Bax suppresses tumorigenesis and stimulates apoptosis in vivo. Nature *385*, 637-640.

Youle, R.J., and Strasser, A. (2008). The BCL-2 protein family: opposing activities that mediate cell death. Nat Rev Mol Cell Biol *9*, 47-59.

Yu, Q., Ciemerych, M.A., and Sicinski, P. (2005). Ras and Myc can drive oncogenic cell proliferation through individual D-cyclins. Oncogene *24*, 7114-7119.

Yuan, J., and Horvitz, H.R. (1992). The Caenorhabditis elegans cell death gene ced-4 encodes a novel protein and is expressed during the period of extensive programmed cell death. Development *116*, 309-320.

Zeller, K.I., Haggerty, T.J., Barrett, J.F., Guo, Q., Wonsey, D.R., and Dang, C.V. (2001). Characterization of nucleophosmin (B23) as a Myc target by scanning chromatin immunoprecipitation. J Biol Chem *276*, 48285-48291.

Zeller, K.I., Zhao, X., Lee, C.W., Chiu, K.P., Yao, F., Yustein, J.T., Ooi, H.S., Orlov, Y.L., Shahab, A., Yong, H.C.*, et al.* (2006). Global mapping of c-Myc binding sites and target gene networks in human B cells. Proc Natl Acad Sci U S A *103*, 17834-17839.

Zhang, H., Gao, P., Fukuda, R., Kumar, G., Krishnamachary, B., Zeller, K.I., Dang, C.V., and Semenza, G.L. (2007). HIF-1 inhibits mitochondrial biogenesis and cellular respiration in VHL-deficient renal cell carcinoma by repression of C-MYC activity. Cancer Cell *11*, 407-420.

Zheng, N.Y., Wilson, K., Wang, X., Boston, A., Kolar, G., Jackson, S.M., Liu, Y.J., Pascual, V., Capra, J.D., and Wilson, P.C. (2004). Human immunoglobulin selection associated with class switch and possible tolerogenic origins for C delta class-switched B cells. J Clin Invest *113*, 1188-1201.

Zhou, P., Levy, N.B., Xie, H., Qian, L., Lee, C.Y., Gascoyne, R.D., and Craig, R.W. (2001). MCL1 transgenic mice exhibit a high incidence of B-cell lymphoma manifested as a spectrum of histologic subtypes. Blood *97*, 3902-3909.

Zhou, P., Qian, L., Bieszczad, C.K., Noelle, R., Binder, M., Levy, N.B., and Craig, R.W. (1998). Mcl-1 in transgenic mice promotes survival in a spectrum of hematopoietic cell types and immortalization in the myeloid lineage. Blood *92*, 3226-3239.

Zimmerman, K.A., Yancopoulos, G.D., Collum, R.G., Smith, R.K., Kohl, N.E., Denis, K.A., Nau, M.M., Witte, O.N., Toran-Allerand, D., Gee, C.E.*, et al.* (1986). Differential expression of myc family genes during murine development. Nature *319*, 780-783.

Zindy, F., Eischen, C.M., Randle, D.H., Kamijo, T., Cleveland, J.L., Sherr, C.J., and Roussel, M.F. (1998). Myc signaling via the ARF tumor suppressor regulates p53-dependent apoptosis and immortalization. Genes Dev *12*, 2424-2433.